Understanding and Developing Capabilities for Large Area and Continuous Micro Contact Printing

By

Ambika Goel
Bachelor of Engineering, Manufacturing Processes and Automation
University of Delhi, 2006

Sowmya Laxminarayanan
Bachelor of Engineering, Production Engineering
University of Bombay, 2006

Yun Xia
Bachelor of Science, Mechanical Engineering
Tsinghua University, 2006

Submitted to the Department of Mechanical Engineering in Partial Fulfillment of the Requirements for the Degree of

Master of Engineering in Manufacturing
At the
Massachusetts Institute of Technology

[September 2007]
August 29, 2007

Signatures of Authors

.....

Department of Mechanical Engineering
August 29, 2007

Certified by

.....

David E. Hardt
Professor, Mechanical Engineering
Thesis Supervisor

Accepted by

.....

Lallit Anand
Chairman, Departmental Committee on Graduate Studies
Department of Mechanical Engineering

Understanding and Developing Capabilities for Large Area and Continuous Micro Contact Printing

By
Ambika Goel
Sowmya Laxminarayanan
Yun Xia

Submitted to the Department of Mechanical Engineering on August 29th, 2007 in Partial Fulfillment of the Requirements for the Degree of Master of Engineering in Manufacturing

Abstract

Micro contact printing is a high spatial resolution-patterning tool that can be used for printing on large and non-planar surfaces because of which it has begun to find important applications in printed organic electronics and fiber optics. However, problems like achieving precise alignment and registration, air bubble trapping and low production rate still remain unresolved. The goal of this thesis is to conceptualize and implement a low cost solution to these problems to be used by a nano-technology based company in Cambridge, Massachusetts. In this dissertation, we first present an extensive literature review of soft lithography techniques, focusing more on micro-contact printing and critical factors for taking this technology from laboratory to commercial production. We then introduce another printing technique called flexography and discuss how this method when combined with micro contact printing can help in overcoming the above stated limitations and at the same time achieve high throughput rate at low cost. We propose a Flexography style micro contact printing mechanism with rotating cylindrical stamps enabling reel to reel processing. Finally, results from the experiments conducted to study the effect of parameters like ink concentration, speed and pressure on the print quality are documented.

Acknowledgements

We would like to dedicate this thesis to Professor David Hardt (Professor, MIT), Karan Chauhan (Engineer, Nano-terra LLC) and each other. We as a team coordinated closely as friends to finish an ambitious project within the limited time.

Professor Hardt was with us whenever we needed advice and also took a most important role of monitoring our progress. The long and rather informal meetings with him always provided us with new ideas as well as deepened our commitment to the success of this project and insight into the discipline of manufacturing. We take this opportunity to congratulate him for this new degree program at MIT and wish the future batches our sincere best.

We also thank the whole of the Nano-terra team for providing us with a very friendly and supportive working atmosphere. We appreciate the enormous amount of trust they showed in us and our decisions throughout the project. With Karan as a strong backbone to our projects, we were able to pursue and complete challenging tasks within the short project timeline and we are extremely thankful to his support and valuable inputs.

Table of Contents

List of Figures

Fig 7.5.2 (a) Intersection selection; (b) generating reference grid and displaying distortion of Moiré pattern; (c) displaying actual distortion of underlying pattern; (d) displaying distortion distribution histogram.

Fig 7.5.3 (a), (b) Actual regional deformations and distortion distribution histogram of substrate printed at 15 rpm and 10 psi; (c), (d) Actual regional deformations and distortion distribution histogram of substrate printed at 25 rpm and 10 psi.

List of Tables

Chapter 1

Overview of the Thesis Work

The potential rise of the Printed Organic Electronics industry serves as the fundamental motivation behind much of the work described in this thesis. Micro-Contact Printing is undoubtedly one of the enablers of printed electronics due to its ability to print micro- and nano scale features at a low cost [8,9]. This process, combined with the low cost and high throughput printing technology such as Flexography, can create a new wave in the electronics manufacturing industry by providing a potential means of mass producing organic electronics for less sophisticated applications. This thesis elucidates the transformation in the cost structure and cycle times that can be achieved through this union.

1.1 Introduction

Until recent times, Inorganic Silicon, Gallium Arsenide semiconductors, Silicon dioxide insulators and Aluminum and Copper conductors have been the dominant choice of materials in the semiconductor industry. However, chemists around the world are now involved in a growing research effort to improve the semi-conducting, conducting and light-emitting properties of Organic materials (Polymers, Oligomers) and their hybrids (Organic-Inorganic Composites) through novel synthesizing methods and self-assembling techniques[1].

Organic Electronics are particularly appealing for less sophisticated applications such as RFID tags, Organic batteries, disposable sensors, smart packaging as well as some logic components. Such a market would require these products to be manufactured at a low cost and have a high throughput. Conventional Semiconductor manufacturing processes therefore become inappropriate choices as they fail to meet these cost and throughput requirements.

A promising solution exists in the printing industry. The reason for this is three fold. First is *compatibility* of the properties of Organic electronics with printing technologies.
Organic Substances,

- Have the potential for deployment as Inks that enable printing of electronic circuitry
- Do not rely on thin film growth to achieve control over the crystal and electronic structure of materials introduces an unprecedented freedom in the choice of substrates used for device fabrication. For the first time the use of flexible substrates becomes possible [2].

Ink and flexible substrates are the backbone to the printing industry.

Second is *high throughput* of printing technologies relative to semiconductor manufacturing processes. And third is, *low capital expenditure* because Organic electronics do not require ultrahigh vacuum or a complex equipment intensive clean room processing [2].

Therefore, a potential transition from the traditional subtractive process involving growth of films and selective etching, semiconductor technology [3] can now migrate to a simplified additive manufacturing method based on the selective transfer of structures of the desired geometry.

1.2 Objectives

The main objective of our project was to design a working prototype machine that marries the science of Micro-Contact[1] printing with the technology of Flexographic[2] printing in order to achieve a reel-to-reel printing of substrates. This means printing Micro-Scale patterns with a feature size of the order of 10μm at a throughput rate of up to 10 feet per minute.

1.3 Approach

In order to achieve our objectives we developed a system that essentially mimics a flexography printing press. Our initial thought process and design concept is illustrated in Fig 1.3. As shown in the figure, the prototype machine consists of three rolls as described below:

- Inking Roll: This roll rotates in an anticlockwise direction over an ink bath. It is in mesh with the stamp roll and has two functions. One, it is the driving roll of the entire mechanism and two, it transfers the ink onto the stamp mounted on the stamp roll as it rotates in mesh with it
- Stamp Roll: The Stamp with the desired pattern engraved in it is mounted onto this roll and it rotates in a clockwise direction
- Impression Roll: The main purpose of this roll is to enable a conformal contact between the substrate and the Stamp Roll. It also facilitates feeding and removal of the substrate which is in the form of a sheet

---

[1] Micro-Contact Printing is a flexible new technique that forms patterns of self-assembled monolayers (SAMs) of inks on the surface of the substrate through conformal contact. Patterns of SAM are formed using an alkanethiol as an `ink', and printing the alkanethiol on a metal support with elastomeric `stamp' having a relief pattern of micrometer dimension [9].

[2] Flexography or Flexographic Printing is a method of direct rotary printing that uses a resilient plate made of an elastomeric material with relief features on it. The plate is affixed to a plate cylinder which is inked by an ink-metering roll that carries fast drying fluid ink to the plate that can print onto virtually any type of a substrate [5].

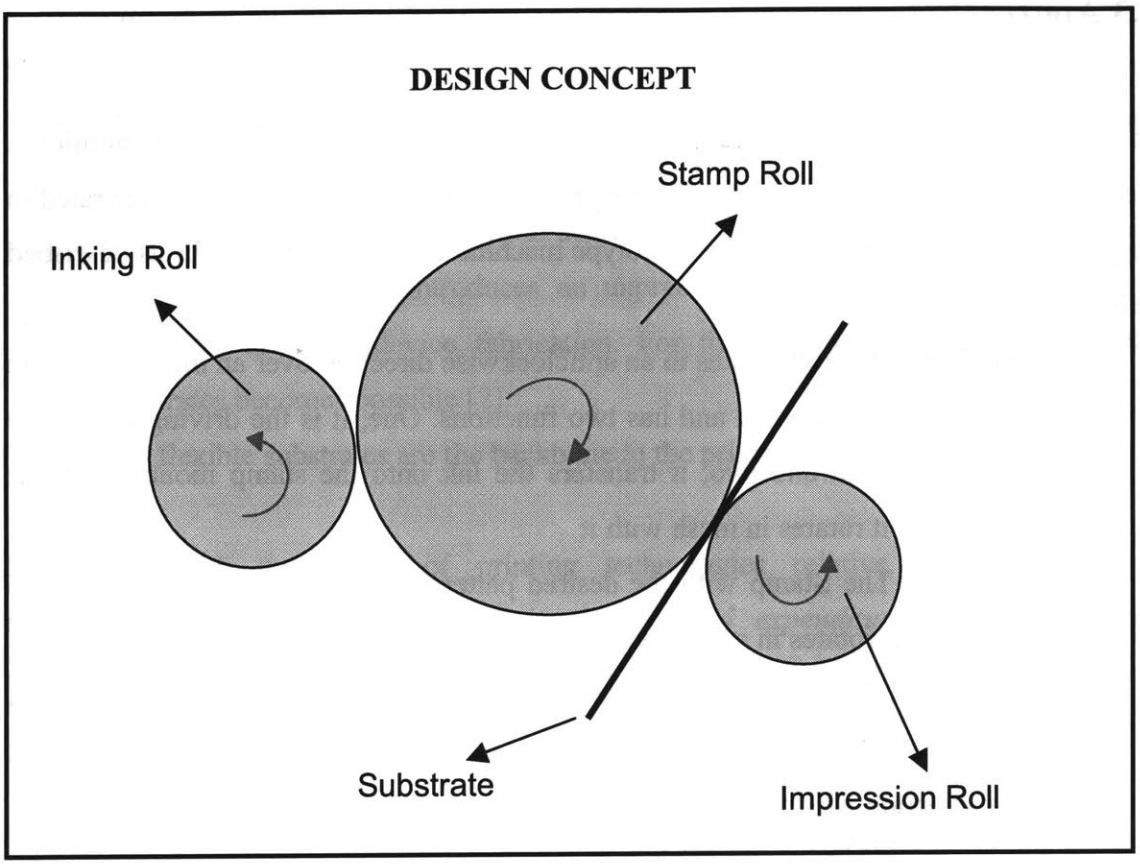

Fig 1.3 shows a Schematic diagram of a flexography printing press (Side View). The arrows in red show the direction of rotation of the rolls.

1.4 Scope

It is extremely important to emphasize that the scope of our project is limited to Micro-Contact printing on Gold Substrates using Hexadecane Thiol [4]. Our project is just the first step in an ongoing research effort towards developing a complete system for printing Organic Electronics. It is also necessary to mention that our focus was to demonstrate successful *transfer* of the desired pattern onto the substrate at a target productivity rate. Micro-Scale pattern transfer using commercial printing technologies is still in its infancy. Therefore, in our project we have made a reasonable amount of compromise with the Quality of the pattern that was printed. This simply means that our main focus has been on understanding the process and achieving effective pattern transfer using the machine

setup which was designed rather than, optimizing a quality function. And so, we have accepted a considerable amount of defects and distortions in the printed pattern.

1.5 Conclusion

In this chapter we discussed the fundamental need for developing a system for delivering low cost and high volume Micro-Scale printing. We also described the design concept that was pursued throughout this project. The next chapter will take the reader through a comprehensive literature underscoring the science and technology that forms the basis for the prototype and the process which was developed.

1.6 Project Breakup

All the three authors have been equally involved in all efforts relating to the project. The machine design process was led by Xia Yun and the hardware built by Ambika Goel and Sowmya Laxminarayanan. Researching and implementing different ways of tool making, one of the most important factors of the process was done by Ambika. Experimental process was led by Sowmya and she also contributed along with Ambika in calibrating and developing a real time output excel sheet for the pressure sensors. Visual analysis of data was conducted by Sowmya based on which further experiments and quantitative analyses were determined. Ambika led the quantitative analysis, making dimensional variation analysis where as Yun analyzed distortions using in house software developed by all three authors over the winter.

Chapter 2

Scientific and Engineering Foundation

2.1 Soft Lithography

2.1.1 Introduction

Micro-fabrication, through its role in microelectronics and optoelectronics, is an indispensable contributor to information technology. It is also ubiquitous in the fabrication of sensors, micro-reactors, combinatorial arrays, micro-electromechanical systems (MEMS), micro-analytical systems, and micro-optical systems. Micro-fabrication uses a variety of patterning techniques; the most powerful of these is photolithography, and essentially all integrated circuits are fabricated using this technology [5].

Although photolithography is the dominant technology, even for large (μm-scale) features, it is not always the best and/or the only option for all applications: For example, it is not an inexpensive technology; it is poorly suited for patterning non-planar surfaces; it provides almost no control over the chemistry of the surface and hence is not very flexible in generating patterns of specific chemical functionalities on surfaces (e.g. for anchorage-dependent tissue culture or combinatorial chemistry); it can generate only two-dimensional microstructures; and it is directly applicable only to a limited set of photosensitive materials (e.g. photoresists). The characteristics of photolithography are such that it is little used for micro-fabrication based on materials other than photoresists. To work with other materials it is necessary to attach chromophores or add photo sensitizers, and neither type of procedure is convenient [5].

An alternative, non-photolithographic set of micro-fabrication methods has been developed and attracted significant attention from both academia and industry due to their tremendous potential to support or even replace conventional means of micro

manufacturing. It is called soft lithography because all its members share the common feature of using a patterned elastomer as the stamp, mold, or mask (rather than a rigid photomask) to generate features on a wide range of dimensional scales, ranging from nanometers to centimeters [5]. These techniques follow a strategy for pattern transfer based on self-assembly of molecular layers and replica molding for carrying out micro and nanofabrication.

The low capital costs and potential of soft lithography for high volume manufacturing with a variety of materials are significantly attractive. For example, the control over surface chemistry, required for some applications in medicine, is possible by the use of soft lithography [98]. E-papers and soft screens consist of LED or OLED are promising applications of it as well [1]. Other potential applications in the near future could include simple optical devices such as polarizers, filters, wire grids, and surface acoustic wave (SAW) devices [6]. Longer term goals include working towards optical data storage systems, flat panel displays, and quantum devices [7].

2.1.2 The Soft Lithography Taxonomy

As mentioned before, several different techniques are known collectively as soft lithography. The soft lithography family covers more than 9 techniques, including microcontact printing (μCP), replica molding (REM), microtransfer molding (μTM), micromolding in capillaries (MIMIC), solvent-assisted micromolding (SAMIM), phase-shift photolithography, cast molding, embossing, injection molding and etc [8]. As shown in **Fig 2.1.2A**, soft lithography relies on replication of a patterned elastomeric stamp from a master to form an elastic stamp that can be inked with a monolayer-forming ink using either wet inking or contact inking. The inked stamp is then used to print a pattern that selectively protects the noble-metal substrate during the subsequent etch.

Six popular techniques in Soft Lithography have been studied by *George M. Whitesides'* group [8], including:

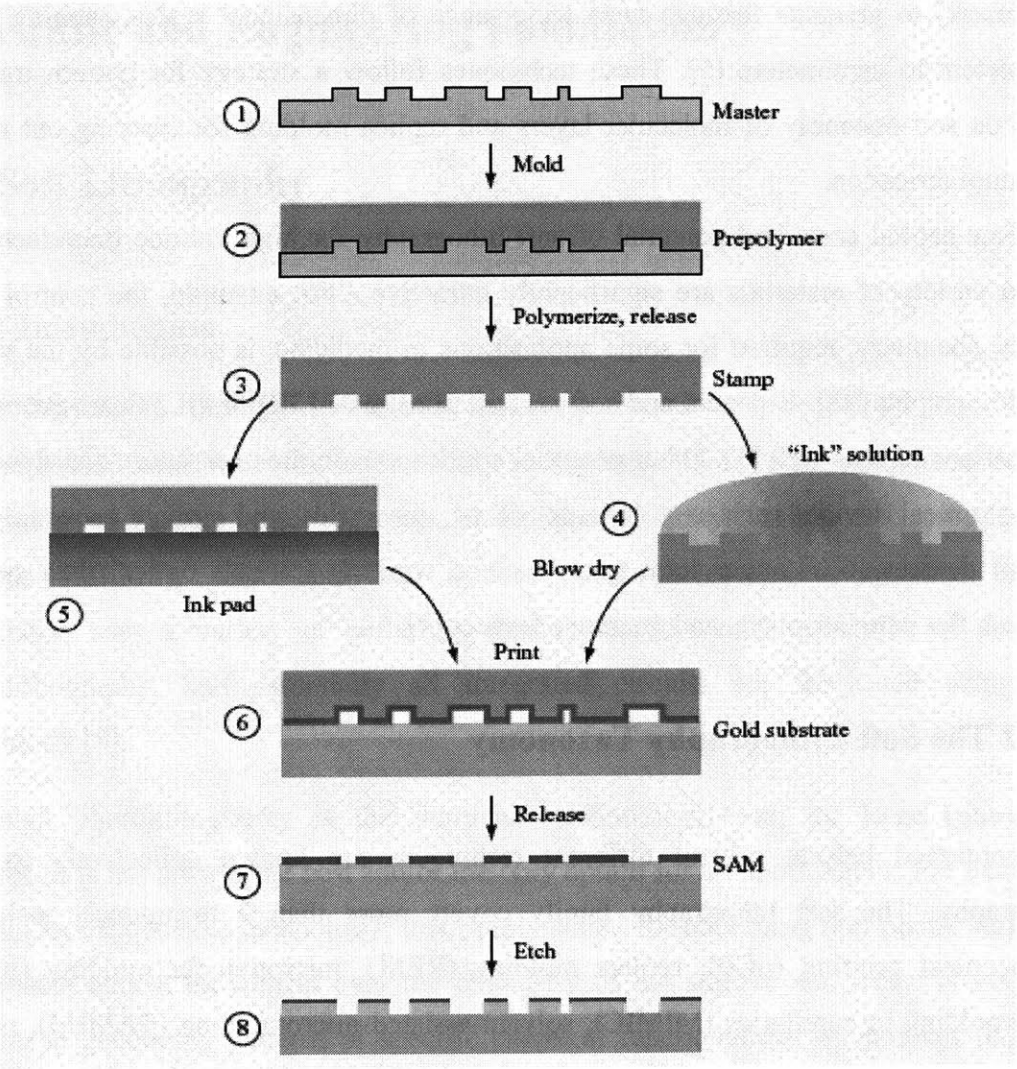

Fig 2.1.2A: Diagram of process: A prepolymer (2) covering the master (1) is cured by heat or light, and demolded to form an elastomeric stamp (3). The stamp is inked by immersion (4) or contacted with an ink pad (5), and printed onto the substrate (6), forming a self-assembled monolayer (SAM). The ink pattern (7) is then transferred into the substrate by a selective etch (8)[9].

a) *Near Field Optical Lithography*

A transparent PDMS mask with relief on its surface is placed in conformal contact with a layer of photo resist. Light, from a source, passing through the stamp is modulated in the near-field. If the relief on the surface of the stamp shifts the phase of light by an odd

multiple of π, a null in the intensity is produced. Features with dimensions between 40 and 100 nm are produced in photo resist at each phase edge [99].

b) Micro-contact Printing (μCP)

Figure 2.1.2B illustrates the procedures for μCP of hexadecanethiol (HDT) on the surface of gold. A thin layer composed of an alkanethiol and ethanol, called "ink", is spread on a patterned PDMS stamp by different methods. Then the stamp is brought into conformal contact with a substrate, which can range from coinage metals to oxide layers. The thiol molecules are transferred to the substrate where they form a self-assembled monolayer, or SAM, that can act as a resist against. Features on the substrate are revealed after etch treatment. Features as small as 300 nm have been produced this way [10]. This process shall be discussed in detail in section **2.2**.

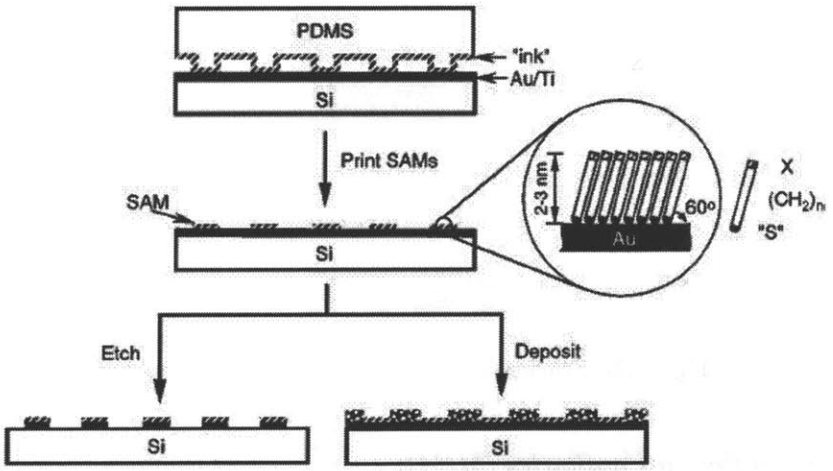

Figure 2.1.2B: Schematic procedures for μCP of hexadecanethiol (HDT) on the surface of gold [11].

c) Replica Molding

As shown in **Fig.2.1.2C**, a PDMS stamp is cast against a conventionally patterned master. Polyurethane is then molded against the secondary PDMS master. In this way, multiple copies can be made without damaging the original master. The fidelity of this process is largely determined by Van der Waals interactions, wetting, and kinetic factors such as

filling of the mold. These physical interactions are short range and should allow more accurate replication of small (<100 nm) features than does photolithography. The value of replica molding is that is allows duplication of three-dimensional topologies in a single step It also enables faithful duplication of complex structures in the master in multiple copies with nanometer resolution in a simple, reliable, and inexpensive way. Replica molding against a rigid mold with an appropriate material (usually a thermoplastic polymer) has been used for the mass-production of a wide range of structured surfaces such as compact disks (CDs), diffraction gratings, holograms, and micro-tools [5]. Xia et al [8] have extended the capability of this procedure by molding against elastomeric PDMS molds rather than against rigid molds; the use of elastomers makes it easier to release small, fragile structures.

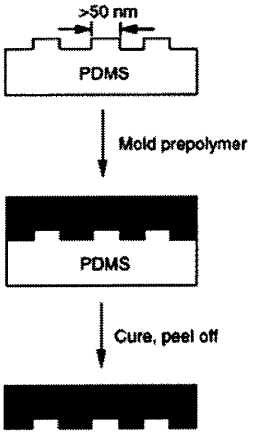

Fig 2.1.2C Schematic procedure for Replica Molding [5].

d) Micro molding in Capillaries (MIMIC).

In MIMIC (**Fig 2.1.2D**), a PDMS mold is placed on the surface of a substrate to form a network of empty channels between them. A low-viscosity prepolymer is then placed at the open ends of the channels, and this liquid spontaneously fills the channels by capillary action. After curing the prepolymer into a solid, the PDMS mold is removed to reveal patterned microstructures of the polymer. MIMIC is able to generate features down to the size of 1 μm [12].

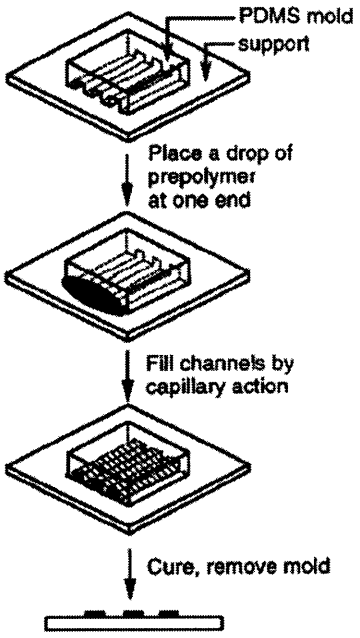

Fig 2.1.2D Shows schematic procedures for MIMIC [5].

e) Micro transfer Molding (μTM)

In μTM (**Fig.2.1.2E**), a thin layer of liquid prepolymer is applied to the patterned surface of a PDMS mold and the excess liquid is removed by scraping with a flat PDMS block or by blowing off with a stream of nitrogen. This mold, filled with the prepolymer, is then placed in contact with the surface of a substrate, and the prepolymer is cured to a solid by illuminating the mold with UV light or by heating it. When the mold is peeled away carefully, a patterned microstructure is left on the surface of the substrate. The technique generates features as small as 250 nm and is able to generate multilayer systems [13].

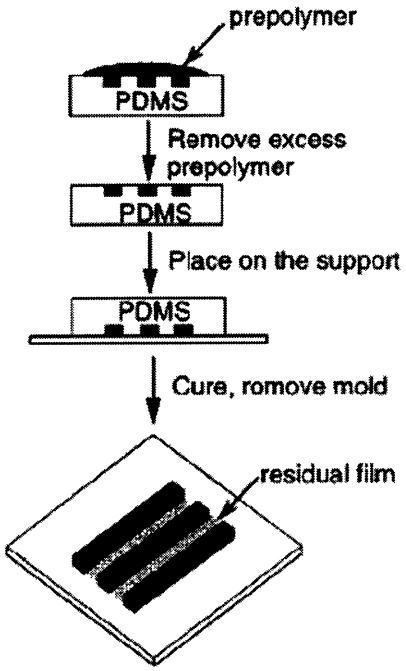

Fig 2.1.2E Shows schematic procedures for Micro Transfer molding [5].

f)) Solvent-assisted Micro contact Molding (SAMIM).

SAMIM (**Fig.2.1.2F**) generates relief structures in the surface of a material using a solvent that can dissolve (or soften) the material without affecting the PDMS mold. The PDMS mold is wetted with the solvent and brought into contact with the surface of the substrate (typically an organic polymer). The solvent dissolves (or swells) a thin layer of the substrate, and the resulting fluid or gel is molded against the relief structures in the mold. When the solvent dissipates and evaporates, the fluid solidifies and forms a patterned relief structure complementary to that in the surface of the mold. SAMIM can be used with a wide variety of materials, generating features as small as 60 nm have been produced [14].

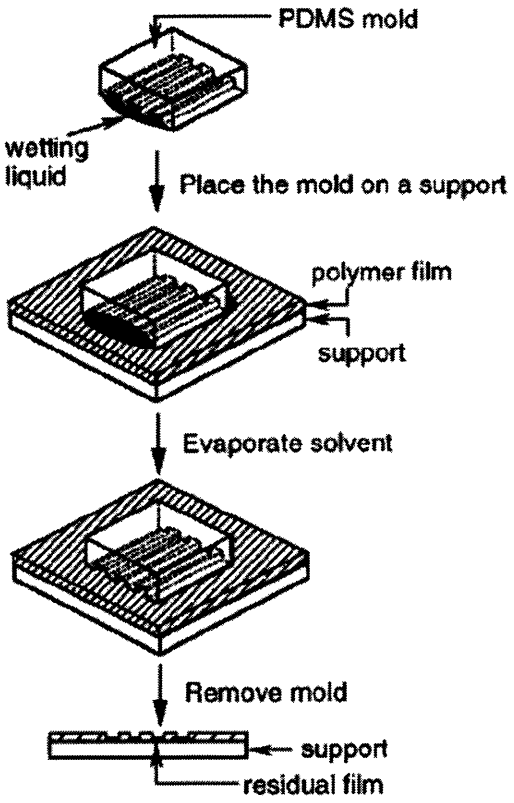

Figure 2.1.2F Shows schematic procedures for replica molding [8].

2.1.3 Soft Lithography versus photolithography

Compared to the traditional photolithography, soft lithographic techniques are low in capital cost, easy to learn, straightforward to apply, and accessible to a wide range of users. They can circumvent the diffraction limitations of projection photolithography; they provide access to quasi-three-dimensional structures and generate patterns and structures on non-planar surfaces; and they can be used with a wide variety of materials and surface chemistries. **Table 2.1.3** gives a comparison between Soft Lithography and conventional optical lithography.

Comparison between photolithography and soft lithography

	Photolithography	Soft lithography
Definition of patterns	Rigid photomask (patterned Cr supported on a quartz plate)	Elastomeric stamp or mold (a PDMS block patterned with relief features)
Materials that can be patterned directly	Photoresists (polymers with photo-sensitive additives)	Photoresists[a,e]
	SAMs on Au and SiO_2	SAMs on Au, Ag, Cu, GaAs, Al, Pd, and SiO_2[a] Unsensitized polymers[b–e] (epoxy, PU, PMMA, ABS, CA, PS, PE, PVC) Precursor polymers[c,d] (to carbons and ceramics) Polymer beads[d] Conducting polymers[d] Colloidal materials[a,d] Sol-gel materials[c,d] Organic and inorganic salts[d] Biological macromolecules[d]
Surfaces and structures that can be patterned	Planar surfaces 2-D structures	Both planar and nonplanar Both 2-D and 3-D structures
Current limits to resolution	~250 nm (projection) ~100 nm (laboratory)	~30 nm[a,b], ~60 nm[e], ~1 μm[d,e] (laboratory)
Minimum feature size	~100 nm (?)	10 (?) - 100 nm

[a–e]Made by (a) μCP. (b) REM. (c) μTM. (d) MIMIC. (e) SAMIM. PU:polyurethane; PMMA: poly(methyl methacrylate); ABS: poly(acrylonitrile-butadiene-styrene); CA: cellulose acetate; PS: polystyrene; PE: polyethylene; and PVC: poly(vinyl chloride)

Table 2.1.3 Gives a tabular comparison between Soft Lithography and conventional optical lithography [15].

2.1.4 Conclusions

This section introduced the reader to the discipline of soft lithography. A brief overview of the various soft lithography techniques and a comparison between soft lithography and photolithography was also presented. The next section will discuss one of the soft lithography techniques called Micro-contact printing, which is closely related to our project, in greater depth.

2.2 Micro contact Printing

2.2.1 Introduction

Microcontact printing is a flexible new technique that forms patterns of self-assembled monolayers (SAMs) of inks on the surface of the substrate through conformal contact. Patterns of SAM are formed using an alkanethiol as an `ink', and printing the alkanethiol on a metal support with elastomeric `stamp' having a relief pattern of micrometer dimension [16].

In this section, we will provide a detailed account of ongoing research in this field that formed the basis of our work. We will discuss the principles, its distinguishing features and also some of the limitations posed by it.

2.2.2 Principles and characteristics of Micro contact Printing

Micro Contact printing uses an elastomeric stamp-PDMS (Polydimethyle Siloxanes) to deposit molecules on surfaces. It can be considered as a two step process- Inking and Stamping.

Inking: First, the PDMS stamp is wetted with the ink, which is capable of forming SAMs. Ethanol is used as a solvent to transfer the ink and hence has to be removed after this step, which is done by drying. The solvent can be dried in the air, but a steam of nitrogen gas helps to reduce time for drying. Inking and drying times depend on factors such as ink concentration, printing area, and printing method. Typically, the inking step takes 30 ~ 60 seconds and drying requires 10 ~ 60 seconds.

Stamping: This requires 3 sub-steps: Initial contact & propagation, full contact, and separation. Achieving full contact through gradual contact is important in order to minimize air trapping between stamp and substrate. After achieving full contact, a certain contact time is required to transport ink from stamp to substrate and form SAMs. The soft PDMS stamp makes conformal contact with the surface and molecules are transferred directly from the stamp to the surface in the space of a few milli-seconds. The required

contact time can vary according to ink type, concentration of ink or target thickness of SAMs. The figure below summarizes the principle behind micro-contact printing.

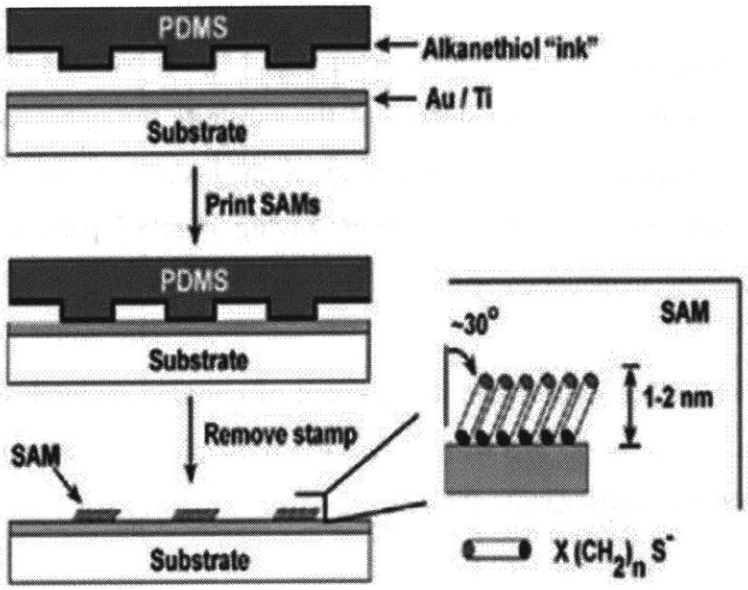

Figure 2.2.2A: Micro contact printing procedure [23].

Table 2.2.2 sums up the various sub-steps of the printing process, their required time, typical failure modes and critical control factors affecting Micro contact printing.

Process	**Inking**		**Stamping**		
Step	Immersion	Drying	Initial contact and propagation	Self assembly full contact	Peeling off
Time	30 ~ 60 sec	10 ~ 60 sec	1 ~ 5 sec	0.3 ~ 60 sec	1~5 sec
Failure Modes	Swelling	Distortion (by capillary force)	Air trapping	- Diffusion of ink - Deformation of stamp	
Control factors	- Inking time - Concentration	- Drying Time - N_2 flow	-Propagation method -Propagation velocity	- Contact time - Pressure - Temperature	- Velocity

Table 2.2.2: Micro contact Printing Process and characteristics [23].

The masters for stamps for micro contact printing are made using micro-machined silicon wafers. The wafers form part of a mould in which liquid PDMS is poured and then

polymerized. On de-molding, a flexible transparent stamp is obtained, with features that can be as small as 100nm.

The alkanethiol ink used, is capable of forming Self Assembled Monolayers (SAMs) between the topographically patterned elastomeric (PDMS) stamp and the surface of the substrate. Hence, the most distinct characteristic of *μCP* is its use of self-assembly (especially, the use of SAMs) to form micro patterns on a substrate [17].

Another important characteristic of micro contact printing is that it makes use of the PDMS elastomer as stamps. This polymer has low interfacial energy and good chemical stability, so the molecules do not adhere to the surface and it can be easily released from the rigid moulds. It can also conformal contact with the surface to be printed with little external normal force and at the same time can compensate for the surface roughness of the substrate. This is important in transporting molecular level SAMs.

Self Assembled Monolayers or SAMs

Self-Assembled Monolayers (SAMs) are layers formed on a solid surface by spontaneous organization of molecules into a stable, well-defined structures via non-covalent interactions having the lowest energy form [18]. SAMs can be easily prepared by immersion of a substrate in the solution containing a ligand ($Y(CH_2)_nX$) reactive towards the surface. The thickness of a SAM can be controlled by change in the number (n) of Methylene groups in the alkyl chain [18]. The surface properties can be easily modified by changing the head group, X [20]. The selectivity in the binding of the anchoring group is a major limitation of this method for forming thin films. For example, some surfaces like Au and Ag [19] are easier to form SAMs on than are others such as metal oxides [21]. The transportation of the ink takes place mainly because of a diffusion process between the stamp and the substrate that then forms SAMs. Diffusion from the edges of the stamp and vapor transport are the non-contact mechanisms that can also form SAMs as can be seen from the figure 2.2.2B.

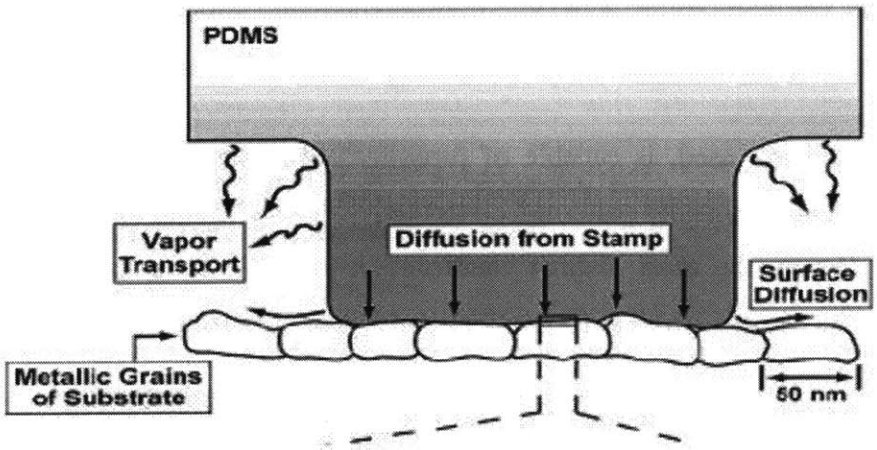

Figure 2.2.2B: Schematic illustration depicting the application of a PDMS stamp containing thiols to a polycrystalline metal film. The mechanisms of mass transport from the stamp to the substrate are also shown [22].

2.2.3 Control Factors affecting *μCP*

In this section, we will elaborate on the critical control factors affecting micro-contact printing.

1. PDMS Properties

As stated above, the elastomeric properties of the PDMS stamps allow micro contact printing to achieve conformal contact with different materials having flat or curved surfaces. PDMS stamps with low young's Modulus (1~3 MPa) are widely used because they provide near perfect conformal contact. Young's modulus is determined by the mixing ratios between the prepolymer precursor and curing agent, and the preparation conditions, such as curing time and temperature.

Because of its elasticity, it can be easily released from rigid masters. In addition to its elastic properties, it has a low interfacial free energy (~21.6 dyn/cm), which prevents it from adhering to the substrate. The interfacial properties can be easily changed either by modifying the prepolymers or by treating the surface with plasma, followed by the formation of siloxane SAMs [18].

2. Concentration of the Ink Solution

With higher ink concentration, printing time is reduced. Also, concentration affects the width of the pattern transferred and the defect rates shown in Figure 2.2.3A.

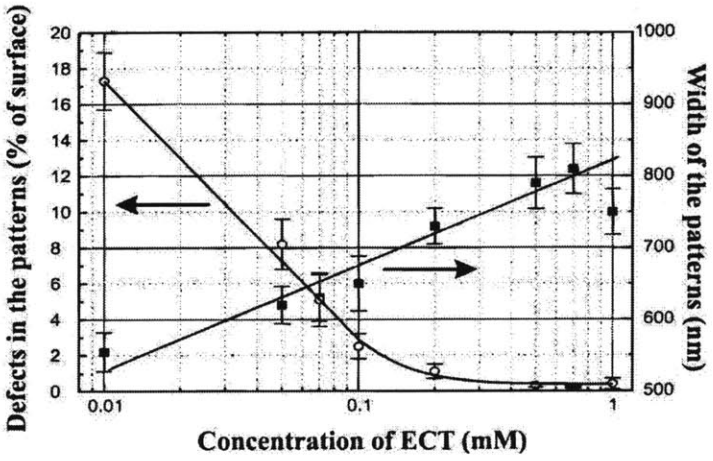

Figure 2.2.3A: Quality of Micro contact printed gold structures performed in the case of an ECT contact-inked stamp. Note that defects in patterns are decreased when concentration of ECT gets higher [24].

3. Stamp-Substrate Contact Time

The thickness of the printed SAMs is proportional to contact time as shown in figure 2.2.3B. Also, longer contact time results into lower defect rates but larger pattern widths as can be seen from Figure 2.2.3C.

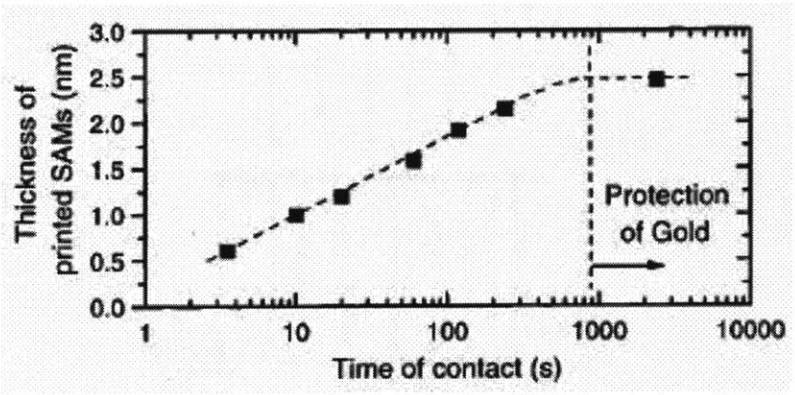

Figure 2.2.3B: Relationship between thicknesses printed with 0.2 milli Mole solution of ECT ink [25].

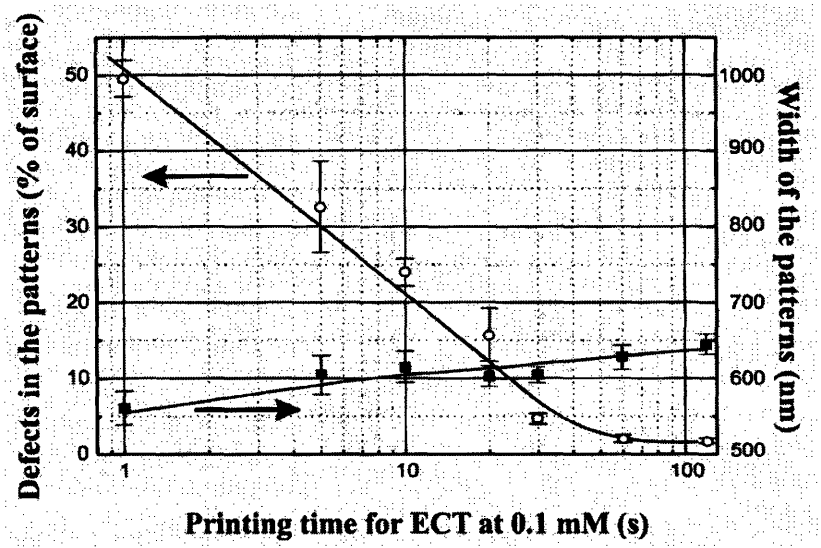

Figure 2.2.3C: Relationship between printing time and the number of defects in the pattern [24].

4. Contact Pressure

Some amount of external pressure is required to establish conformal contact between the stamp and the substrate. On the other hand, excessive pressure can cause the relief features of the stamp to collapse and cause unexpected printing. Figure 2.2.3D shows a basic geometry of a stamp that consists of periodic relief line features with height of *h*, feature width of *l*, and trench width of *d*. When pressure is applied to the stamp, several deformations occur [26].

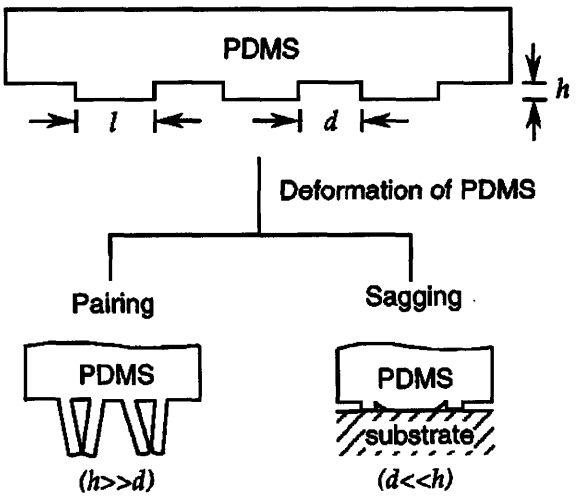

Figure 2.2.3D: Schematic Illustration of deformations caused in the PDMS stamps.

Here, the aspect ratio that is height-to-width ratio of the relief features on PDMS stamps is important. It should be between 0.2 and 2 in order to obtain defect free printing [27]. If the aspect ratio of the PDMS feature is too low, the roof of the feature may come into contact with a substrate under its own weight or under an external pressure, which is called collapse. When the aspect ratios are very high, the relief structures do not withstand the stamp weight and because of the adhesive force they stick together [27].

High interfacial adhesion force can also cause a collapse. K. J. Hsia et al. [28] observed collapse of grooves regardless of self-weight or normal force. According to their study, interfacial adhesion force is the main driving force of groove collapse, and they developed a parameter, which is a function of feature width, height, surface energy, and Young's modulus, that determines the adhesion force.

5. Inking Methods

Inking can be carried out in three different ways – Wet inking, Pen-Type inking, and Contact inking as shown in fig 2.2.3E.

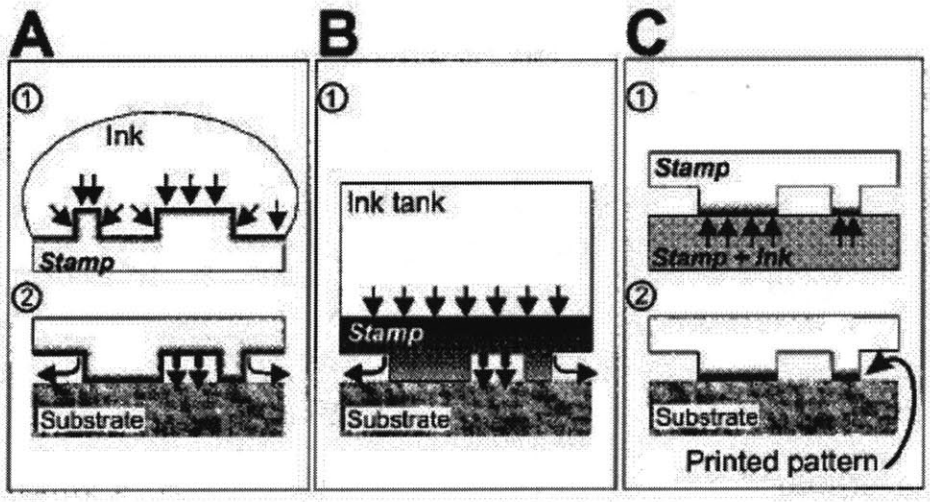

Figure 2.2.3E: Three different types of inking for Micro contact printing [29].

1. Wet inking: In this method the stamps are coated with a droplet of solution for 2 minutes. The excess ink is dried with a nitrogen flow for 30 – 40 seconds. Then the stamp

is immediately placed onto the substrate for printing without any external pressure. The wet inking method is the simplest inking method, but it has problems with diffusion.

2. Pen-type inking: The stamp is inked by transferring the ink from a liquid reservoir of alkanethiols through the PDMS. This way, the stamp gets completely inked including the areas which are not required to be printed.

3. Contact Inking: In this method, the patterned stamp is not exposed to liquid ink but only to an ink-impregnated PDMS block that mediates the transfer of thiols from solution to the elastomeric pattern. After the inker pad is equilibrated with a solution of thiols in ethanols, it is withdrawn from the solution and then dried with a stream of Nitrogen. Then, it is contacted by the patterned face of the stamp. The similar texture of both PDMS surfaces in contact and the elastic property help in easy transfer of thiols. This way, the patterns on the stamps are not subjected to wetting or de-wetting by the ink. This is particularly beneficial for high resolution stamps for which the aspect ratios of parts of their patterns render these stamps more susceptible to mechanical changes [29].
The table below shows a comparison of three methods of inking for micro contact printing.

	Wet Inking	**Pen Stamp**	**Contact Inking**
Distortion of stamps	Capillary effects, slight swelling	Strong swelling	No distortion
Adversary diffusion of the ink (HDT)	Strong	NA	Strongly minimized
Geometric effects	Some	NA	Strongly minimized
Surface crystallization	Strong (>=0.5mM)	Strong (>=0.01mM)	Strong (>=0.5mM)
Ease for repeated inking/printing	Bad	Very good	Fair
Scalability	Unknown	NA	Plausible
Economy of reagent	Bad	Very Good	Fair

Table 2.2.3 Comparison of Three Methods of Inking Stamps for μCP [29].

6. Contact Propagation Methods.

There are several problems that hinder high quality micro-contact printing. Problems like air bubbles getting trapped between the substrate and the stamp, separation of stamp after printing, and the deformations caused in the stamp because of high printing pressure or interfacial adhesive forces can be reduced by using proper methods of contact initiation and propagation between stamp and substrate. The contact propagation can be categorized into three methods: radial, linear, and rolling as shown in fig 2.2.3F.

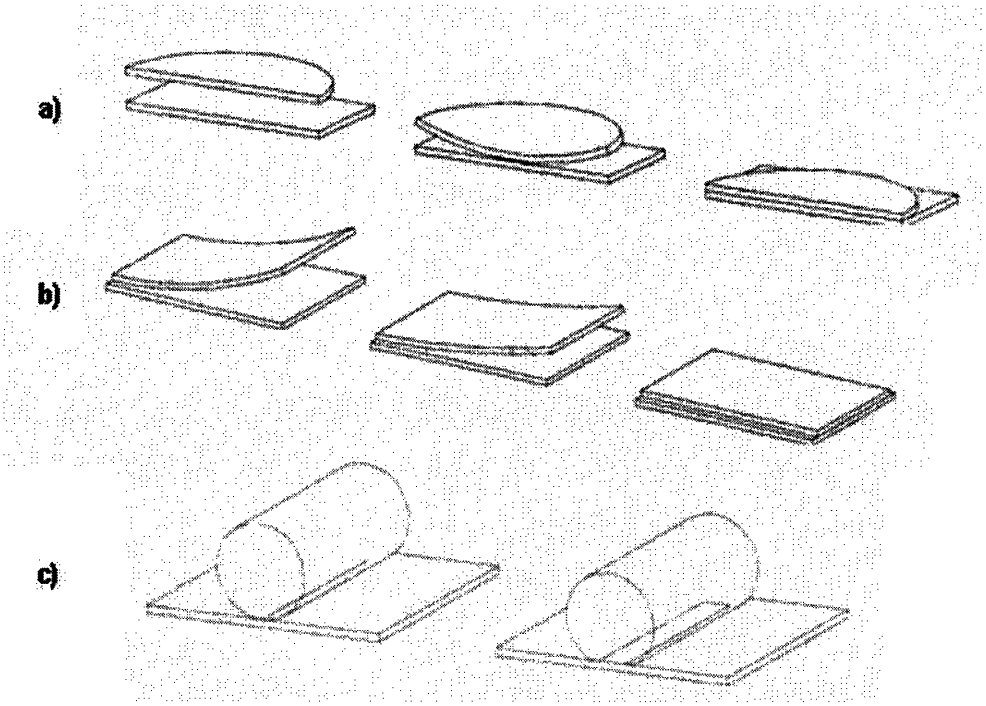

Figure 2.2.3F: Three contact propagation methods (a) Radial contact propagation (b) Linear contact propagation (c) Rolling contact propagation [28].

Radial contact propagation is done by making a convex stamp. The contact initiation starts from the center, and convexity is decreased gradually along with spreading contact region. [23]. Linear contact propagation starts from line contact instead of point contact. The end of a bent stamp creates line contact initiation and contact area gradually increases by dropping the stamp gently. A thin bendable layer of metal or polymer can be used for backing the soft stamp. The third contact propagation method is rolling contact, using cylindrical stamp. In terms of automation, rolling propagation has benefits in that it does not require another mechanism or process for separation of stamps after printing.

Moreover, rolling propagation can simply scalable to mass production process of Micro contact printing such as reel to reel process. However, the deformation of stamp is difficult to predict during preparing cylindrical stamp and printing.

2.2.4 Limitations of Micro Contact Printing

In all, micro contact printing is a very powerful method for surface structuring. The major advantages of this technique is the high quality sub-micrometer features that can be patterned onto the substrate with very little capital investment and under ambient laboratory conditions as opposed to the well known photolithography process which requires very expensive equipment and clean room facility.

But, with the cost benefits and the high quality that micro-contact printing offers, there are certain limitations to this method as listed below:

1. Large area printing

Micro-contact printing when carried out with flat PDMS stamp with surface patterned with relief structures results in air bubbles getting trapped between the stamp and the substrate. This limits the use of very large patterns (>50cm^2).

2. Alignment & Registration

It is difficult to print features that require multiple superimposed patterns with accurate registration and alignment between them on large areas. Also, proper alignment between substrate and the stamp is difficult to achieve.

3. Conformal Contact

Establishing a uniform conformal contact between the substrate and the stamp is another key issue.

4. Stamp Deformation

Stamps used in micro contact printing are made of PDMS. But, it also presents a number of technical problems as listed below [16].

1. PDMS shrinks by 1% upon curing and the cured PDMS can be readily swelled by a number of nonpolar organic solvents such as toluene and hexane.

2. The elasticity and thermal expansion of PDMS makes it difficult to get high accuracy in registration across a large area and may limit the utility of micro contact printing in multilayer fabrication.

3. The softness of an elastomer limits the aspect ratio *(h/d, figure 2.2.3D)* of microstructures in PDMS. When the aspect ratio is too high, the relief structures are not able to withstand the stamp weight and because of the adhesive force they stick together, called as pairing. If the aspect ration is too low, the roof between the relief features will collapse called as sagging.

5. Slow Rate of Production

Micro contact printing is a two step process- inking and then followed by stamping. Rate of production is very slow if the inking and stamping processes are kept coupled as individual processing times get added up. Also, PDMS curing takes a considerable amount of time.

6. Lack of Flexibility

At present, micro contact printing has its limitations when it comes to the repeated use of inked stamps for a long period of time. Because of problems like swelling up of the PDMS and relief features getting distorted as discussed above, flexibility of fast tooling mechanism becomes important.

2.3 Flexography

2.3.1 Definition

Flexography is a method of direct rotary printing that uses a resilient plate made of an elastomeric material with relief features on it. The plate is affixed to a plate cylinder that

is inked by an ink-metering roll that carries fast drying fluid ink to the plate that can print onto virtually any type of a substrate [30].

The heart of the flexographic printing process is the simple inking system. Flexography uses fluid ink. This dries very quickly between the print stations of the press. Both solvent based and water based inks are used depending on a wide variety of requirements.

Flexographic presses generally print on a continuous web of material. The exit end of the press winds the finished printing into a roll, hence the term roll-to-roll or reel-to-reel printing.

2.3.2 Description of the Process

A typical flexographic printing layout is shown in Fig 2.3.2 below.

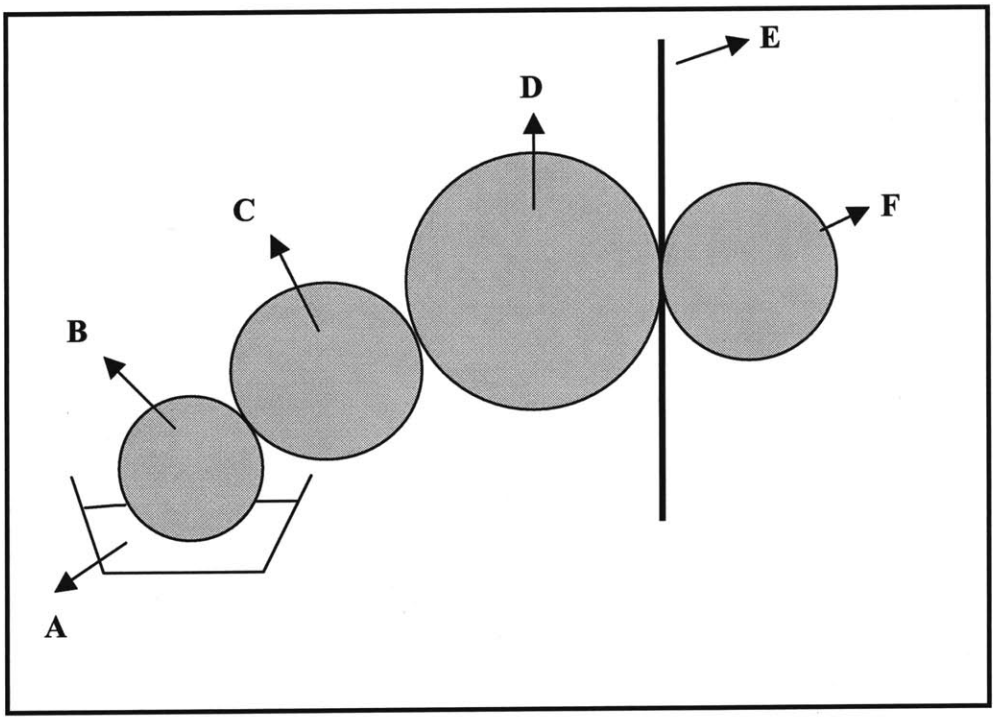

Fig 2.3.2 Shows typical printing station. A. Ink bath with fluid Ink. B. Rubber Ink Fountain roll. C. Ink metering roll. D. Printing Plate Cylinder. E. Substrate passing through press. F. Impression Cylinder.

Briefly, the ink-fountain pan (A) supplies ink to the elastomeric fountain roll (B), which then supplies ink to the metering roll (C). The ink metering roll (C) transfers uniform levels of ink from its cells onto the surface of the printing plate (D) containing the relief features. The substrate (E) that runs through the press is pressed against the plate cylinder (D) with the help of the impression cylinder (F) and ink transfer or printing takes place [30].

2.3.3 Types of Flexographic printing processes

There are three basic types of flexographic presses[1] [30]. Given below is a brief description of the three types.

1. The Stack Press

   The stack press consists of individual color stations stacked one over another on one or both sides of the main press frame. The main advantage of stack presses are that one can reverse the substrate such that both sides get printed. The stack press can print on any kind of substrate but is limited to an accuracy of the order 700 μm [30].

2. The Central Impression Press

   The central impression press is unique in its design because it supports all its color stations around a single steel impression cylinder mounted in the main press frame. The impression cylinder supports the web of substrate which is thereby locked into the cylinder as it passes through all the color stations. The greatest advantage of the central impression cylinder is its excellent registration capabilities [30].

1 Pictures of the different types can be viewed in [30, pg.181].

3. The In-Line Press

   The in-line press is designed such that its color stations are separate complete units, horizontally mounted to one another and driven by a common line shaft. The advantage with the in-line press is its ability to print on very wide substrates and additionally being able to print on both sides of the substrate [30].

2.3.4 Advantages of Flexography

Flexography offers the following advantages [30].

- It can print on a wide variety of absorbent and non-absorbent substrates including extensible plastic films
- It uses fast drying inks, whether solvent, water-based or UV curable
- It uses elastomeric image carriers that can print millions of impressions
- It can print continuous patterns
- Press speeds are up to 2000 feet per minute
- It is cost effective for many applications towing to its very high throughput and simple mechanism
- It enables fast turnaround time between different types of prints
- It can do short-run work profitably
- It has alignment and registration accuracies on the order of 50 μm

2.4 Conclusion

The section introduced the reader to another printing technique, flexography, which is critical for the concept generation of our machine. A brief overview of flexography is presented together with a summary of its advantages. Based on all the background knowledge introduced, the next chapter will discuss in detail how the elements of flexography can be borrowed and adjusted in a novel micro-contact printing machine.

Chapter 3

Flexography Test Machine Concept Design and Realization

3.1 Introduction

As described in the previous chapter, although it has been shown that micro contact printing can offer cost benefits and the high quality, there are still certain limitations which prevent this technique from entering lithography industry. This particular project focuses on increasing the productivity of micro contact printing. In addition, in order to make this technique more attractive and competitive, the solution should be applied to existing equipments with minimum adjustment instead of demanding each manufacturer spending millions of dollars to buy a new set of firmware. To achieve these goals, a thorough understanding of the process physics involved in micro contact printing was required besides identifying the critical factors that could contribute to output quality and production rate. The familiarity of related fields and industries is also critical to the success of the project. Based on the advantages of flexography, which has been discussed in detail in chapter 2, it was chosen on the process for more thorough study. To this end a prototype machine was designed and built to allow lab scale testing of flexographyic micro contact printing. The test machine design was derived after several design iterations, which will be cover in this chapter as well as in following chapters. The key breakthrough in the design process was achieved with the realization that the target substrate, which is a flexible sheet of gold coated plastic film, could be continuously fed into rolling cylinders where printing actually takes place.

This chapter takes the reader through some of the most important design iterations towards the final design, followed by a detailed description of each component in the machine. Though some of the designs are not present in the final prototype, they are

included as a complete design history and for possible future use. Finally, we propose a complete manufacturing system for high-rate continual micro contact printing.

3.2 Target functions and concept generation

3.2.1 Target Function

Applying new technologies to existing machines with minimal adjustment is always preferred by industries to building or purchasing a completely different system. In order to develop a technique compatible with existing systems, at the beginning of the project, a careful study of potential candidates was conducted. With its high throughput and simple mechanism, plus the similarity in flexible substrates with microcontact printing, flexography was finally selected to be process on which the prototype machine is developed.

Designing a micro contact printing machine on the flexography principle has never been demonstrated by any organization. However, a good understanding of both flexography and micro contact printing provided important hints for the exploration. First, the five most important factors that determine the quality of micro contact printing were listed as: ink concentration, temperature, printing pressure, printing time and the quality of stamps. In order to explore the feasibility of the combination of the two techniques as thoroughly as possible, within the certain constrains we were facing, maximum flexibility should be included in the prototype machine, namely the machine should be capable of adjusting the first four parameters listed above while printing. This served as the benchmark in the concept generation stage. As for the quality of stamps, a thorough discussion will be presented in next chapter.

3.2.2 Concept generation

The process of micro contact printing involves two sub-stages, namely inking and printing, which is the same for flexography. The two steps will be discussed separately.

3.2.3 Inking process

Although it looks like that the inks used in micro contact printing and flexography share a lot of commonalities, there is actually a fundamental difference between them. As shown in Fig 3.2.3A, Flexography uses liquid ink which form a thin layer on top of the features while in microcontact printing, there is no liquid ink at all, instead, the "ink" is molecules residing inside the features.

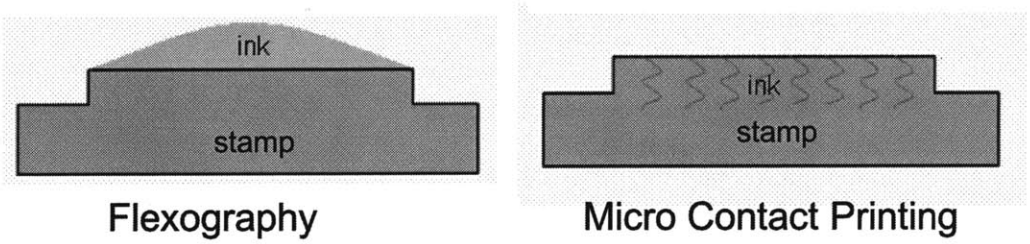

Figure 3.2.3A: The difference of inks between flexography and micro contact printing.

This difference leads to a modification of the flexography concept to meet the new standard for micro contact printing. In a flexography machine, liquid ink is transferred from ink bath to the plate cylinder which is covered with stamps through one or multiple rolls engraved with mini cells to precisely control the amount of ink. Those features are neither necessary nor desired in micro contact printing. In this project, the goal of inking is to guarantee that there are always enough molecules in the stamp.

Taking into consideration the strength and weakness of each method and the principles of flexography, among the three inking methods, namely wet inking, pen stamp and contact inking, we agreed that wet inking and contact inking both are suitable for our machine. Several feasible solutions for inking were then generated based on the two inking methods. They all share three commonalities: first, their inks all start from liquid form, namely solvent with molecules dissolved inside; second, before printing actually happens, there is no liquid, only ink molecules on the stamp; third, they all use PDMS sheets which are mounted on the rolls as carriers of ink (solvent and ink molecules). As explained in Chapter 2, PDMS is ideal to play this role for three reasons:

1. PDMS can carry significant amount of molecules and transfer them easily, which

has been proved in contact inking [10];

2. PDMS sheets can form conformal contact between each other, enhancing the ink transfer process;
3. The friction between PDMS sheets is high, which prevents slip. This is very important when we later decided not to build a synchronized system.

Figure 3.2.3B illustrates four inking concepts.

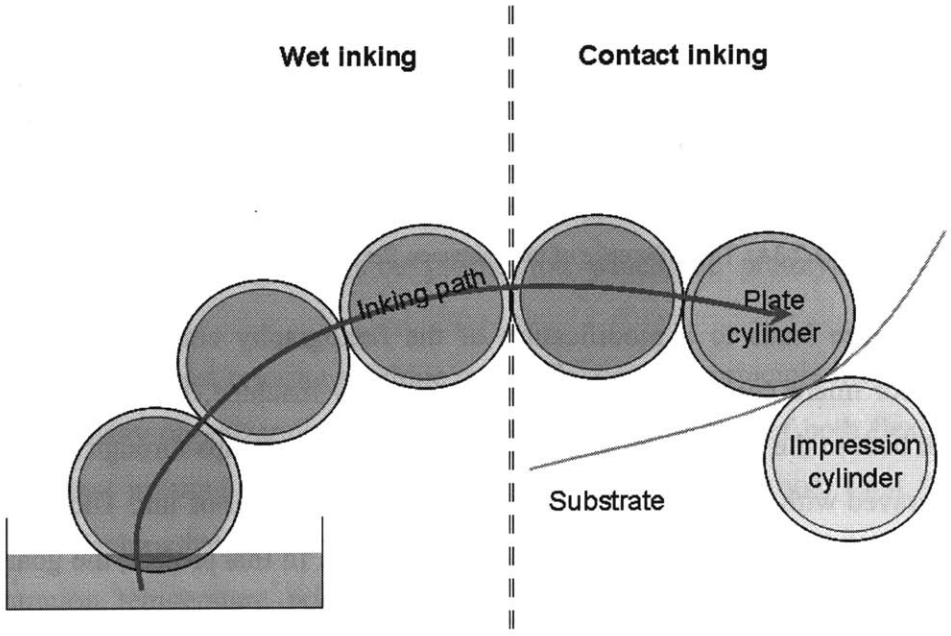

(a)

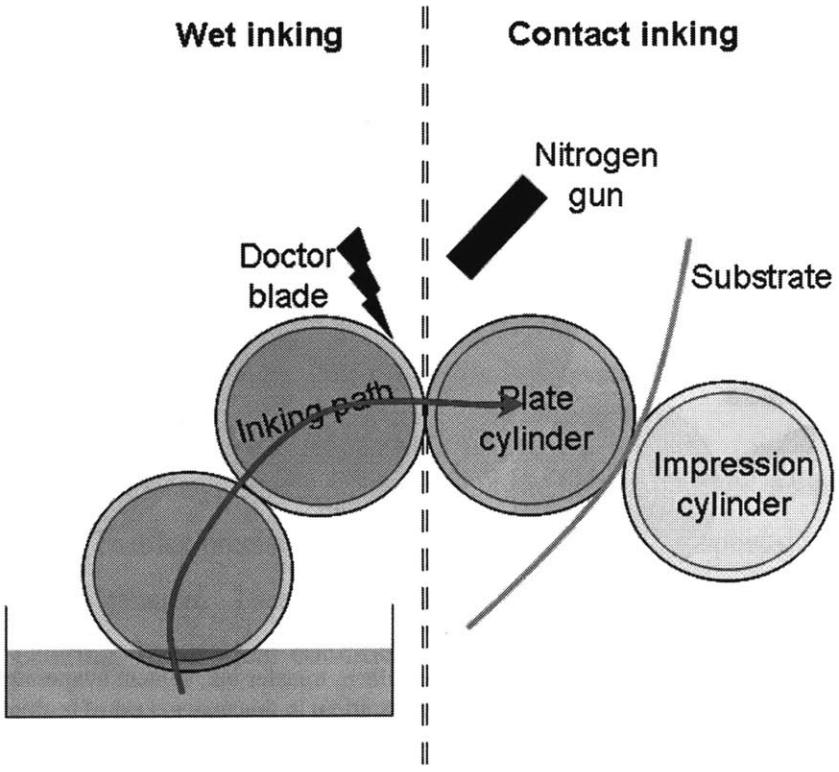
Wet inking
Contact inking
Nitrogen gun
Doctor blade
Substrate
Inking path
Plate cylinder
Impression cylinder

(b)

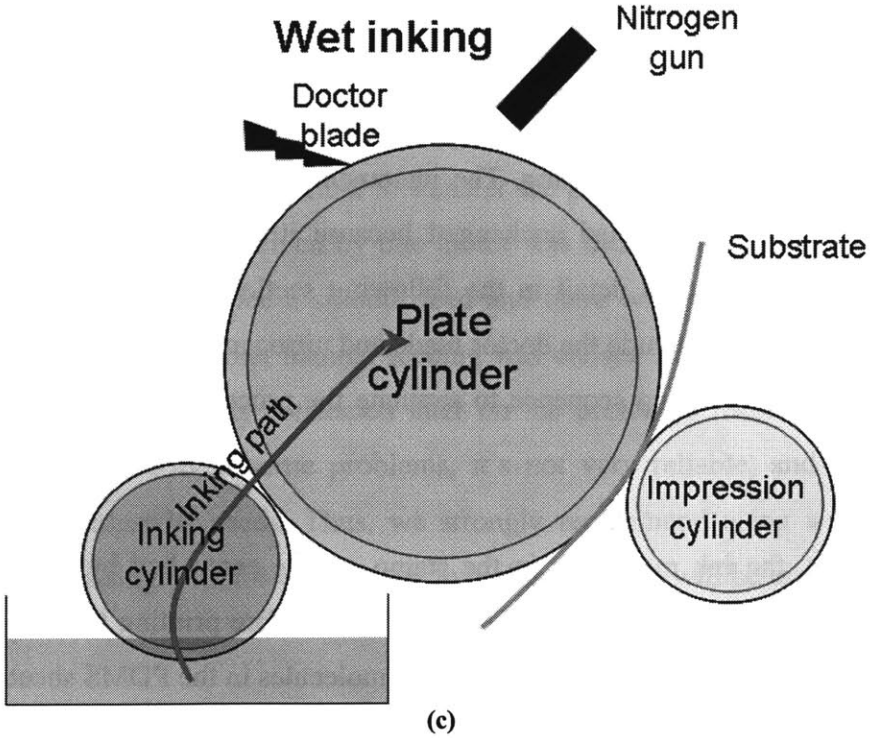
Wet inking
Nitrogen gun
Doctor blade
Substrate
Plate cylinder
Inking path
Inking cylinder
Impression cylinder

(c)

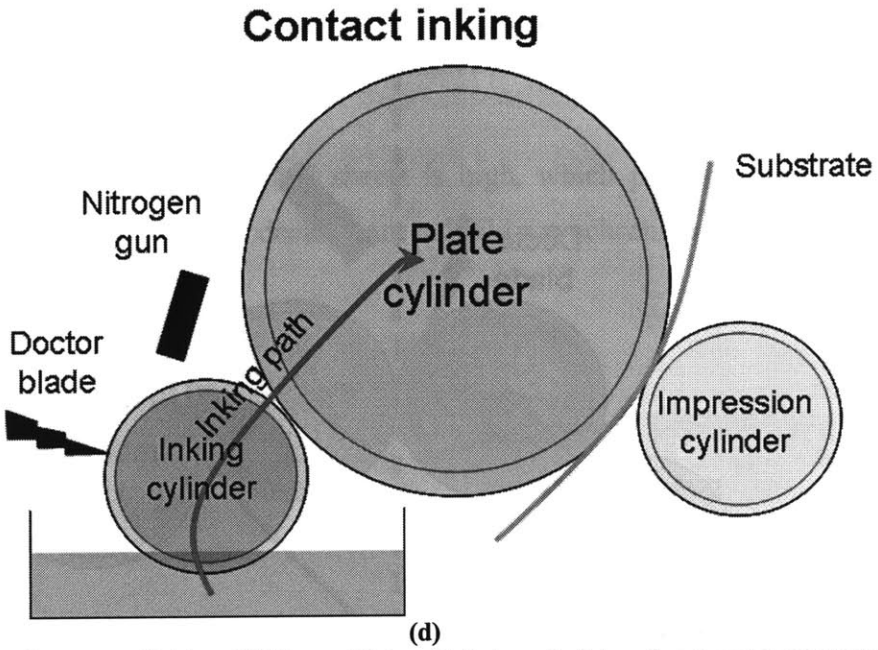

Figure 3.2.3B: Concepts of inking. (a) Use multiple rolls to transfer ink, solvent evaporates naturally; (b) Use doctor blade and nitrogen gun to expedite the evaporation, in this way get rid of multiple cylinders; (c) Simplify the system again by ruling out the last ink carrier and increasing the dimension of plate cylinder to leave enough time for the liquid solvent to evaporate; (d) Modified (c) from wet inking to contact inking; this required stronger nitrogen gun to avoid wet inking.

Concept (c) and (d) are preferred to (a) and (b) because of their simplicity and compactness. Concept (d) was finally selected because it has been shown that contact inking leads to less distortion of the stamp, which in turn increases the life of the stamp and improves the quality of printing. The increment in the dimension of plate cylinder shown in concept (c) remained unchanged because it's desirable in printing process, which will be discussed in detail in the following section. However, because of time constraints, we did not include the doctor blade and nitrogen gun in our machine; instead, we used a simplified inking sequence to simulate the process. This will be discussed in Chapter 4.

In our concept, the ink molecules in the stamp can be controlled by changing the ink concentration in the solvent. It should be noted that before printing takes place, 5 to 15 minutes pre-inking is required to make sure the molecules in the PDMS sheet wrapped on inking cylinder reach a preset concentration.

3.2.4 Printing process

As the most critical part of the machine, the actual printing process requires tight control as well as maximum flexibility. Careful considerations are given to five aspects of the design in order to fulfill the requirements within the constraints we were facing.

(A) Synchronized system versus single-motor-driving system

In the flexography industry, synchronized roll systems are widely adopted because delicate equipment enables precise control over cylinder rotation speeds; substrate feed rate and substrate tension. These abilities are equally, if not more desirable in microcontact printing. In an ideal condition, building a synchronized system should be the best solution. However, given a tight time limit of two months, we had to give up a synchronized system and instead, find some way to control the printing speed while preventing slide between cylinders and the substrates.

As mentioned in previous section, the coefficient of friction between PDMS sheets is high, which gives a solution to prevent slipping. With sufficient amount of pressure between cylinders, friction is sufficient to transfer the power from one drive cylinder to the overall system. A system driven by one motor was then developed. Because certain tension is required to guarantee a smooth feed and there was no suitable winding and unwinding equipment available, manual feeding was chosen for this system. However, the results of the experiments conducted later on the prototype machine suggests that although the solution solved some problems, it's not very reliable, and not yet good enough to meet industrial needs. Thus, we strongly recommend using a synchronized system instead of a single-motor-driving one in real industry. It will be discussed in detail in Chapter 6.

There are three places to mount the motor in the concept generated based on the requirements of inking, inking cylinder, plate cylinder and impression cylinder. Table 3.2.4A gives a comparison among the three.

Motor location	Advantages	Disadvantages
Inking cylinder	Flexibility in inking, namely pre-inking inking cylinder is possible	Indirect printing speed control
Plate cylinder	Direct printing speed control	Less flexibility and harder to drive (larger moment of inertia)
Impression cylinder	None	Indirect printing speed control

Table 3.2.4A Comparison between different motor locations

In order to get the best tradeoff, we evaluated our goal of the project and decided to mount the motor on the inking cylinder. The reason is that the capability of pre-inking gives us more flexibility in both machine design and experiments while precise speed control is not critical the exploration stage.

(B) Temperature control

Temperature at which printing takes place may significantly affect diffusion rate, thus affect the printing process. We planed to incorporate heating equipment in the machine to control the temperature at first. But it turns out that if the ink concentration and the printing time are within a certain range, the effect of temperature is insignificant. To simplify the prototype, we eliminated the heating equipment from our machine. However, if a thorough understanding of the reel-to-reel micro contact printing is desired, temperature control should be included.

(C) Pressure control

Another important factor determining the quality of micro contact printing is the printing pressure. If the pressure is too low, the ink transfer will be insufficient, or not happen at all. On the other hand, if the pressure goes too high, there is a high risk of collapse. Clearly some mechanism to adjust and control the pressure is a must in our machine. The

basic idea is to make the cylinders movable with respect to each other. Two types of movement are considered, vertical movement and horizontal movement (including the combinations of the two). After careful consideration of the whole system, we finally chose horizontal movement, because horizontal movement is easier to realize and integrate in our design.

(D) Printing time control

In the reel-to-reel concept, printing time is primarily determined by the speed at which the plate cylinder rotates. A simple solution is to use a drive motor that is capable of providing multiple speeds. One critical issue here, as mentioned earlier in this chapter, is that there should be no slip between substrate and stamp. Since manual feeding is selected, operators of this machine must be careful of the tension they apply on the substrate. The tension should be enough to prevent wrinkle, tangle or wrap, yet should it be below certain value to avoid slide.

(E) Machine scale

The test machine must be big enough to simulate real conditions and test the feasibility of the concept without being too costly, slow and difficult to build. Also, since making big PDMS stamp of highly uniform thickness is very difficult at present, the smaller dimensions are desirable. Finally, test substrate material will only be available in 4 inches widths. Accordingly, the final decision was a machine roughly 12'' by 12'' by 14'' in overall dimensions.

Another consideration is the diameter of the plate cylinder. A larger diameter has advantages as shown in Table 3.2.4B.

	Large diameter	Small diameter
Stamp mounting	Easy to mount; less tension	Hard to mount because larger force is required to secure the position of stamp
Conformal contact	Smaller curvature provides better conformal contact and enables more flexibility in contact area control	Worse conformal contact; less flexibility
Reference availability	Closer to flat stamp printing from which experience and knowledge can be borrowed	Little reference is available

Table 3.2.4B Comparison between cylinders of different diameters

With those advantages, a plate cylinder of the largest diameter for the overall scale of the machine was selected.

With a thorough consideration of both process and function targets, a workable concept was generated. The next step is to build a prototype machine based on the concept.

3.3 Concept realization

This section guides reader through the selections of each component used in the prototype machine which realizes the concept.

3.3.1 Machine overview

As shown in Figure 3.3.1A, a detailed three-dimensional model was designed in Solidworks. Note that motor is not included in the Solidworks drawings shown in this paper since it is considered as a part of electrical system which will be discussed in Chapter 5. Please also note that all dimensions in the drawings are marked in inches.

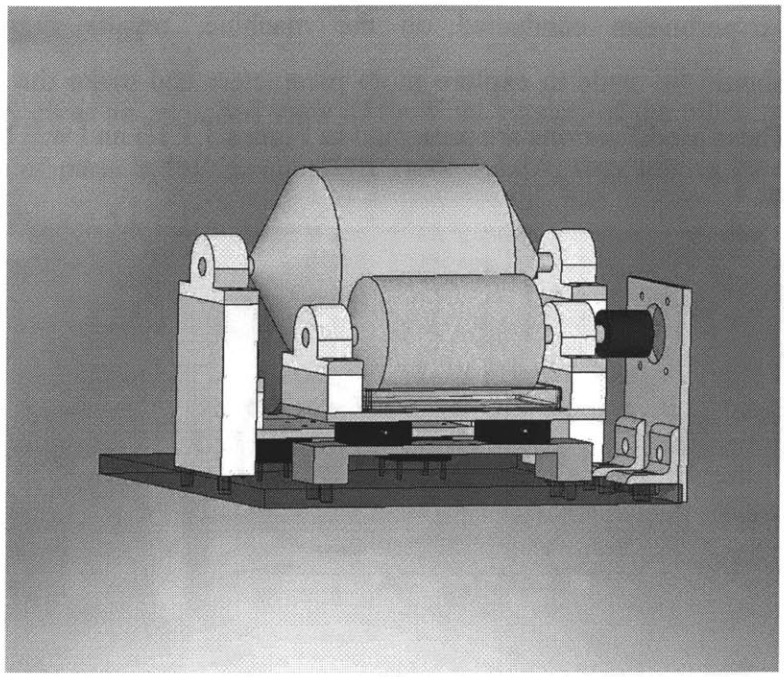

(a)

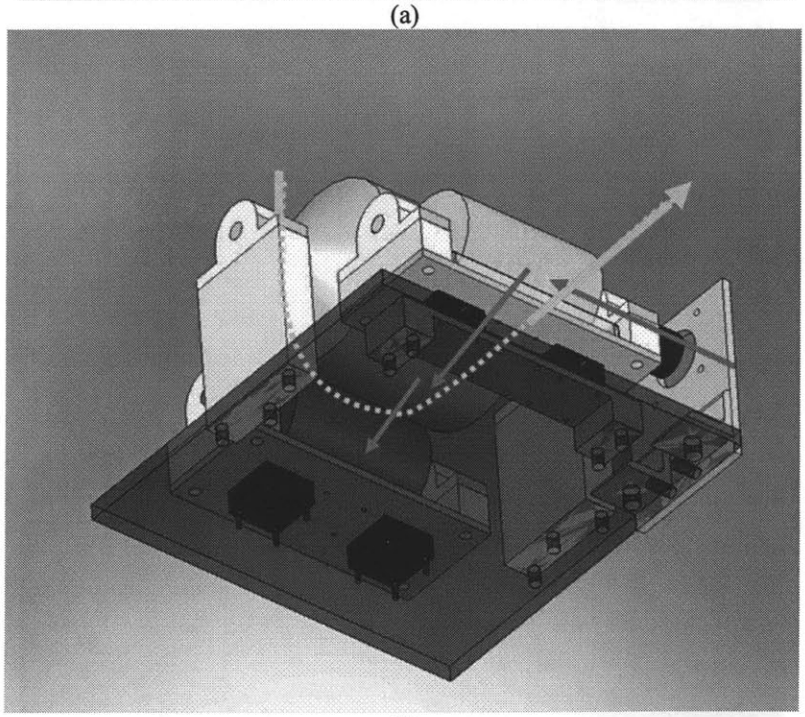

(b)

Figure 3.3.1A: 3-D model design in Solidworks, detailed dimensions are shown in following drawings. In (b), red arrows indicate the drive path, (1) drive motor drives inking cylinder through flexible coupling,(2) inking cylinder drives plate cylinder, (3) plate cylinder drives the impression cylinder; the green arrow indicates the substrate feeding path: the substrate is fed between plate and impression cylinder where printing takes place, then the substrate is pulled off the system through the hollow part of the inking desk.

In the early experiments conducted on the machine, results suggested several modifications should be made to explore more parameters and make the machine more user-friendly. These modifications are presented in Figure 3.3.1B and will be discussed in detail in Chapter 4.

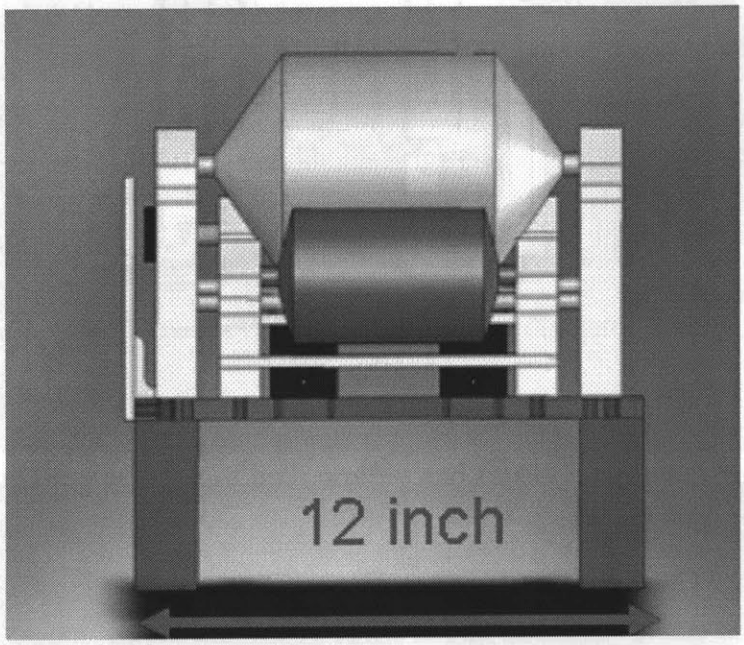

(a)

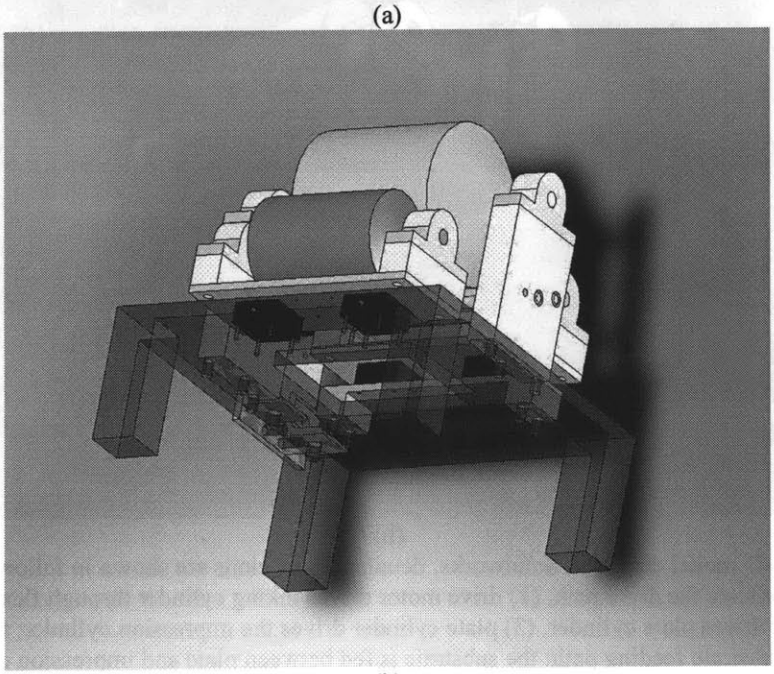

(b)

Figure 3.3.1B: Modified 3-D model

3.3.2 Bill of material

Figure 3.3.2A gives an exploded view of the final version of the machine. There are 15 different kinds of parts in this machine. In Table 3.3.2A, they are all listed according to the number in Fig 3.3.2A

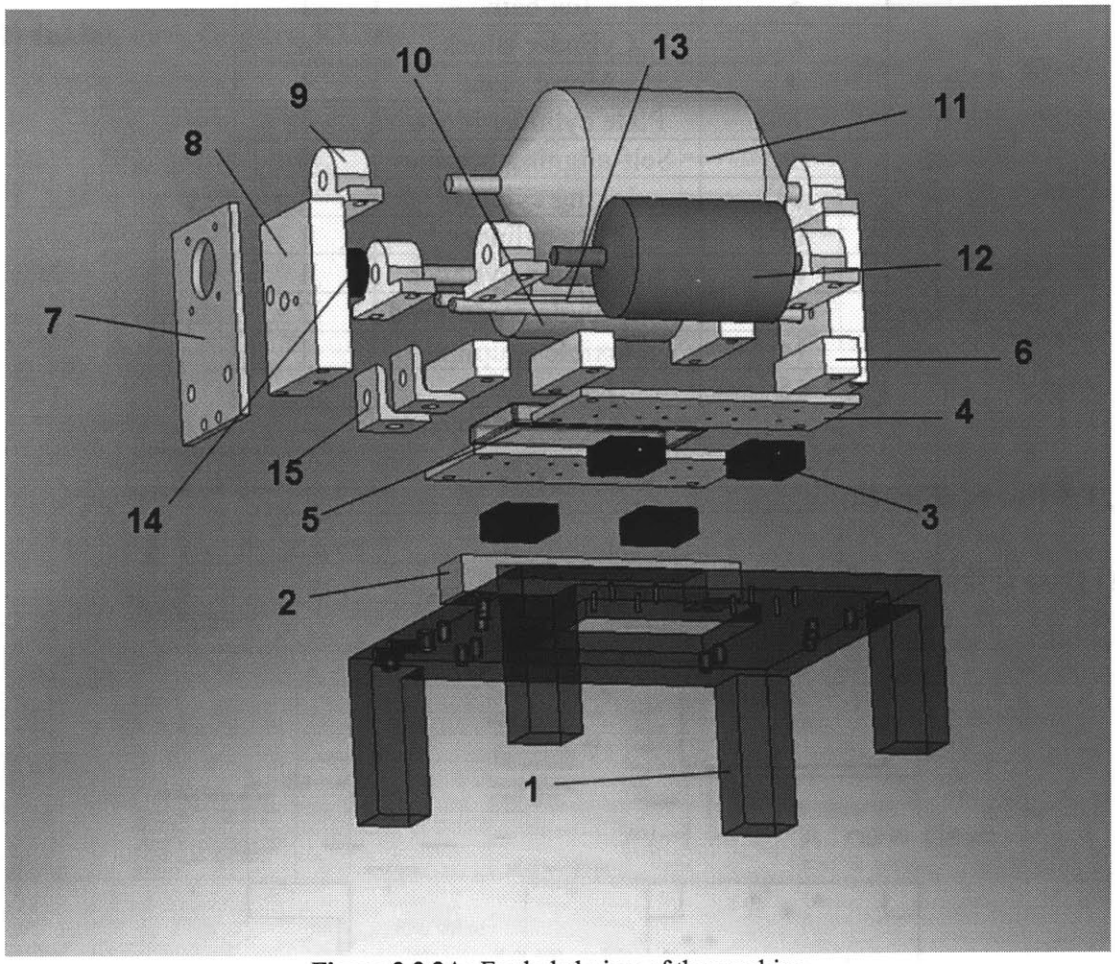

Figure 3.3.2A: Exploded view of the machine

Part number	Part name	Quantity
1	Base	1
2	Inking desk	1
3	X stage	4
4	Cylinder plate	2
5	Ink bath	1
6	Cylinder Block	4
7	Motor plate	1
8	Plate cylinder block	2
9	Self-aligning bearing	6
10	Inking cylinder	1
11	Plate cylinder	1
12	Impression cylinder	1
13	Wrap angle control rod	2
14	Flexible coupling	1
15	L-connector	2

Table 3.3.2A Bill of material

3.3.3 Parts selections

(1) Base (Figure 3.3.3A)

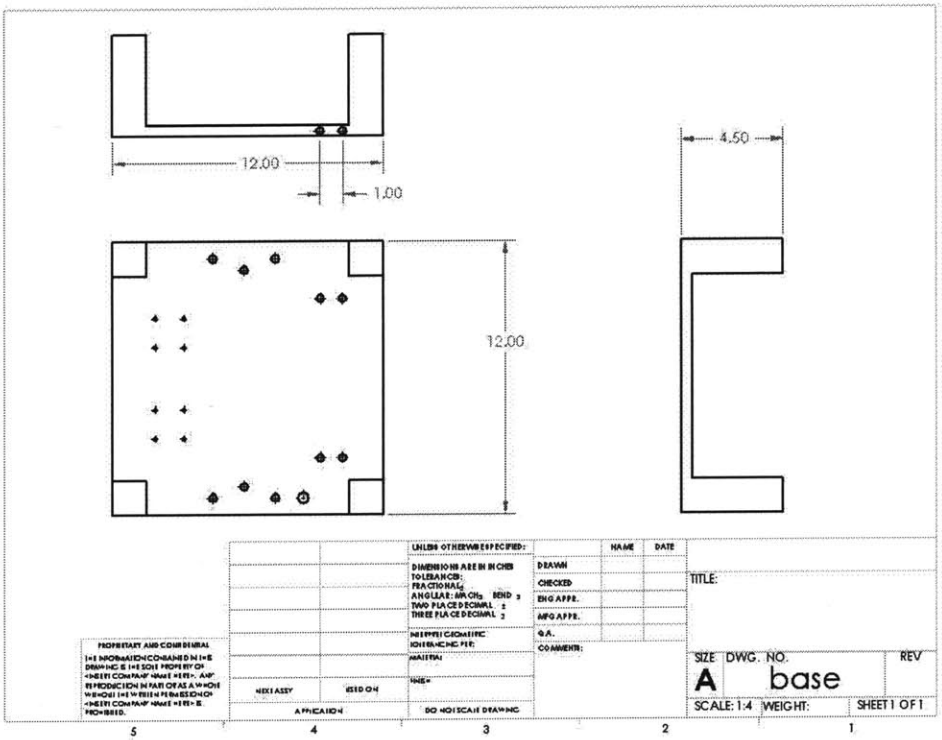

Figure 3.3.3A: Base, for the detailed locations of the holes refer to the corresponding parts.

The function of base is to provide a rigid and stable platform for the system. It decides the layout of other components.

The raw material, an aluminum block with high level surface flatness, comes from McMaster-Carr. The machining was done in LMP machine shop of MIT.

(2) Inking desk (Figure 3.3.3B)

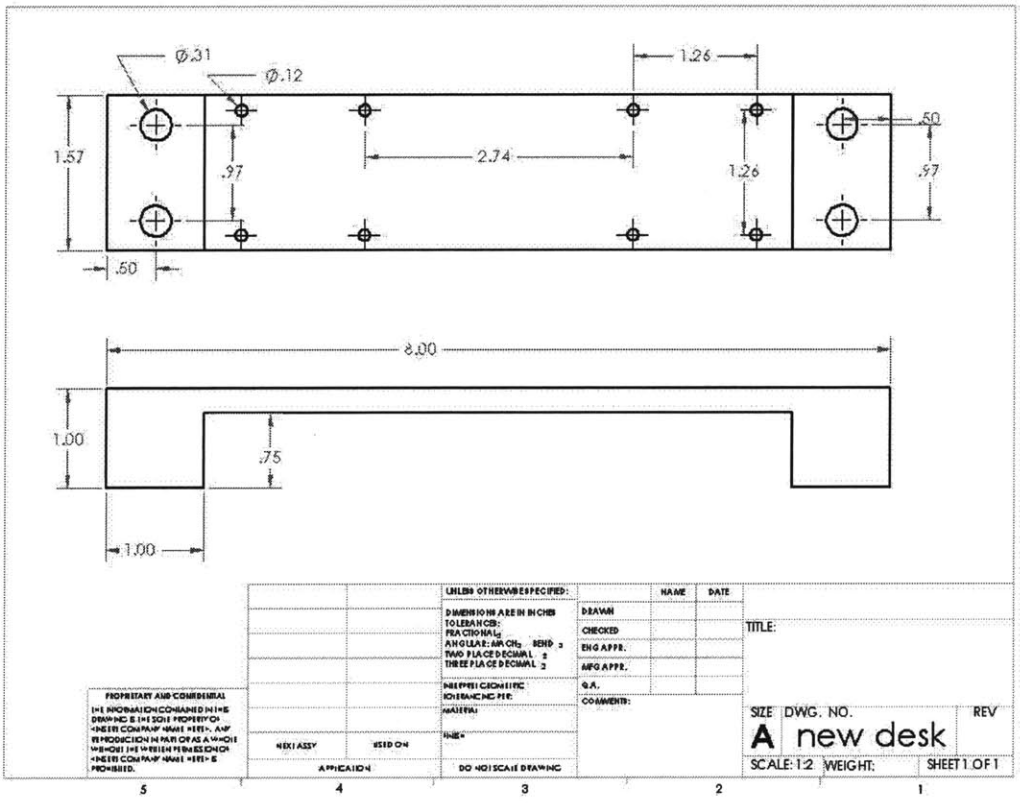

Figure 3.3.3B: Inking desk

The reason to design a desk for the inking cylinder is to leave an exit for the substrate from where it can be collected although we later changed the substrate path and no longer needed the desk.

The raw material, an aluminum block with high level surface flatness, comes from McMaster-Carr. Machining is done in LMP machine shop of MIT.

(3) X stage (Figure 3.3.3C)

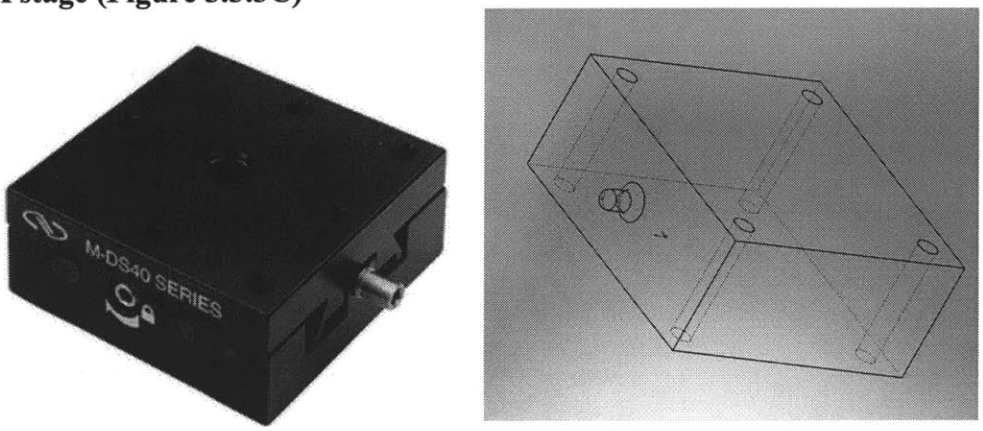

Figure 3.3.3C: M-DS40X stage

The primary function of stage is to give the machine the ability to adjust the positions of inking and impression cylinders. With the help of the pressure sensors that will be discussed in Chapter 5, the pressure control can be realized.

The prototype machine itself is compact, so a precise stage with compact shape is desired. In addition, the requirement of travel is small because the relative movement is kept in a scale of millimeter. The M-DS40X stage from Newport provides a good solution.

Taking into consideration the dimensional constrains, the load capacity of M-DS40X stage and user-friendly factor, we decided to fix the position of plate cylinder and mount inking and impression cylinder on stages. At the beginning, one stage was used for each cylinder, as shown in Fig 3.3.3D (a). After assembling the machine, we realized due to the small size of the stage, the two cylinders not well supported, and we could not adjust the parallelism of the cylinders. The final design has two stages for each cylinder. With two stages functioning separately; the pressure and parallelisms between cylinders can be independently adjusted.

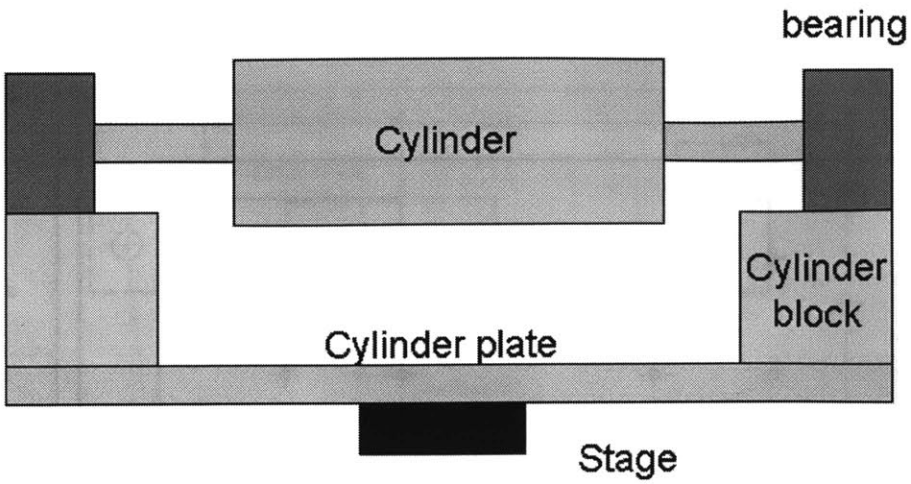

Figure 3.3.3D: Cylinder subassembly with one stage (front view)

(4) Cylinder plate (Figure 3.3.3E)

The primary function of the cylinder plate is to serve as a movable platform mounted on stages for the inking and impression cylinder. The one used for inking cylinder also provides an area to place the ink bath.

The raw material, aluminum plates with high level surface flatness, comes from McMaster-Carr and again machining is done in LMP machine shop of MIT.

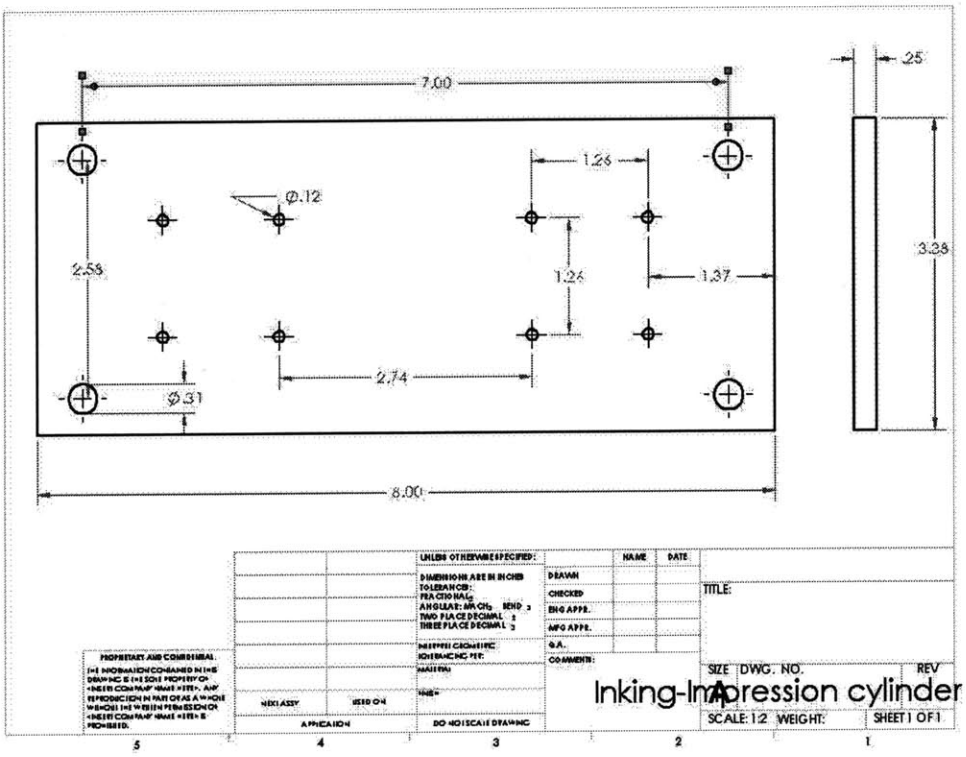

Fig 3.3.3E: Cylinder plate

(6) Cylinder Block (Fig 3.3.3F)

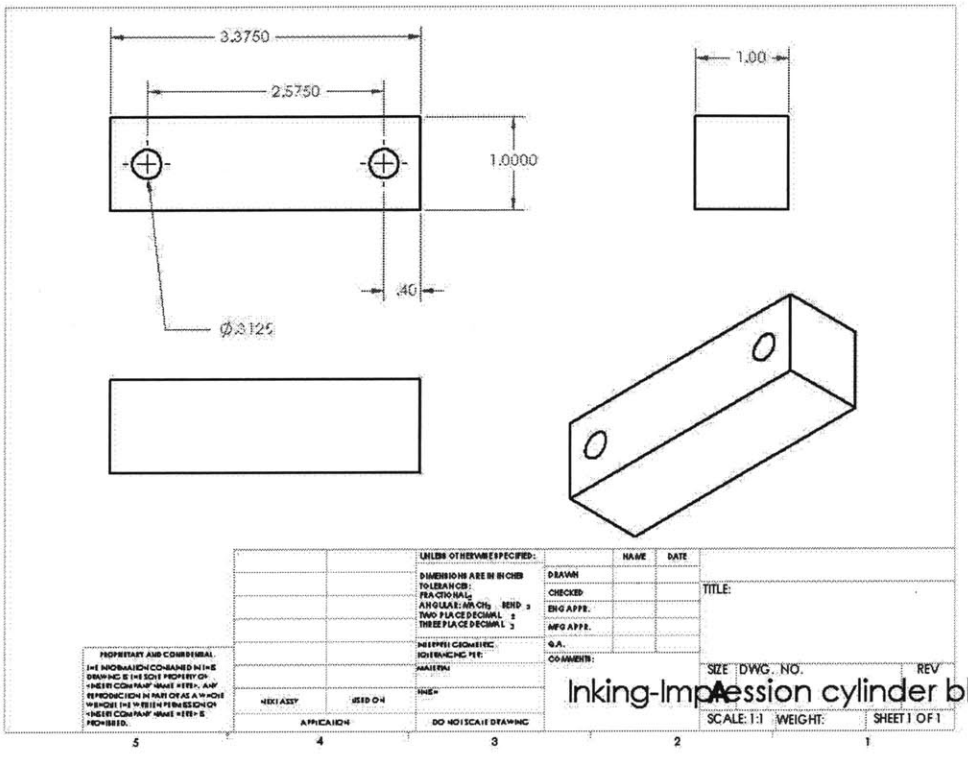

Fig 3.3.3F: Cylinder block

Cylinder blocks serve as adapters, adjusting the height of the self-aligning bearings to prevent any interference. They are made from aluminum blocks with high level surface flatness, purchased from McMaster-Carr and machined in the LMP.

(7) Motor plate (Fig 3.3.3G)

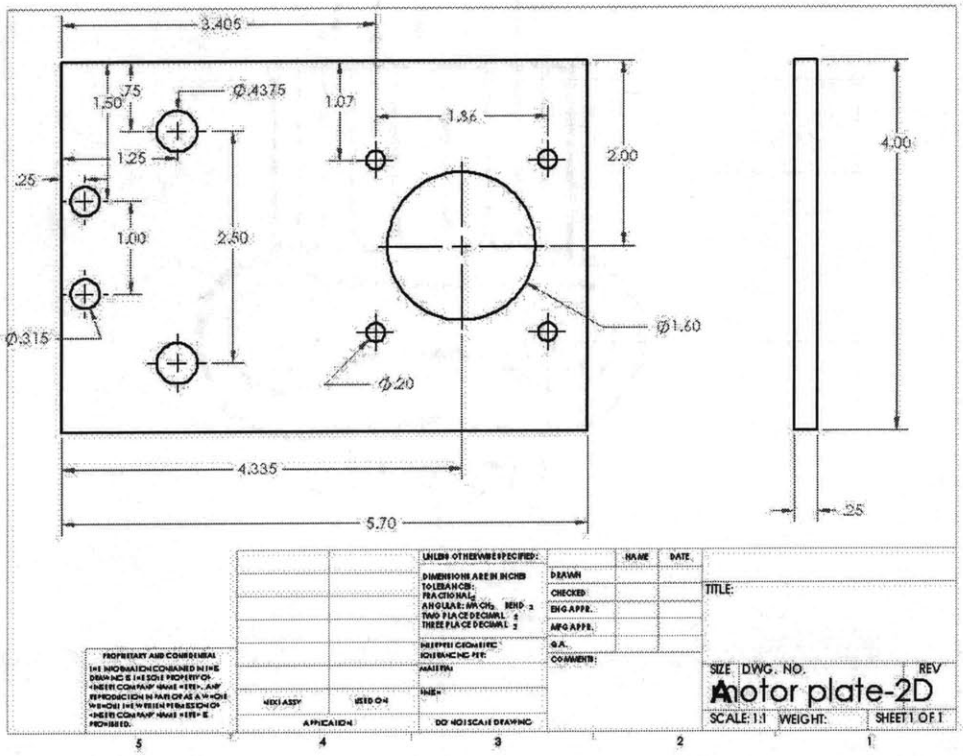

Fig 3.3.3G: Motor plate

The motor plate provides a place to mount the motor and guarantee that the motor shaft and inking cylinder shaft are concentric at their original positions.

(8) Plate cylinder block (Fig 3.3.3H)

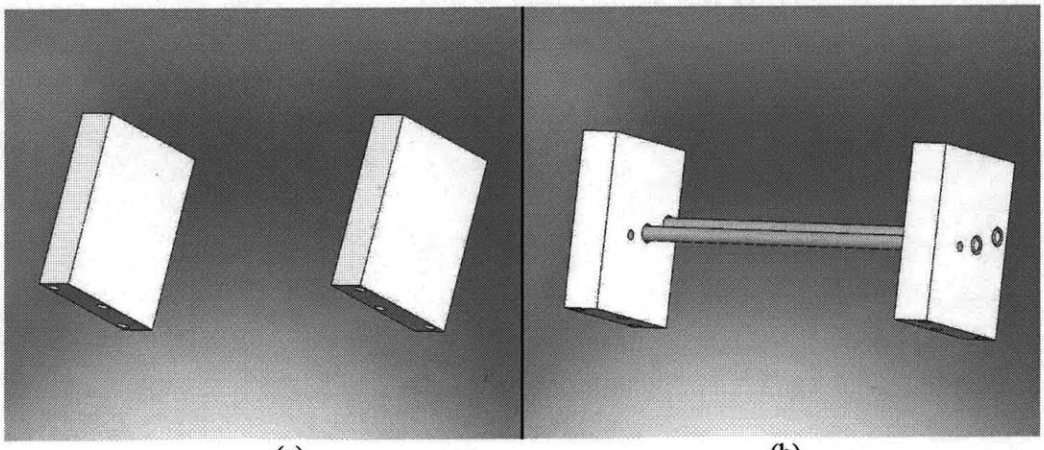

(a) (b)

Fig 3.3.3H (a) Original design of plate cylinder blocks; (b) Final version of plate cylinder blocks.

In the original design, plate cylinder blocks serve only as adapt blocks, adjusting the height of the self-aligning bearings to prevent any interference. In the final version of the machine, they also provide a method to control wrap angle, as shown in Fig (b). Please refer to Chapter 5 details.

(9) Self-aligning bearing (Figure 3.3.3I)

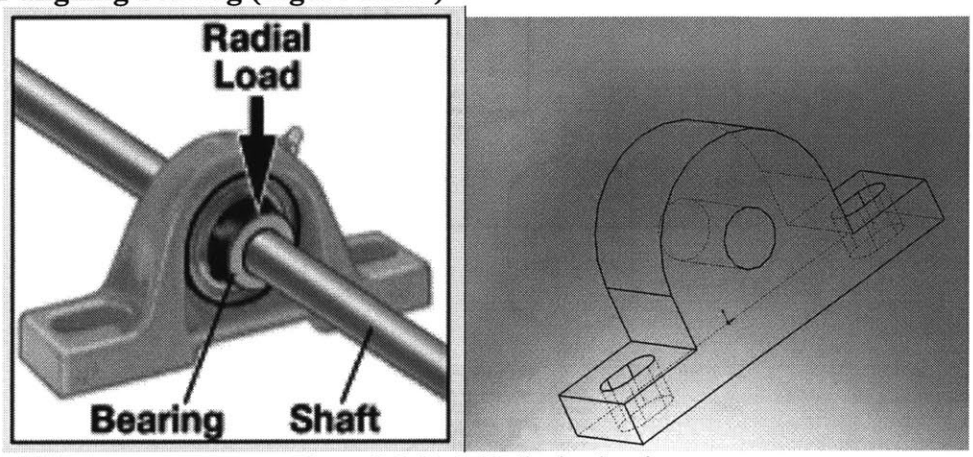

Figure 3.3.3I: Self-aligning bearing

Self-aligning bearings are ideal for conditions where misalignment can happen. Given the limitations of access to highly precise machining, we decided to use self-aligning bearing to avoid any potential problem caused by misalignment. Since the radial load and rotation speed both are low compared to the specifications of commercially available bearings, selection was based on dimensional consideration.

All six bearings, two for each cylinder are identical and purchased from Mcmaster-Carr, part number 5913K41, stamped-steel mounted ball bearing.

(10) Inking cylinder (Figure 3.3.3J)

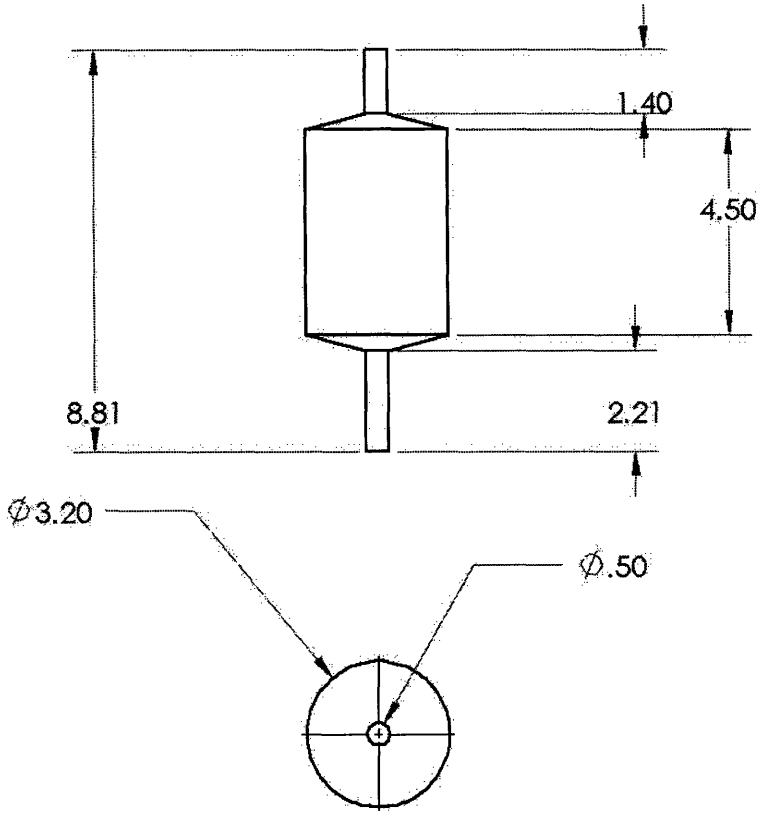

Figure 3.3.3J Inking cylinder

Inking cylinder transfers ink solution to plate cylinder and drives the whole system with the power from motor. The end with longer shaft connects to the motor.

(11) Plate cylinder (Figure 3.3.3K)

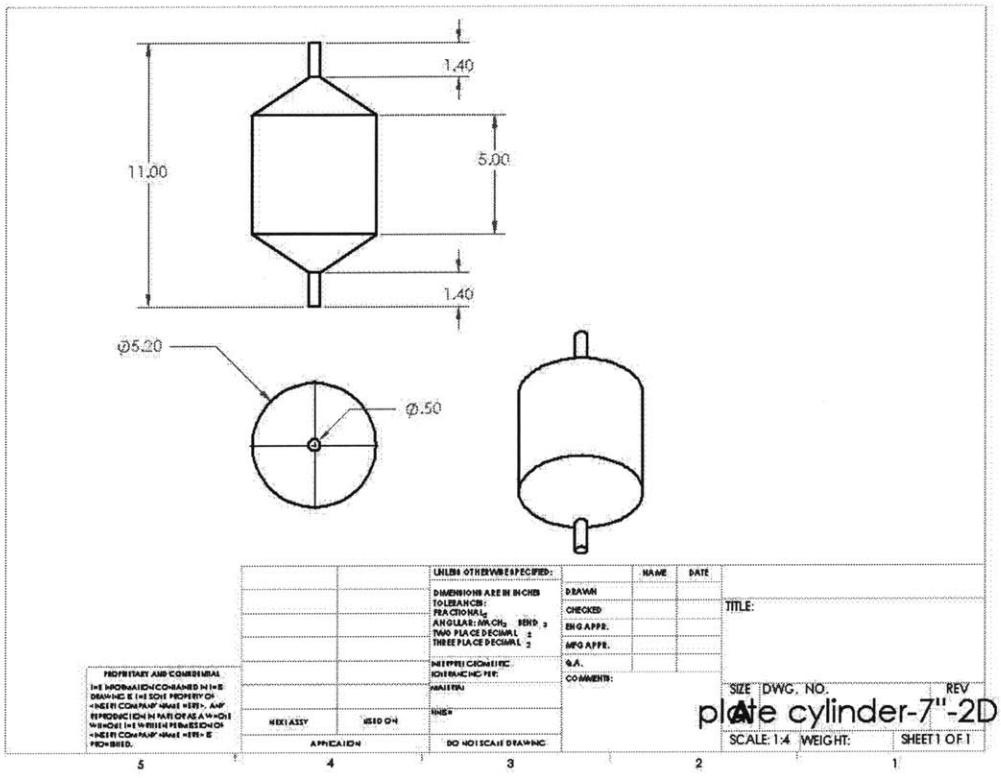

Figure 3.3.3K Plate cylinder

The plate cylinder is where the stamp is mounted. The actual printing happens between plate cylinder and impression cylinder. Ink solution is dried on plate cylinder, leaving only molecules diffused inside the stamp.

(12) Impression cylinder (Figure 3.3.3L)

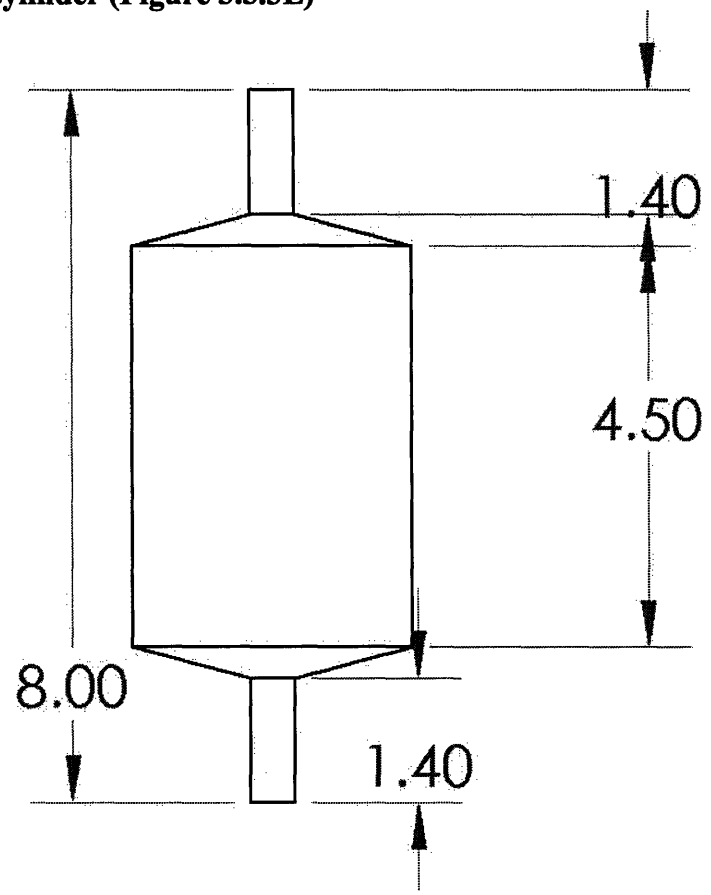

Figure 3.3.3L Impression cylinder

Impression cylinder assists printing and enables pressure control.

All the three cylinders are machined from alloy 6061 aluminum rods purchased form McMaster-Carr.

(14) Flexible coupling

Coupling is the component connects the inking cylinder shaft and motor shaft and enables transmission from motor to inking cylinder. A flexible coupling is used here to deal with small amount of misalignment.

The coupling is purchased from McMaster-Carr, part number 3084K31, machinable-bore one piece clamp-on coupling.

3.4 Conclusions

In this chapter, we described the target functions of our machine. We also discussed the development of our concept design to achieve reel-to-reel continuous microcontact printing and how the concept was realized by a working machine (Figure 3.4). Several recommendations for system improvement were presented as well. In the next chapter, we shall lead readers through a process study which covers tooling, inking and printing.

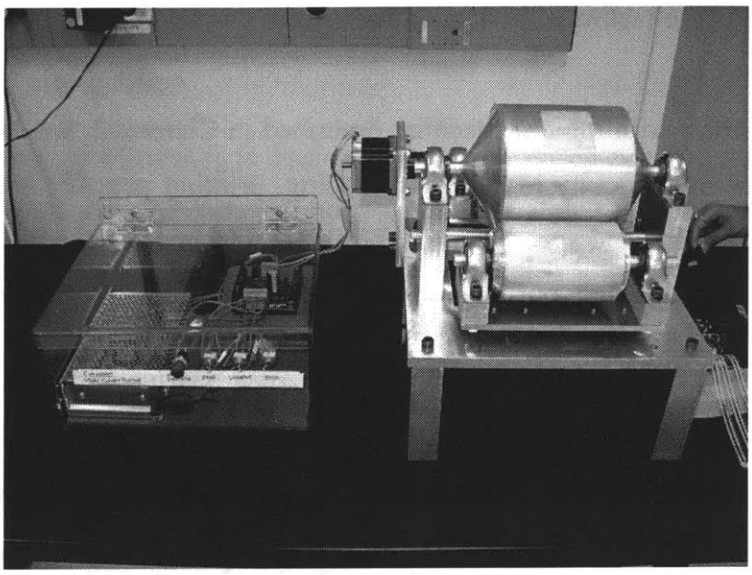

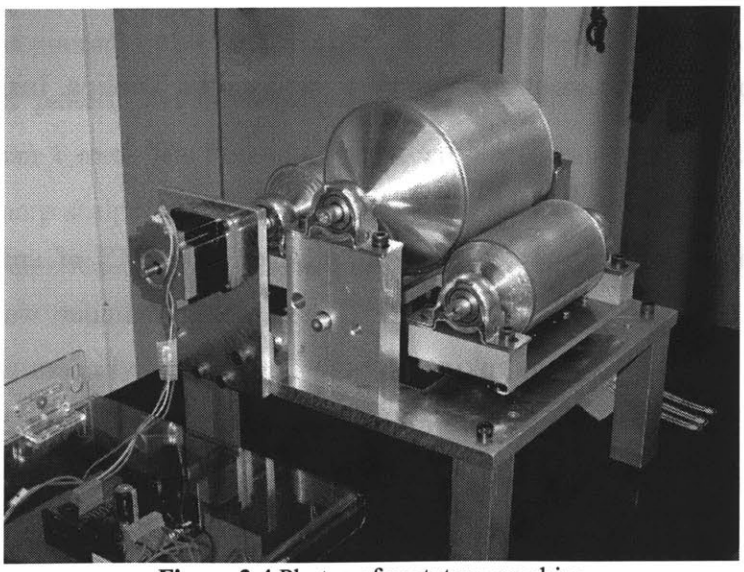

Figure 3.4 Photos of prototype machine

Chapter 4

Process Study

As introduced in Chapter 1, the objective of this project is to design and manufacture a working prototype of a micro contact-printing machine using the flexography principle to achieve a reel to reel printing of substrates. In order to attain this goal, we required a thorough understanding of the process physics of micro contact printing and flexography besides identifying the factors affecting its throughput rate and the quality of print.

While experimenting with the test machine described in Chapter 3, we experienced a lot of problems such as difficulty in substrate feeding, printing pressure measurement and control, area of printing and speed control. While troubleshooting the machine, we made several modifications to suit our requirements and make the system more robust and repeatable.

This chapter takes the reader through some of the most important pre-experiment machine setups and procedures that we standardized. Also, we describe some of the design modifications done to the system to vary the wrap angle and enable easy substrate feeding.

The printing process of this machine comprises three stages: Tooling, Inking and Printing.

4.1 Tooling

The tool used in our design was essentially a sheet of PDMS of uniform thickness, wrapped around the Aluminum Cylinder. The stamping cylinder was covered with patterned PDMS sheet while the inking and the impression cylinders were wrapped in plain PDMS casts. Maintaining a uniform thickness throughout the length of long PDMS sheets during casting was very important which not only determined smooth functioning of the machine but also the quality of print. Also, non-uniformity in the thickness of PDMS sheets prevented the cylinders from meshing properly with each other, resulting into unequal pressure exertion on different areas of the stamp. Besides uniformity, there

were other factors like air bubbles trapping in the cast, PDMS swelling, shrinkage and dust particle deposition which largely deteriorated the quality of tools.

This required us to thoroughly understand the characteristics of PDMS and its behavior while curing, and then come up with innovative but feasible ideas to cast the required PDMS tools. In the section below, we describe the stamp properties, its fabrication and several failed attempts before we figured out the right method to mount the stamps on the cylinders.

4.1.1 Stamp Fabrication

PDMS (Polydimethyl Siloxane) is basically a silicon based organic polymer which is made by mixing 10 parts of Sylgard 184 prepolymer with 1 part of curing agent. Our method of mixing, while ensuring complete mixing, also introduced many air bubbles into the mixture. The mixture was then placed in a dessicator to degas for sometime. The air bubbles raised to the surface were removed by gently blowing in air by mouth. This mixture was used to make patterned as well as plain PDMS sheets, which were used as the machine tooling.

1. **Patterned PDMS sheet for the Stamping Cylinder**

This mixture was poured onto a patterned silicon wafer placed flat and face-up in a Petri-dish. The master pattern was covered with enough liquid PDMS to obtain a stamp of thickness less than 1 mm. The Petri dish was then placed in an oven and cured at 70° C for 2 hours. A sharp scalpel was used to evenly and gently cut around the pattern and then the stamp was removed using tweezers. Figure 4.1.1A shows a stamp fabricated in this way.

Figure 4.1.1A: PDMS stamp. Pattern includes gratings and array of squares, rectangles and circles of different sizes.

For our experiments, we examined a variety of master patterns having feature sizes ranging from 500 to 2 microns with an aspect ratio of 1:10. We printed square grids, gratings, arrays of triangles, squares, circles and rectangles of varying sizes.

To ensure uniformity in thickness of PDMS casts, we used the following two mechanisms to make the curing plate parallel to the base surface.

a) Tilt stage

The curing tray was placed on a tilt stage. Levelers were placed on the tray and the tilt stage was moved until the bubbles got positioned in the center of the levelers. The tray became completely parallel to the surface as shown in the figure 4.1.1B.

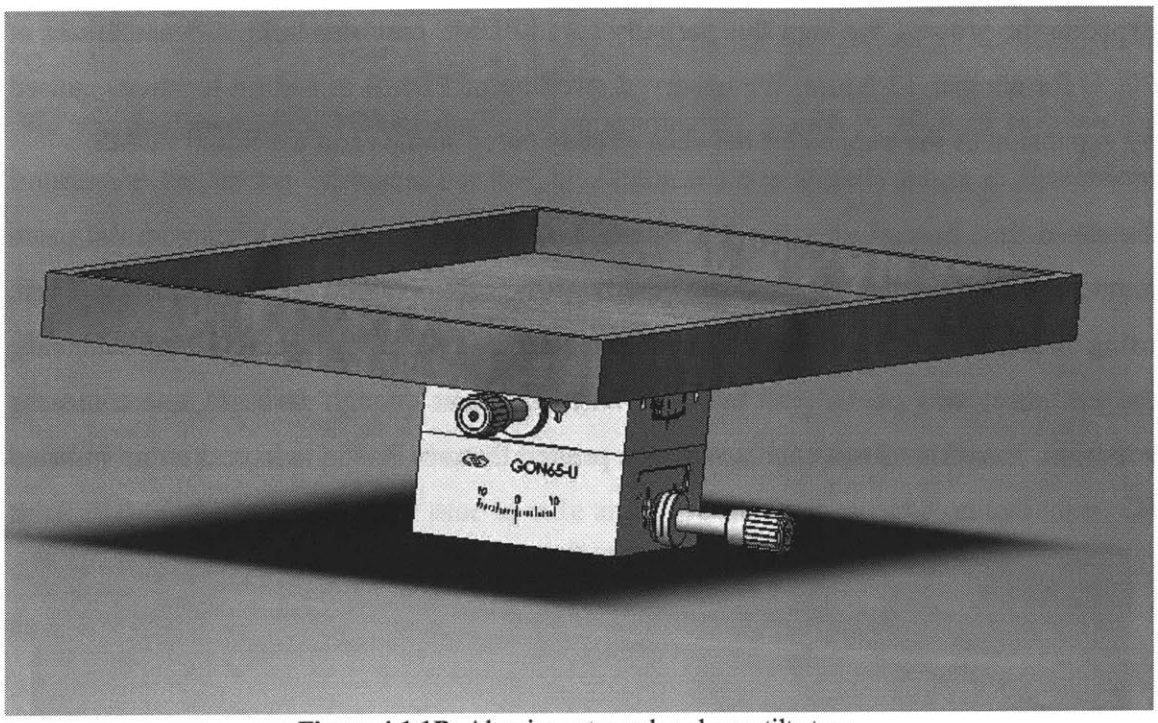

Figure 4.1.1B: Aluminum tray placed on a tilt stage.

b) Three Z stage- balls setup

Three mini Z stages were screwed onto a flat steel tool plate. Steel balls were attached on them using epoxy and on this, a curing tray was placed. The three z stages defined a plane and the balls allowed the movement of the tray as the stages was moved. The heights of the two z stages were adjusted while keeping the third one stationary. With the help of levelers, the curing tray was made parallel to the surface.

Four stamps manufactured by this process were placed face-down on to the center of an Aluminum tray in a line, making sure that they made a conformal contact with the tray and that no air was trapped between them. Then the tray was made parallel to the surface as described above. The mixture was gently poured into the tray covering the stamps. It is advisable to first start pouring the mixture on to the stamp, and then covering its edges properly. Next, the rest of the area was covered. The air bubbles on the surface were removed by gently blowing in air by mouth. The tray was left in the same position for 12 hours until the PDMS solidified but was still sticky enough to be readily peeled off. To

expedite the process, we kept this partially cured PDMS cast on a hot plate maintained at 70° C for another 12 hours. We observed swelling of PDMS in certain locations caused by expansion of the trapped air between already cured stamps and the liquid PDMS.

To avoid this, instead of using a hot plate, we allowed the PDMS to cure in the room temperature for another day and the quality of the cast obtained was much better. Then, using a ruler and a scalpel, PDMS sheet of required dimension was cut. Using two hands, the cut sheet was peeled off from the tray with just enough force to overcome the adhesion. Excessive force can damage the printed features owing to excess strain induced.

Figure 4.1.1C: Patterned PDMS sheet cured with four stamps placed in a line.

While wrapping the patterned PDMS sheet onto the printing cylinder, the following problems were experienced:

1. The stamp edges popped out from the rest of the PDMS sheet. This occurred because the liquid PDMS shrunk on curing while the already cured stamps (on which the liquid was poured) did not.
2. Wrapping of the stamp over a roller also caused deformation of the features on the stamp.

2. Plain PDMS sheets

We required two plain PDMS sheets of approximately 5 inch X 10 inch to wrap the impression and inking cylinders. For this, an Aluminum tray slightly larger in dimensions was placed on a tilt stage and sheets were cast exactly the same way as described above. The flexibility in the system to adjust the gap between the cylinders using linear stages prevented us from casting PDMS sheets of same thickness every time. However, in the present design, because of very small clearance between the inking cylinder and the ink bath underneath it, the PDMS sheet thickness could not be more than 5 mm. Also, too thick PDMS sheets took longer time to cure and were difficult to wrap on cylinders. On curing, shrinkage takes place~1% and this results into bowing of PDMS at the surface [1] as shown in the figure 4.1.1D.

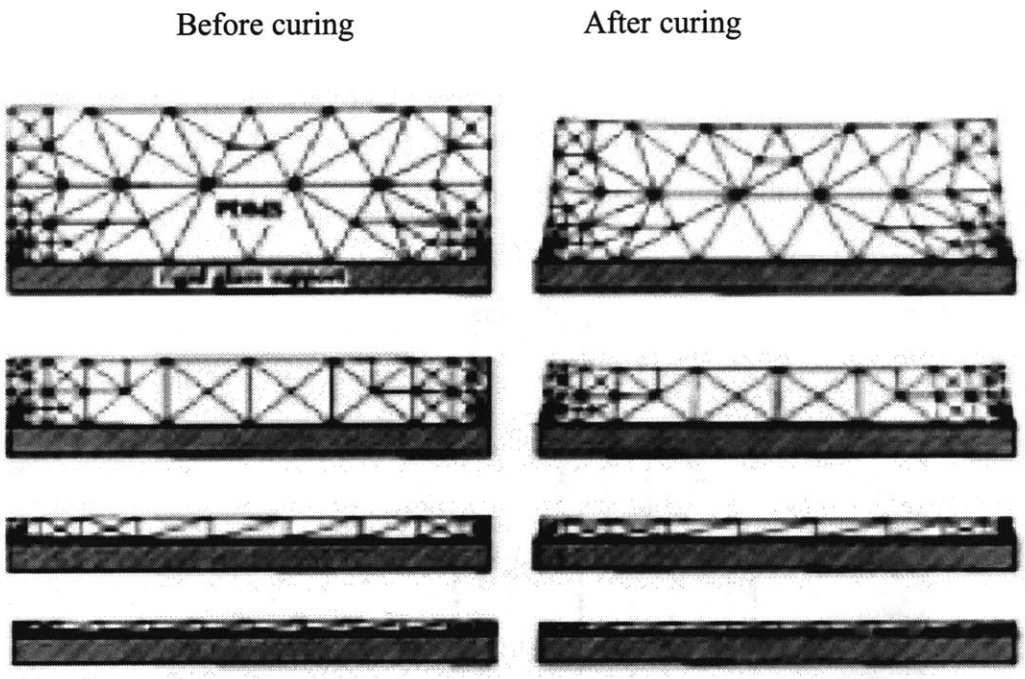

Figure 4.1.1D: Results of finite element calculations of shrinkage of PDMS tightly bound to glass. The results suggest that the elastomeric elements cast against rigid supports are bowed at the surface. The bowing disappears as the thickness approaches to zero [1].

Besides this, because of larger volume there was a greater chance of casting defects like swelling, air trapping and contamination. On the other hand, thin PDMS sheets are difficult to peel off from the tray. Accordingly, we tried maintaining the thickness of the PDMS sheets between 3 to 5 mm.

Stamp Casting Defects

PDMS stamp casting should be done in a clean room environment and on a leveled surface. Proper curing temperature of about 70° should be maintained. The following casting defects can occur if proper curing conditions are not maintained.

- Non-uniform thickness:

Non-uniformity in the thickness of the stamp results into formation of humps and depressions all over the area. This results into improper meshing of the cylinders and hence unequal pressures. Because of this, variable location printing defects like partial printing (because of low printing pressure) and collapse (because of excessive pressure) can occur.

- Localized Swelling of Stamp:

While curing the patterned PDMS sheet on the hot plate, the air trapped between the already cured stamps and the liquid PDMS expands and rises on heating. This results into swelling of the PDMS sheet in that region as shown in the figure 4.1.1E.

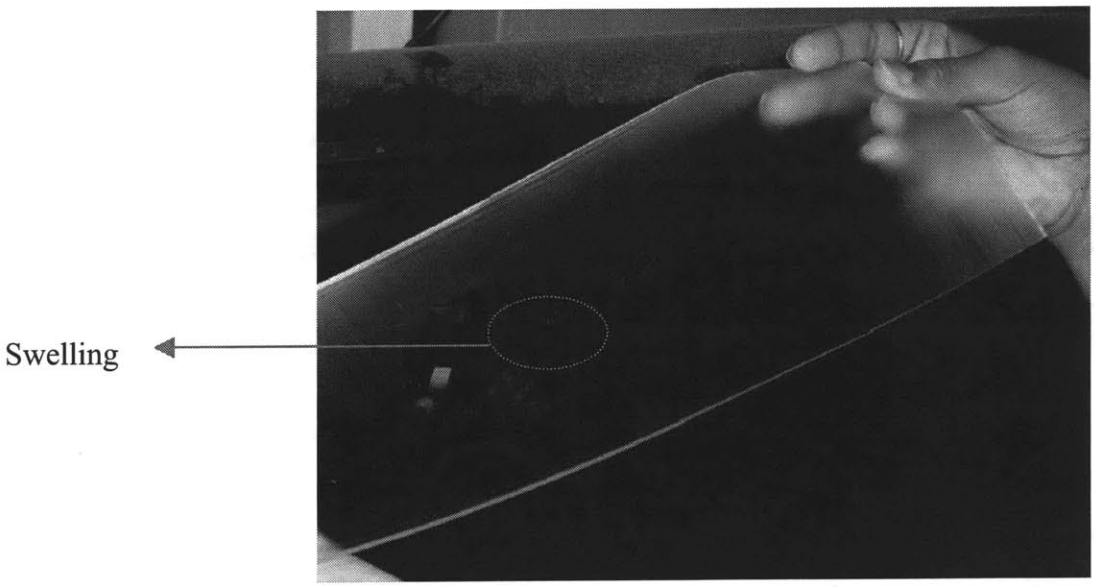

Figure 4.1.1E: Patterned PDMS sheet. The circled area shows the swelled up region on the stamp.

- Contamination with dust particles

PDMS attracts dust. The dust particles sitting on the cast stamp can result into defects like pinholes on the substrate while printing. Kindly refer to Chapter 7 for details.

- Shrinkage while curing~1%.

On curing, PDMS shrinks by 1% that can result into distortions in pattern features.

4.1.2 Stamp Mounting

Mounting PDMS sheets onto the aluminum cylinders was another challenging task. It was while conducting experiments that we got a deeper insight into the problems that arose because of improper PDMS sheet wrapping. After several iterations, we developed a standardized procedure for stamp mounting. In this section, we will describe the various methods we tried along with the causes of failure.

1. PDMS sheet with a foam backing

We tried casting PDMS on a sheet of foam having an adhesive backing for self-attachment. The foam added some extra thickness and compliance to PDMS sheets enabling easy meshing of cylinders without much movement of the linear stages. It also provided a supportive backing to the pliable PDMS stamp which prevented it from stretching while being wrapped on the cylinder. Excessive stretching induces strain in PDMS sheets damaging the stamp features. However, we experienced many problems making this method infeasible.

- Non-uniformity in the thickness of PDMS sheets.

Because of the open cell nature of the foam, unknown amount of PDMS would get into it resulting into humps and depressions all over the sheet on curing.

- Insecure PDMS sheet ends.

Though the foam backing was firmly pasted on the cylinder, the PDMS edges kept popping out, hindering smooth rotation of cylinders in mesh. We tried taping the ends

together, which increased the thickness of the closing line. This hump resulted into jerky motion of the cylinders.

- Difficulty in tool removal.

Once the stamp has been soaked in ink, it cannot be used after 12 hours because the thiol ink results into swelling and distortions of stamp features. Hence, easy removal of tool is required. In this case, the adhesive backing was too strong to be removed easily and an adhesive dissolver had to be used which was a time consuming and a non-value adding process.

- Variability

Variations in physical properties of the foam such as thickness and cell density made repeatability of the process difficult.

2. PDMS sheet with a paper backing

We even tried using paper with an adhesive backing for mounting PDMS sheets on the aluminum cylinders. A sheet of this paper was put on the liquid PDMS in the leveled tray with its adhesive back facing up. PDMS was allowed to cure this way. While mounting, similar problems like thickness non-uniformity, insecure sheet ends and difficulty in tool removal were experienced.

3. PDMS sheet with liquid PDMS as adhesive.

On the backside of the solid PDMS sheet, a thin layer of liquid PDMS was applied. The cylinder was rolled on it to evenly spread the liquid and form a uniform layer. The sheet was then wrapped on the cylinder and the ends held together and tightly taped. It was allowed to cure for 12 hours at room temperature and then the tape was removed. This method turned out to be the most robust way of mounting a stamp. The ends of PDMS sheet were more firmly secured and the tool removal became easier, cleaner and faster as it could be easily peeled off from the cylinder. Figure 4.1.2A shows cylinders wrapped in PDMS sheets using liquid PDMS as adhesive.

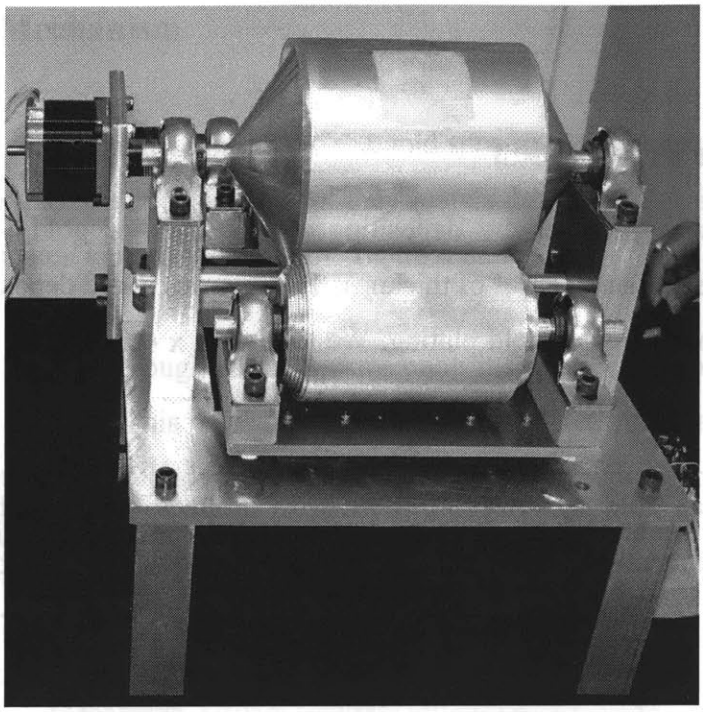

Figure 4.1.2A: PDMS sheets mounted on the Aluminum cylinders using liquid PDMS as the adhesive.

4.2 Inking

After stamp fabrication and mounting, the next step in microcontact printing is inking. Ethanol was used as a solvent to transfer the hexadecane-thiol molecules to the PDMS stamp. 10 mmol/L and 50 mmol/L thiol concentration in ethanol was used as inks. Higher the concentration of the ink molecules in ethanol, lesser is the printing time. Also, with high concentration inks, the defects in the patterns decrease.

4.2.1 The Inking Procedure

The stamp was inked by using the contact inking method. The inking cylinder was allowed to rotate over the ink bath for 10 minutes and then the all the ink was pipetted out from the ink bath. The cylinder was then dried and brought into contact with the stamping cylinder. The similar texture of both PDMS surfaces in contact helped in easy transfer of thiols. This way, the patterns on the stamp were not subjected to wetting or de-wetting by the ink, preventing the stamp distortions.

4.3 Printing

4.3.1 Substrate Preparation

The substrates were prepared by depositing a thin layer of gold (~70nm) on PET (Polyethylene terephthalate) sheet of thickness 150 microns. Gold deposition can be done by sputtering, evaporating or gold plating. We used 4cm x 4cm square substrates of for printing.

High quality, clean gold substrates are needed to produce high quality SAMs and for obtaining consistent results. Many factors influence the quality of the gold substrates and consequently the quality of the resulting self-assembled monolayers. These factors include the gold purity, substrate's roughness, cleanliness, coating method, and the treatment of the coated substrates after preparation.

Handling and Storing Gold Substrates

Utmost care was taken while handling the gold substrates to prevent the possibility of contamination. The work area and the equipment were cleaned with solvents and polyethylene gloves were worn. Clean forceps and tweezers were used to move and handle the gold coated substrates.

Although gold is chemically non-reactive, it is instantaneously coated by adventitious hydrocarbons after exposure to air. Hence, the gold coated samples were stored in sealed Petri dishes backfilled with nitrogen or argon.

Substrate Cleaning

Several methods can be used for cleaning the gold substrates after they have been stored. We cleaned by using argon plasma for 3-5 minutes. This plasma cleaning removes organic contaminants and makes the gold surface negatively charged.

4.3.2 Feeding Mechanism

To facilitate easy feeding and alignment of the gold substrate with the stamp on the stamping cylinder, the two opposite ends of the square substrate were joined to two plastic sheets by scotch tape as shown in the figure 4.3.2A.

The plastic sheet used had rough surfaces preventing it from sticking on PDMS because of the adhesive forces. This substrate sheet was then fed manually between the impression and stamping cylinders with small tension to prevent wrapping. Impression cylinder helped in attaining a conformal contact between the substrate and the stamp during printing.

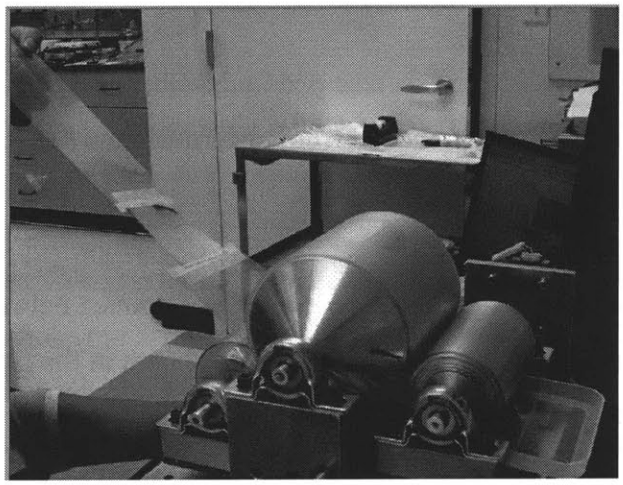

Figure 4.3.2A: The Feeding Mechanism. The picture shows the gold substrate with its ends stuck on two plastic sheets being fed between the impression and the stamping cylinders.

The fixed length of the plastic sheets, determined by the position of stamp on the cylinder helped in alignment. We also used long sheets of gold substrate in which alignment was less of an issue because of the large printing area available.

To further enhance the feeding mechanism, a few design modifications were done as described below.

For easy removal of the printed substrate a slot in the base plate was made as shown in the figure below, which gave more working space

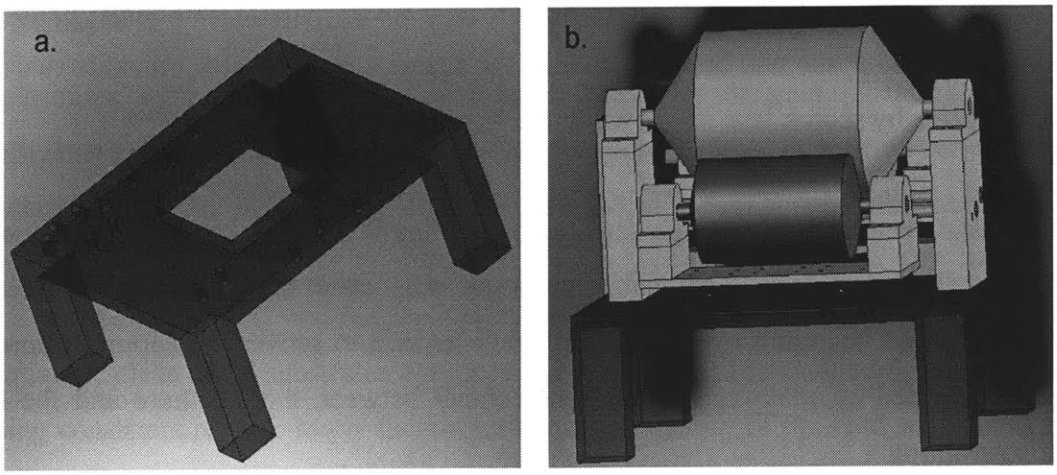

Figure 4.3.2B: a) the new design for the base plate with a square slot in the center and 4 pedestals attached. **b)** Machine mounted on the new base.

The whole setup was made to stand on four pedestals. Now, the printed substrate with plastic sheet tails could be easily removed from underneath the setup.

Print Cylinder Wrap Angle Control

Wrap angle is defined as the angle made by the area of contact between the substrate and the stamp with the center of the stamping cylinder as shown in the figure 4.3.2C.

α denotes the wrap angle.

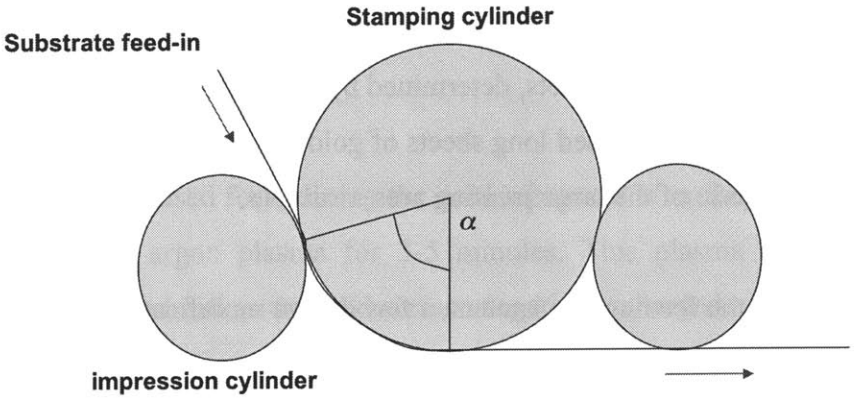

Figure 4.3.2C: Wrap angle: α denotes the wrap angle here.

To allow a variable wrap angle, 3 holes were drilled on each of the stamping cylinder blocks as shown in the figure 4.3.2D. A rod could be passed through these holes connecting the two blocks and was fixed using a C clip. Now, the gold substrate stuck on the plastic sheet was fed by wrapping one end of the sheet over this rod.

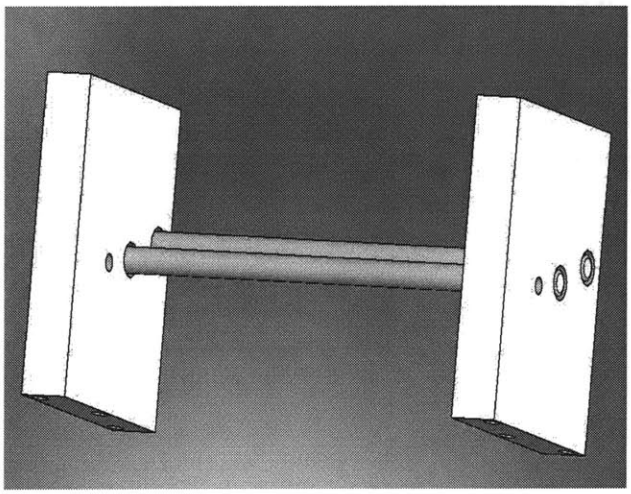

Figure 4.3.2D: Modified design of the stamping cylinder blocks. Three holes were drilled on each block to hold the rod in different positions to vary the wrap angle.

Greater wrap angle implies greater contact area. The figure 4.3.2E illustrates the feeding mechanism using the hole-rod arrangement. The three circles in red depict three different positions in which the rod can be placed. While feeding, one tail of the substrate was wrapped over this rod as shown in the figure below and proper tension was provided on both the ends of the substrate.

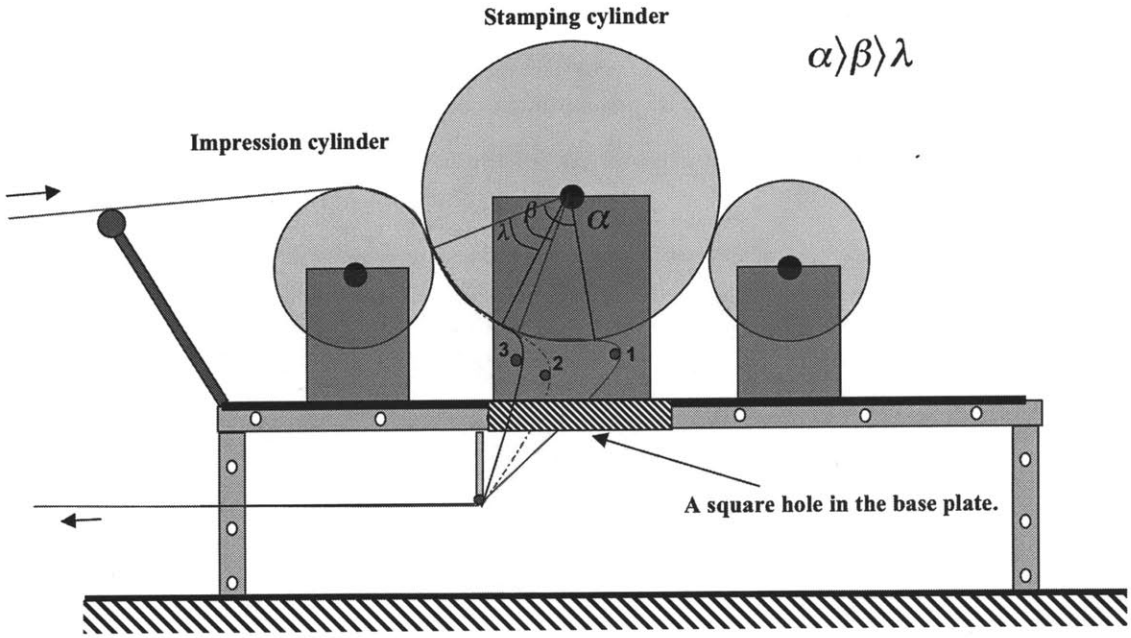

Figure 4.3.2E: The hole-rod design modification to vary the wrap angle: The circles in red depict three different rod positions used for varying the contact printing area between the substrate and the stamp.

The position of the rod determined the wrap angle. As the rod was shifted from the holes set 1 to 3, the wrap angle decreased and so did the contact printing area. It can be clearly seen in the figure above that $\alpha\rangle\beta\rangle\lambda$.

When the substrate was fed continuously using the rod number one, the wrap angle was the greatest and so was the contact area. We called this "continuous printing". When the rod number 3 was used for feeding, the contact area was the minimum. We refer to this as,"reverse printing[1]" in the rest of the chapters. Figures 4.3.2F and 4.3.2G show continuous and reverse printing.

[1] Before any modifications in the design, the substrate was pulled from the same side as feeding when the wrap angle was small, as shown in the figure above. Whereas, when the wrap angles were high, the substrate was removed from the inking cylinder side. Hence, printing with small wrap angles was called as reverse printing and with large angles as continuous printing.

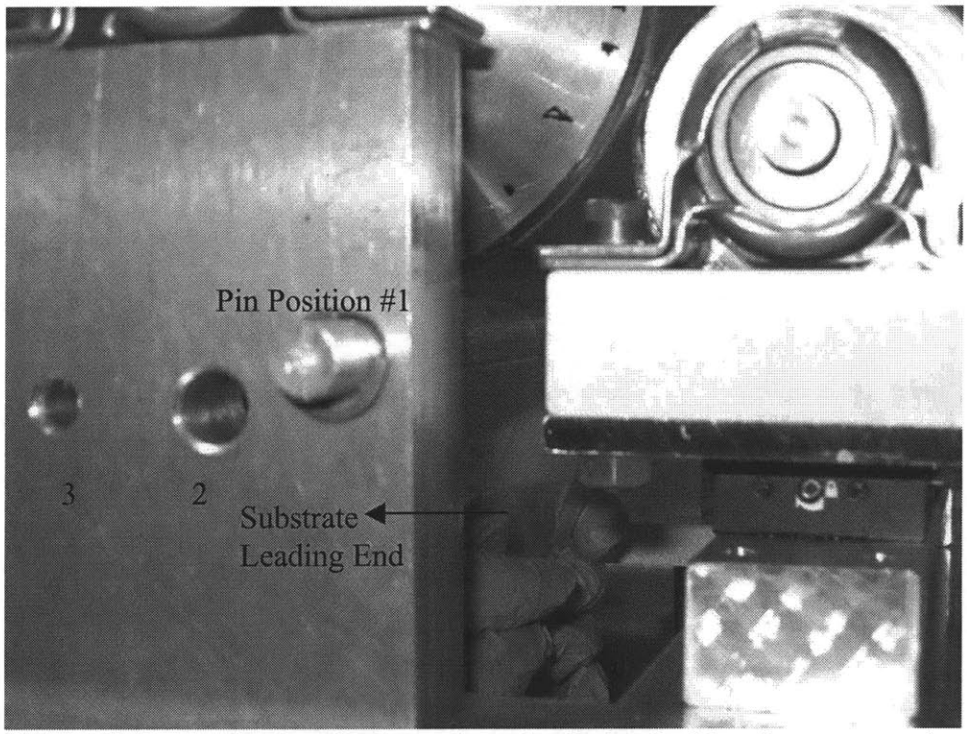

Figure 4.3.2 F: Continuous Printing: The figure shows the plastic tail of the substrate wrapped over the rod 1. The printing area is maximum here.

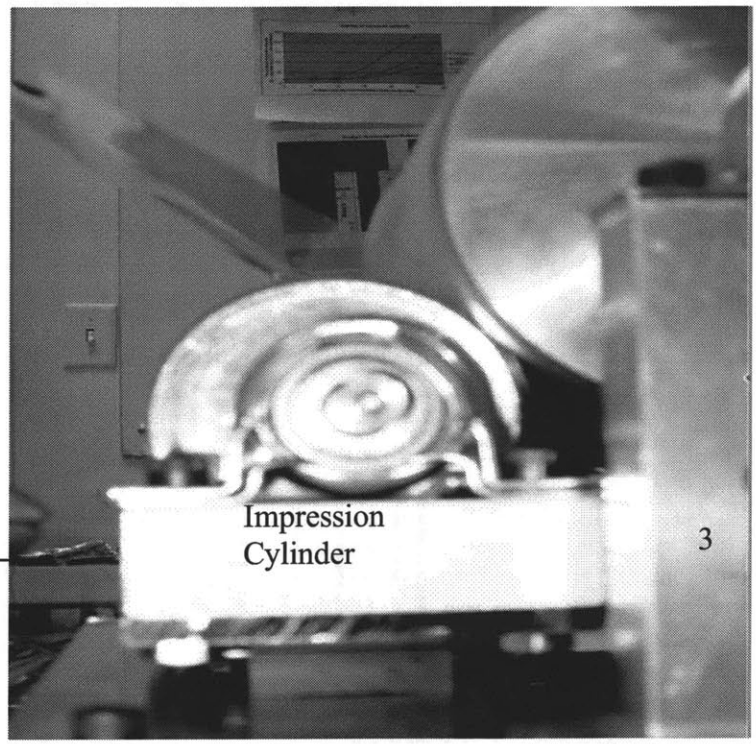

Figure 4.3.2 G: Reverse Printing: Rod 3 is being used. Notice that the contact area is much less.

4.4 Etching

The etching solution was prepared by mixing four grams of Thiourea with 1.14 grams of $FENO_3$ in 50 ml of water at 45° C. The printed substrate was held by tweezers and gently stirred for 2 minutes in this solution. The solution etched away rest of the gold leaving behind the printed portion. Picture 4.3.2H shows an etched pattern on a gold substrate.

Picture 4.3.2H: Etched Gold substrate.

4.5 Conclusion

In this chapter, we described the pre-experiment setup procedure required to conduct experiments on the lab scale flexography machine. Also discussed were the design modifications done to make the system more robust and repeatable.

To conduct experiments and get useful data, a standardized approach has to be used. In the next chapter, we will talk about the Design of Experiments Analysis done on the various input parameters to study their effect on the process output.

Chapter 5

Experimental Study of Flexography style Micro-contact Printing Process

5.1 Introduction

The primary goal of this project was to develop a machine to execute continuous micro-contact printing at a high throughput rate. From an engineering stand point, this is important for the micro-contact printing process to have a commercial value. To achieve this goal, a good understanding of the inherent chemistry of micro-contact printing and self assembly was required along with the knowledge of process parameters that contribute to both, the quality and productivity of the printed pattern. The limits of the lab scale flexography machine capability were tested through a series of experiments designed to determine the feasible parameter space. After a number of iterations, key process noises or disturbances, such as fabrication of uniformly thick stamps, flow of substrate and alignment of pattern, were realized. By minimizing these process noises, a series of experiments identified parameters for both acceptable quality and high productivity.

This chapter will take the reader through the details of the experimentation. A brief description of the experimental designs is given along with the details of the three sets of experiments that were conducted. The chapter then concludes with the complete experimental procedure that was followed during each set of experiments.

5.2 Definitions

5.2.1 Quality

A classical definition of Quality would be "Conformance to Specifications" as quoted by Philip B. Crosby in the 1980s [35]. For our experimental purpose, we gathered an understanding of these so called "specifications" from the feed back given by the company's commercial clients which are enlisted below.

As the electronics industry is most interested in this developing patterning technology, the key customer requirements are as follows

- *Position* and *Alignment* of pattern onto the substrate. This is of extreme importance in both single layer as well as multilayer patterning. Current research has demonstrated an alignment of 2 μm over a substrate of diameter 150mm [36].

- Pattern *Distortion*: Pattern distortion can be defined as the amount by which the elastomeric elements of the stamp stretches or contracts after peeling the stamp from the master and during conformal contact with the substrate. Ideally, a pattern must have no distortions but research has shown that absolute distortions as small as ~ 500nm over areas of 1 cm^2 can be acceptable. This value is dependent on the thickness of the stamp used [32].

- Pattern *Dimensions*: Pattern dimensions which generally include the size and the spacing of the features must have minimal variation. Typical standards are <1% coefficient of variation.

- Pattern *Defects*: A printed pattern is the foundation for the product obtained in subsequent processing steps. Hence, a pattern with minimum defects would result in a product with a better quality. One of the most important requirements of the

pattern is the *completeness of print*. The formation of a uniformly thick monolayer is crucial as it acts as a resist to the etching process that follows the printing.

5.2.2 Productivity

A simple definition of productivity is; the number of parts produced by a process per unit time. A typical flexography printing process has a throughput rate of approximately 2000 feet per minute [30]. The fastest rate at which micro-contact printing has been demonstrated so far is 2 centimeters per second which is approximately 4 feet per minute [4].

5.3 Experimental Objective

The objective of the experiments was to establish a relationship between printing speed of the flexography style micro-contact printing process and the quality of the printed pattern. In order to establish this relationship, first, a study of the effect of various process input variables on the quality of the printed pattern was conducted through two sets of experiments. Using these results, a third set of experiments was conducted to determine the fastest printing speed that could be achieved with the given test hardware.

5.3.1 Process Parameters

The chemistry of micro-contact printing results in a number of controllable and uncontrollable (i.e. noise) factors. Fig 5.3.1a shows a cause and effect relationship for the flexography style micro-contact printing process and fig 5.3.1b is a simple block diagram illustrating the process and the classification of the process inputs.

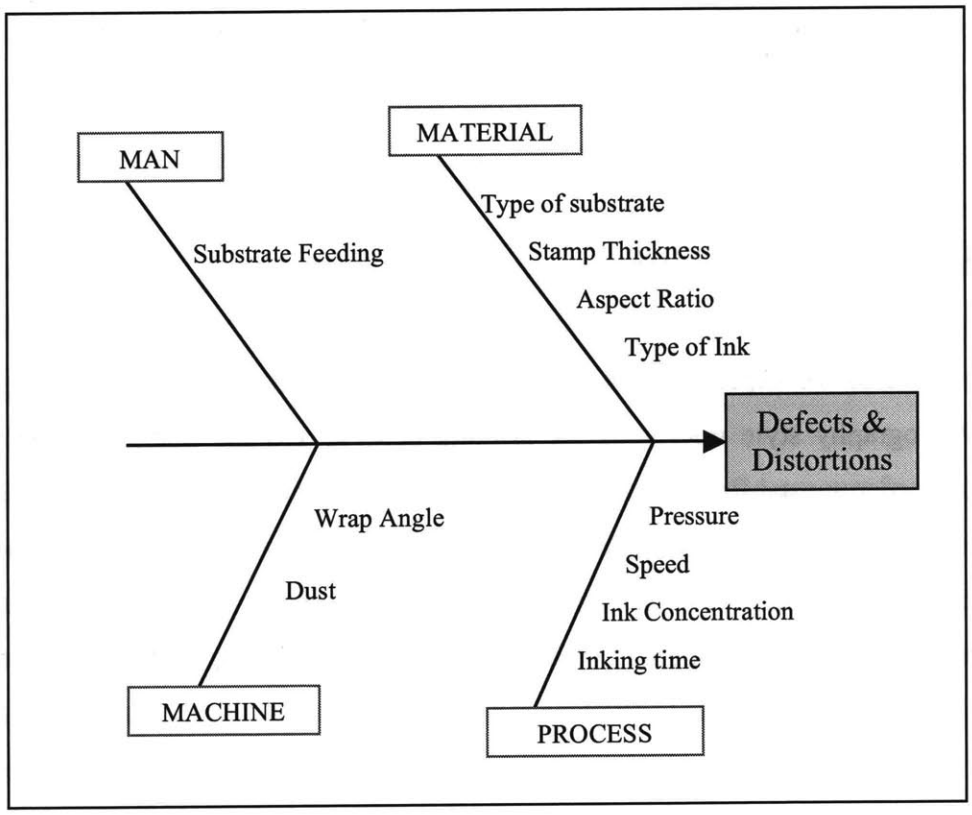

Fig 5.3.1a shows the *Cause & Effect Diagram* for the flexography style micro-contact printing process output quality. The defects and distortions in the printed pattern is caused by the factors grouped into four categories namely man, machine, material and process.

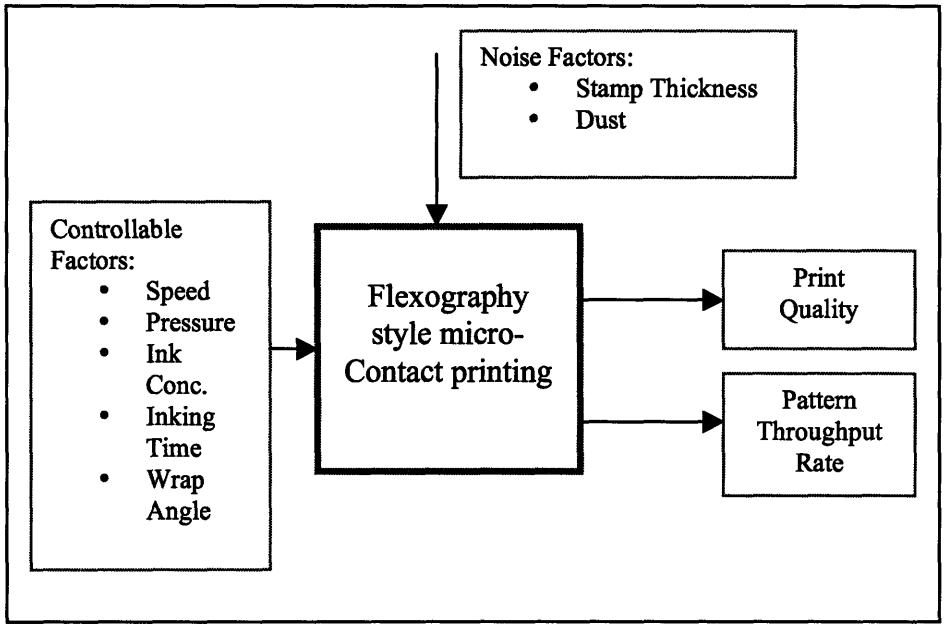

Fig 5.3.1b shows a block diagram illustrating all the variables in the flexography style micro-contact printing process. The final print quality and throughput rate of the process is dependent on these variables.

5.3.2 Output

The output of the micro-contact printing process can be characterized and analyzed in different ways. The main responses of interest are as follows:

- *Defects:* These are visual data such as the presence of 'roof collapse', 'pin holes', 'incomplete printing', 'edge definition' and 'corner definition'.

- *Distortions:* Distortions are defined as the change in the position and orientation of the printed pattern with reference to the master pattern.

- *Dimensional Error:* The dimensions of the printed features and their spacing on the substrate as compared to the specified dimensions of the feature size and spacing.

  The different types of patterns that were printed and their specifications are given below in table 5.3.2:

Pattern	Line Width/Diameter	Spacing
Grid	25 μm	250μm
Grating	10μm	5μm to 150μm
Large Dots	400μm	50μm
Dot Arrays	5μm to 150μm	50μm

Table 5.3.2 gives the dimensional specifications of the different patterns which were printed in the experiments.

5.3.3 Inputs

A brief description of some of the input variables that have a significant effect on the process outputs defined above is given below [6].

- *Type of Substrate*

The type of substrate affects the formation of the Self Assembled Monolayer. Gold is the popular choice as it is the most studied and available easily in the form of thin films. For our experiments, we used gold substrates of size 3cm x 3cm and a thickness of approximately 200 μm.

- *Type of Ink*

The "ink" or in chemical terms the *adsorbate* and its affinity to the composition of substrate is critical to the formation of a good monolayer. *Thiols* have the most affinity to gold substrates and in particular *Hexadecanethiol* (HDT) forms the most protective monolayer to a subsequent etching process [7]. This was the choice of *adsorbate* for experimental purposes.

- *Type of Solvent*

The adsorbate is required to be dissolved in a solvent in order for it to be in a liquid state. Experimental studies show that the type of solvent influences the quality of the print as they affect the kinetics of formation of the self assembled monolayer [6]. Ethanol was the solvent used for the experiments as it enables an organized formation

of self assembled monolayers and also prevents swelling of the stamp unlike in the case of non polar organic solvents.

- *Ink Concentration*

Ink concentration is expressed in Milli-Molars (mM) is the concentration of the adsorbate molecules in the solvent. It is an important factor as it affects the formation of the monolayer and thus the quality of the printed pattern

- *Stamp Thickness*

The thickness of the stamp directly relates to the distortions in the printed pattern. A thin stamp of the order of a few hundred microns thick is preferred to a thick stamp (few millimeters thick) as it will impart less distortions to the print [8].

- *Aspect Ratio*

Aspect ratio of the features on the stamp is defined as the ratio of the width of the feature to its height. Aspect ratio is important as it leads to defects in the printed pattern termed as "roof collapse" [9].

- *Printing Pressure*

Printing pressure is a significant factor in the flexography style micro-contact printing as a certain amount of pressure is required to ensure conformal contact between the stamp and the substrate. The dimensional quality of the printed pattern is believed to be affected by the printing pressure.

- *Speed*

Speed is a parameter that determines the throughput rate of the process. As our prime experimental goal is to determine the maximum throughput rate that can be achieved with the given set up, it is an important parameter for the study.

- *Wrap Angle*

Wrap angle is a factor that determines the time taken for the substrate to flow through the machine system. As described in chapter 4, a change in wrap angle changes the substrate flow from continuous flow to reverse flow or vice versa. Wrap angle affects the output quality of the pattern because it sets the time for which the substrate is in contact with the stamp.

- *Inking Time*

This factor is inversely related to the Ink concentration. Experimental studies conducted by researchers show that lower the ink concentration, higher should be the inking time for the proper formation of self assembled monolayers [6].

5.4 Experimental Design

With the given resources and timeline for the project, we aimed at mainly testing a feasible input space for the lab-scale flexography machine. The experiments which were conducted were more of "Screening Experiments" rather than those that enable us to improve or optimize the process.

Only two factors namely, *Speed* and *Pressure* were chosen as the controllable input variables. The use of a stepper motor limited the range of speeds that could be experimented with. Low range of speeds from 4 rpm to 100 rpm was tested. Pressure values ranged from 3 psi to 15 psi depending upon the uniformity in the stamp and PDMS sheet thickness which was wrapped around the cylinders. Prior knowledge about the relationship between ink concentration and inking time [6], led us to conduct the three different sets of experiments with two different values of these factors thus having them constant within each set. Care was also taken during stamp fabrication to maintain a constant aspect ratio of 0.1 (1:10) throughout the experimental phase. Gold was the substrate and the ink was Hexadecanethiol (HDT) dissolved in ethanol. Stamps were cast as described in chapter 4. Since the thickness and uniformity of the stamps were a challenge to control, it was considered as the noise variable. Table 5.4 gives details of the experimental design.

Parameter Classification		
Constant	Variable	Noise
Aspect Ratio	Speed	Stamp Thickness Dust
Substrate (Gold)	Pressure	
Ink (HDT)		
Solvent (Ethanol)		

a)

Constant Parameters	SET1	SET2	SET3
Ink Concentration	10mM	50mM	50mM
Inking Time	15 minutes	7 minutes	7 minutes
Pattern Type	Grid	Grid	Pattern
Wrap Angle	Small	Large	Small
Replicates	2	2	2

b)

SET	TRIAL	Speed (rpm)	Pressure (psi)
1	1	4	6
	2	25	6
	3	4	15
	4	25	15
	5	10	8
2	1	10	3
	2	50	3
	3	10	8
	4	50	8
	5	25	5
3	1	10	3
	2	50	3
	3	100	3
	4	25	3

c)

Table 5.4 gives the experimental design and the input space tested. a) Shows a classification of the parameters into constant, controllable and noise factors. b) Gives values of the constant parameters for each set of experiments. c) Gives the experimental design for each set of experiments.

5.5 Experimental Procedure

The following flowchart depicts the procedure which was followed for each set of experiments.

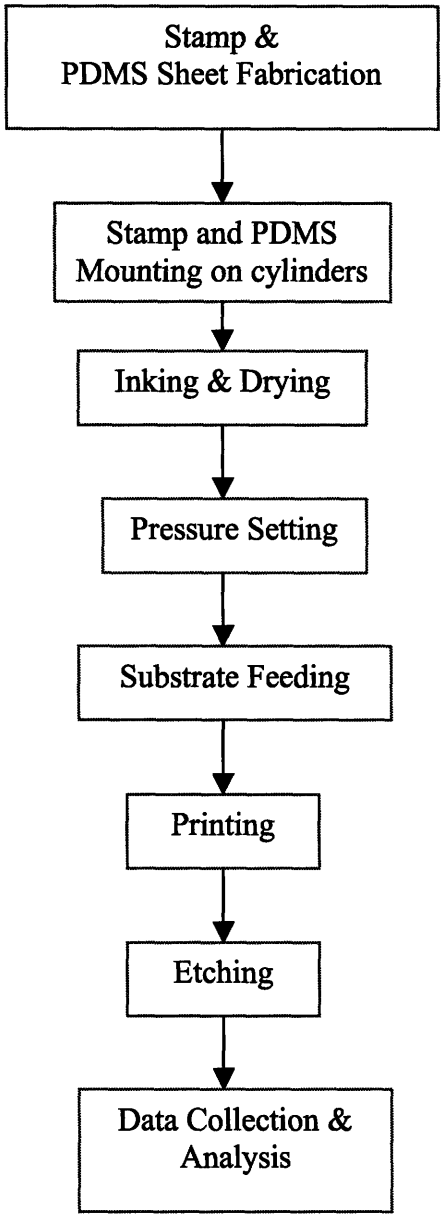

Fig 5.5 is a flowchart showing the complete experimental procedure followed while conducting experiments.

5.6 Conclusion

This chapter gave the reader a description of the experimental approach that was taken and the details of the variables and conditions applied during experimentation.

The next chapter discusses how actual changes in speed and pressure control were achieved during experimentation followed by chapter 7 which explains the analyses of data collected.

Chapter 6

Process Parameters and their Measurements

In the previous chapter, we talked about the input parameters that affect the final output of the machine, which in this case is the quality of the print. The two most important input parameters identified were speed and printing pressure. A stepper motor-driver was selected that could drive the machine at different with sufficient loss. For measuring the printing pressure between the impression and the inking cylinder, three Flexi Force [37] thin film sensors were used.

This chapter will take the reader through the important characteristics and specifications of the stepper motor and the pressure sensors used in this design to measure the input parameters. We will also talk about the integration of the pressure sensors with the PBASIC stamp to get a real time output data and their calibration.

6.1 Stepper Motor and Driver

The stepper motor (US Digital MS23C [38]) was connected to the inking cylinder shaft using a flexible coupling and was used to rotate the cylinder at different speeds. As the inking cylinder rotated, the other cylinders were also driven because of friction. A stepper motor was preferred over a servo motor because of simplicity and cost. It was basically a bipolar motor giving us the flexibility of choice between a range of high and low speed operations. Table 6.1A gives the important specifications of this motor. The technical data sheets have been given in Appendix A.

Parameter	Value
NEMA size	23
Full step angle	1.8 degrees
Full step accuracy	+-5%
Full Step Current	3.00 Amp
Micro Step Current	4.20 Amp
CD Resistance	0.85 ohms
Inductance	1.73 mH
Power Total	15.3 Watts
Holding Torque (static torque)	140 oz-in
Running Torque	110 oz-in

Table 6.1A: MS23 Stepper motor specifications. Source: USDigital [38].

The present design required us to drive the inking cylinder at various different speeds. High torque was required to overcome the friction between the meshed cylinders wrapped in PDMS sheets. This stepper motor was already configured for a bipolar parallel mode, that is, both coils of the two phases were connected in parallel to ensure maximum torque at high speeds.

The torque of a stepper motor is directly proportional to the current flowing through the motor coils. The current must ramp up to +100%, then -100% 50 times per revolution (200 quadrature states for a stepper motor of 1.8 degree step angle). At higher speeds the current does not have enough time to ramp up to maximum. Before it reaches the maximum, it must reverse and go in the other direction. Since the maximum rate of current change is inversely proportional to the square of the inductance, high speed with minimum torque loss can be obtained by minimizing the coil inductance. Compared to a bipolar series mode, bipolar parallel mode has one fourth the inductance because both coils of either phase are connected in parallel. Therefore, a stepper motor in bipolar parallel mode gives better torque performance at higher speed compared to a stepper motor operating in bipolar series mode.

The speed-torque characteristics[1] of the stepper motor are shown below.

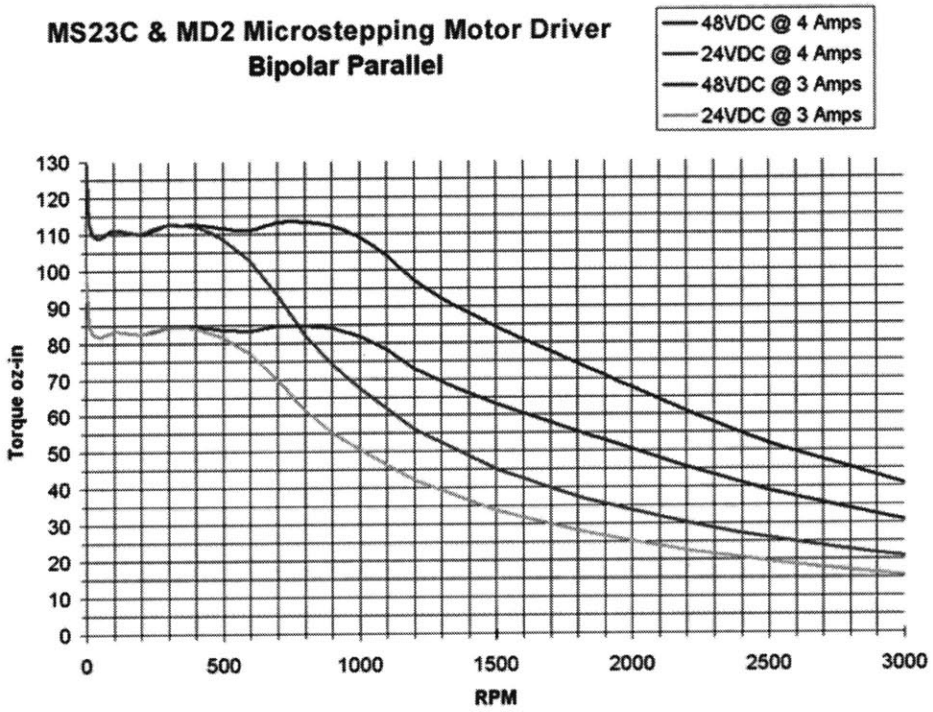

Fig 6.1A: Speed-torque characteristics for the Motor. Source: USDigital [38]

Besides the stepper motor itself, any stepping motor system requires a Driver (or Amplifier) that converts the controller command signals into the power necessary to energize the motor windings.

We used the MD2S-D (Digital Speed Control Version) programmable micro-stepping (uses 51200 microsteps per revolution) motor driver having 4 digital inputs and 8 DIP switches providing the ability to ramp up and down, run slow or fast, and reverse directions. The table 6.1B shows the different low and high speeds at which the motor could be run using this driver.

[1] As supplied by the vendor: USDigital (www.usdigital.com)

Code	RPM	RPS	2 SW3	1 SW4	0 SW5
0	4	0.07	↓	↓	↓
1	10	0.17	↓	↓	↑
2	25	0.42	↓	↑	↓
3	50	0.83	↓	↑	↑
4	100	1.67	↑	↓	↓
5	200	3.33	↑	↓	↑
6	300	5.00	↑	↑	↓
7	360	6.00	↑	↑	↑

Code	RPM	RPS	2 SW6	1 SW7	0 SW8
0	480	8	↓	↓	↓
1	600	10	↓	↓	↑
2	720	12	↓	↑	↓
3	900	15	↓	↑	↑
4	1200	20	↑	↓	↓
5	1500	25	↑	↓	↑
6	1800	30	↑	↑	↓
7	2100	35	↑	↑	↑

Table 6.1B: Low and High speeds. Source: USDigital [38].

Figure 6.1B shows the layout of the acquired driver with its key features and integration with the motion controller and the motor.

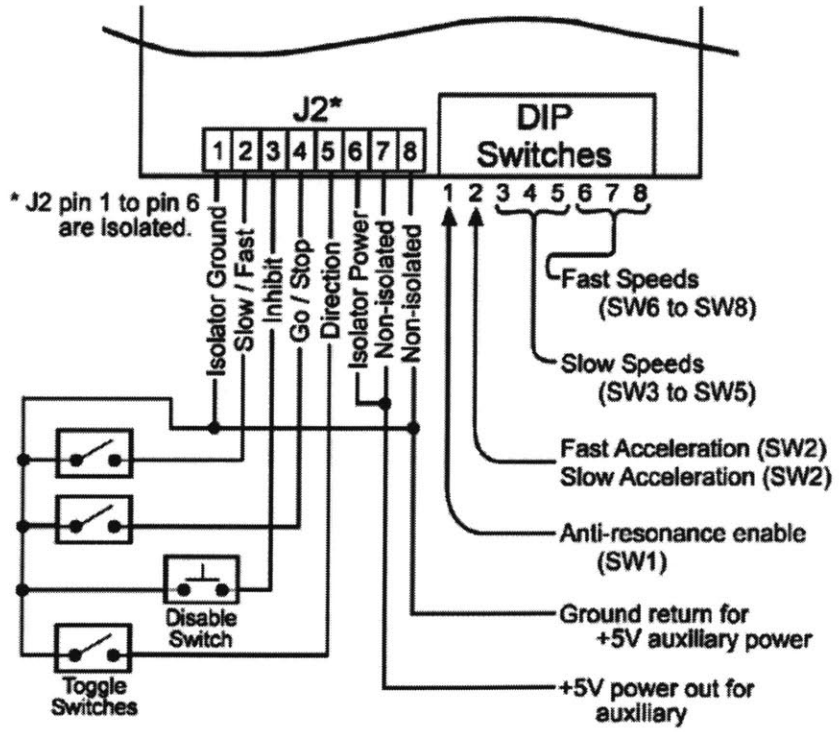

Fig 6.1B: The layout of the acquired driver MD2S-D. Source: USDigital [38].

6.2 Printing Force Measurement

Again give a data sheet reference for all of this.

The force between the stamping and the feeding cylinders was measured by using a Flexi Force Sensor A201-1 having a force range of 0-1 lb. It is a flexible printed circuit, having a circular sensing area (~0.0986 in^2) on its tip, The Flexi Force specifications have been listed in the table below. Further details can be found in Appendix A.

Physical Properties	**Typical Performance**
Thickness 0.005" (0.127 mm)	Linearity (error) < ±5% (Line drawn from 0 to 50% load)
Length 8.000" (203 mm)	Repeatability < ±2.5% of Full Scale (Conditioned Sensor, 80% of Full Force Applied)
Width 0.55" (14 mm)	Hysteresis < 4.5 % of Full Scale (Conditioned Sensor, 80% of Full Force Applied)
Active Sensing Area 0.375" diameter	Drift < 3% / logarithmic time (Constant Load - 25 lb.)
Connector 3 pin post connector	Operating Temperature 15°F – 140°F (-9°C – 60°C)

Table 6.2A: Flexi Force Specifications: Source: Technical Data Sheet-Tekscan Inc. [39].

The flexiforce single element force sensor acts as a resistor in an electric circuit. When the sensor is unloaded, its resistance is very high. Resistance decreases when force is applied to the sensor. The conductive leads are easy to connect to a breadboard or through-hole area. The Flexiforce has an ideal output for A/D conversion - 0V is no force and 4.2V is 100 lbs. We connected the sensor in a resistor/capacitor discharge time measurement circuit on the Parallax Basic Stamp 2 breadboard [39] as shown below.

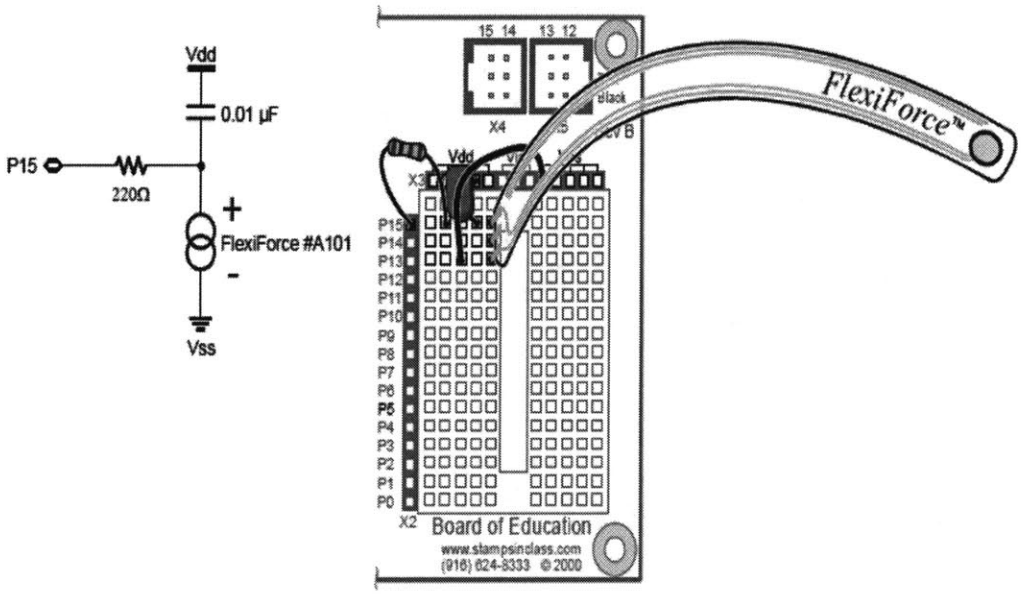

Fig 6.2A: Resistor/capacitor discharge time measurement circuit on the Parallax Basic Stamp 2 breadboard. Source: Flexiforce Demo Kit [37].

A code was written using RCTIME command with a lookup table to monitor the sensor, which acted like a variable resistor on application of load in an RC-time circuit and the discharge time, was calculated. With a capacitance of .01µF, the discharge time was as low as 1500 µs. Using PBASIC programming, the RCTIME numbers were scaled to resistance values by performing some mathematical operations. Real-time streaming data from the sensor was obtained by using StampDAQ which is an Excel 2000 (or greater) add-on.

The code in the BASIC Stamp 2 module was run. Then, the experimental circuit was connected to the PC with a serial cable and StampDAQ Excel add-on was started. The BASIC Stamp was reset and we obtained the real time resistance values into Excel spreadsheet. A snapshot of the excel sheet has been shown below.

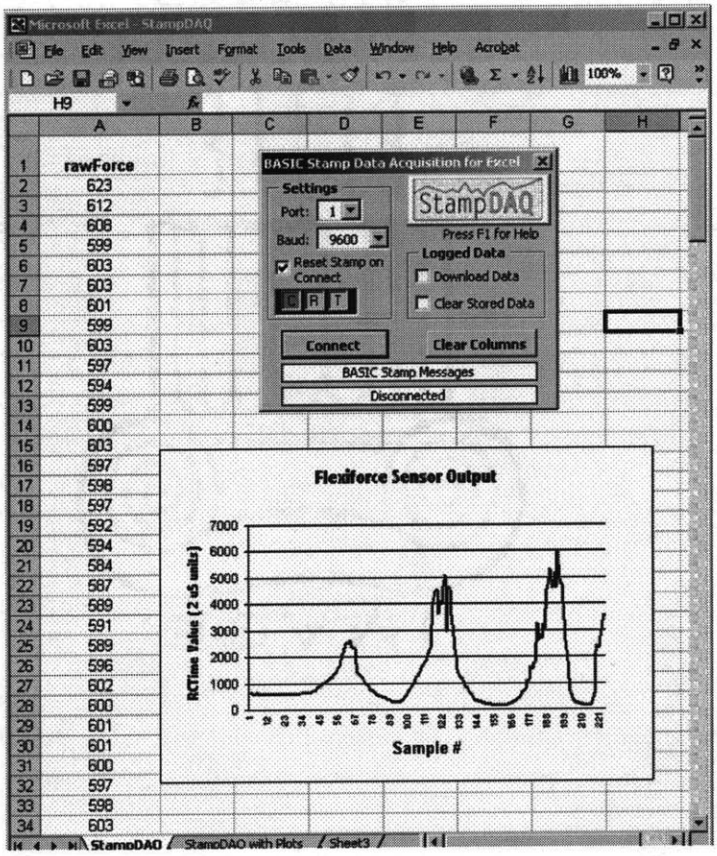

Fig 6.2B: Snapshot of StampDAQ Excel sheet used for displaying real time output data.

6.2.1 Sensor Loading Considerations

The following points were taken into consideration while sensor loading.

1. The applied load was distributed evenly across the sensing area to ensure accurate and repeatable force readings.
2. The sensor was loaded in the same way each time.
3. The entire load path was used as the sensing area and we made sure that no load was supported by the area outside it.
4. The Flexiforce sensor was placed between the cylinders in such a way that the force was perpendicular to the sensor plane to get accurate readings as shown in figure 6.2.1A.
5. To protect the sensor from shear forces, it was covered with tape. This also added to the thickness of the sensors.

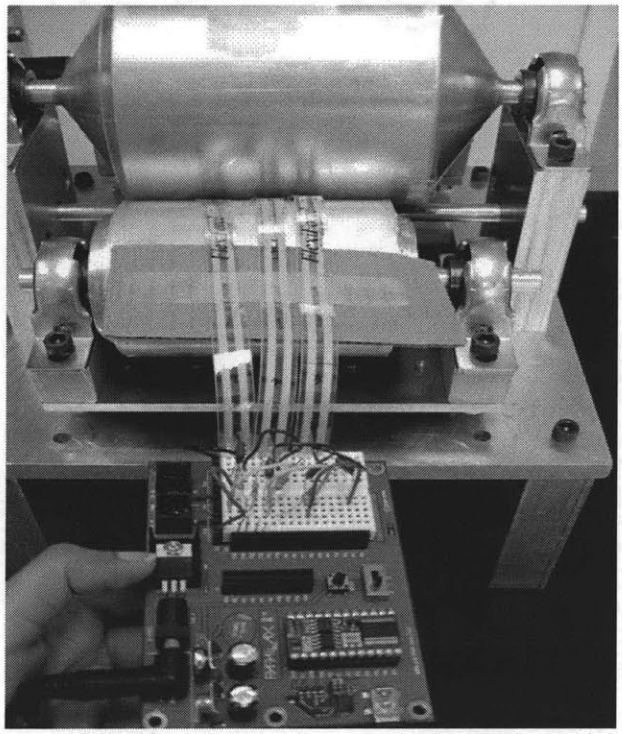

Figure 6.2.1A: Placement of Flexiforce Sensors between the impression and the stamping cylinders.

6.2.2 Calibration of Sensors

Calibration was required to relate the sensor's electrical output to force values. In our design, we used 3 flexiforce sensors to measure the printing pressure and ensure uniform force across the printing area. Prior to calibration, sensors were properly conditioned to lessen the effects of drift and hysteresis. 110% of the test weight was applied on the sensor placed on a PDMS piece. It was allowed to stabilize and then the weight was removed. The process was repeated four to five times.

Procedure

1. A known force was applied to the sensor and the sensor resistance output was equated to this force.
2. This step was repeated with a number of known forces. Kindly refer to the appendix for the collected data.
3. For the given sensing area of the sensor (~0.0986 in^2), corresponding pressure values were calculated and plotted against the resistance values.

4. Using regression analysis, best fits were obtained as shown in the graphs below.
5. Using the obtained equations, we are able to calculate the actual pressure values corresponding to the sensor output range.

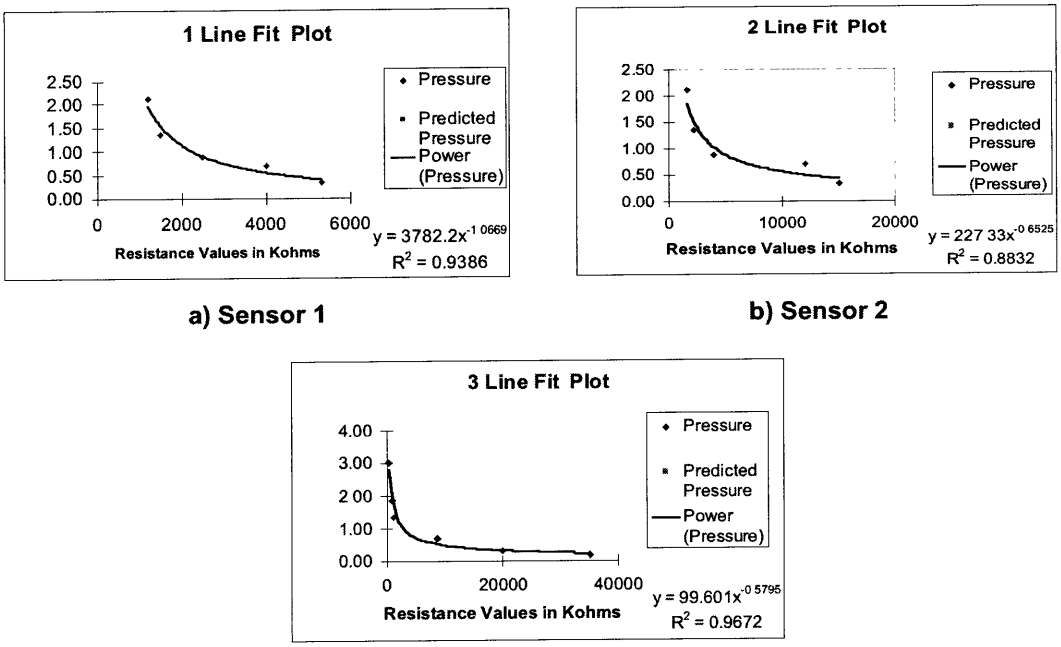

Fig 6.2.2 a, b & c: Pressure Vs Resistance Best fit plot for sensors 1,2 and 3.

6.2.3 Substrate Printing Pressure

The calibration procedure actually defines the pressure with the sensors in the roller pinch zone. Fortunately, the senor thickness with the applied tape was approximately the same as the substrate (150 microns) so the assumption was made that a similar pressure would be present during stamping. In truth, the absolute printing pressure is not exactly known, however the pressure increments are well defined by this procedure.

6.3 Conclusion

The chapter explained the procedure followed to vary and measure the two most important input parameters- speed and printing pressure that affect the process output. The specifications and characteristics of the stepper motor and flexi-force sensors were also briefly discussed. While conducting experiments, the input parameters were varied and optimized to get the best print quality at high throughput rate. In the next chapter, we shall talk about the experimental results that were obtained.

Chapter 7

Experimental Data and Analysis

7.1 Introduction

The three sets of experiments that were conducted in the flexography style micro-contact printing resulted in various observations each of which depicted something unique about this process and the hardware used to execute this process. In order to maximize the useful knowledge obtained from the experiments, the observations and data that were collected was classified and analyzed in two different ways as shown in fig 7.1

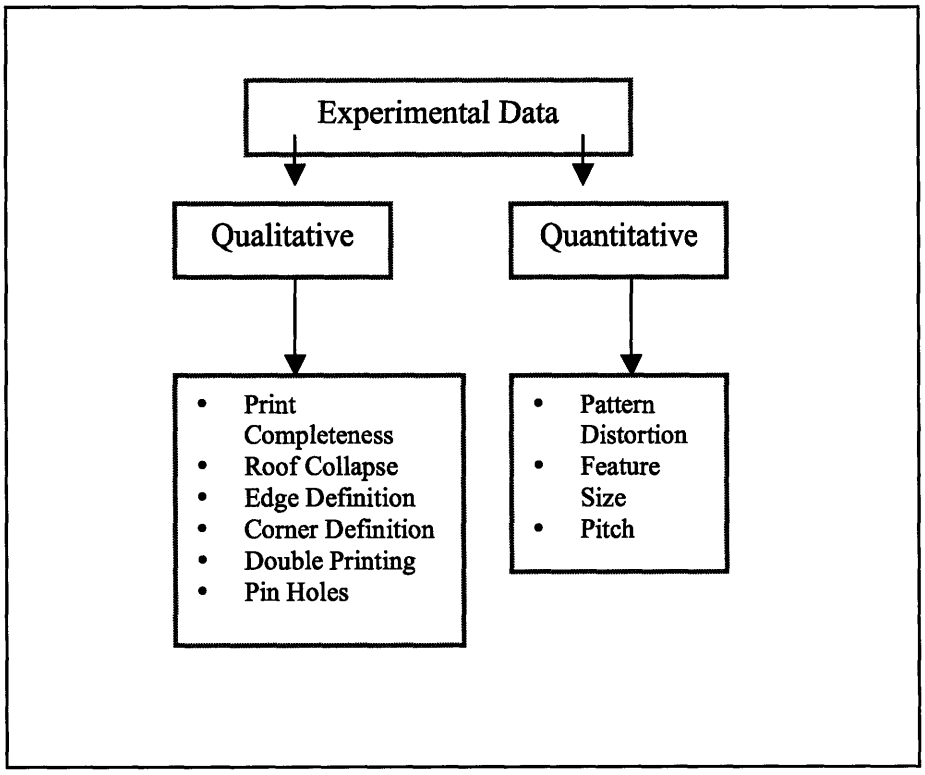

Fig 7.1 shows the classification of data which was collected from the three sets of experiments.

7.2 Analysis of Qualitative Data

Qualitative data includes all the defects observed in the printed pattern. Study of defects in the self assembled monolayers is a good start to understanding the process. Defects in the monolayers can be directly related to the following namely,

- Chemistry of micro-contact printing
- Design of the stamp
- Fabrication of stamp
- Treatment of substrate and stamp

A number of different types of qualitative data are of interest as enlisted below:

- Roof Collapse: An unintended touching of the inked recesses of the stamp onto the substrate, fig 7.2A.

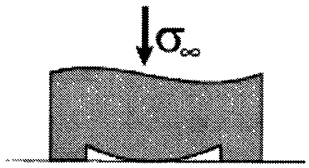

Fig 7.2A taken from [33], shows an exaggerated view of a stamp with recessed features. A pressure of σ psi causes the roof to touch the substrate.

- Incomplete Printing: Absence of the complete or a specific region of monolayer onto the substrate.
- Double or Multiple Printing: This is self explanatory. When the substrate comes into contact with an inked stamp multiple times, it leads to multiple prints.
- Pin holes: As the name suggests, these are tiny dots interspersed throughout the features of the pattern.

Naturally, in order for a subsequent quantitative analysis to be made, the above mentioned defects must be eliminated. Therefore, a study of these occurrences is vital to the development of the flexography style micro-contact printing process and to the achievement of the desired goals.

The details of the qualitative observations from three sets of experiments are shown in table 7.2.

a) Experimental SET 1 Observations:

	Treatment		Print Completeness	Roof Collapse	Pin Holes	Edge Definition	Corner Definition
Trial	Speed	Pressure					
1	4	6	Faint lines overall, Incomplete print in the middle	None	Yes	Rough	Rough
2	25	6	Faint lines overall, Incomplete print in the middle	none	Yes	Difficult to define	Difficult to define
3	4	15	Faint lines overall, Incomplete print in the middle	Over a large area of the print	Yes	Rough	Nodes
4	25	15	Faint lines overall, Incomplete print in the middle	Over the center of the printed pattern	Yes	Good	Good
5	10	8	Faint lines overall, Incomplete print in the middle	Over a small area	Yes	Good	Good

b) Experimental SET 2 Observations:

	Treatment		Print Completeness	Roof Collapse	Pin Holes	Edge Definition	Double Print
Trial	Speed	Pressure					
1	10	3	Complete	None	Yes	Good	NO
2	50	3	Complete	None	Yes	Rough	Yes
3	10	8	Complete	None	Yes	Good	Yes
4	50	8	Complete	None	Yes	Rough	Yes
5	25	5	Complete	None	Yes	Rough	Yes

c) Experimental SET 3 Observations:

	Treatment		Print	Roof	Pin	Edge	Corner
Trial	Speed	Pressure	Completeness	Collapse	Holes	Definition	Definition
1	10	3	Complete	None	Yes	Good	Good
2	25	3	Complete	None	Yes	Good	Good
3	50	3	Complete	On Triangles near the edges	Yes	Good	Good
4	100	3	Complete	On all the triangles	Yes	Good	Good

Table 7.2 gives details of the observations made from the samples obtained in the three experimental sets.

7.3 Qualitative Results

Experiments were conducted with different types of patterns such as Grids, Gratings, Triangles, Array of Dots, Large Dots, perpendicular lines etc. Table 7.3 summarizes the types of patterns used for each experimental set and gives their dimensional specifications.

Experimental Set	Pattern	Line Width/Diameter	Spacing
1,2	Grid	25 µm	250µm
3	Grating	10µm	5µm to 150µm
3	Large Dots	400µm	50µm
3	Dot Arrays	5µm to 150µm	50µm

Table 7.3 summarizes the types of patterns printed during experimentation.

7.3.1 Results of Experimental Set 1

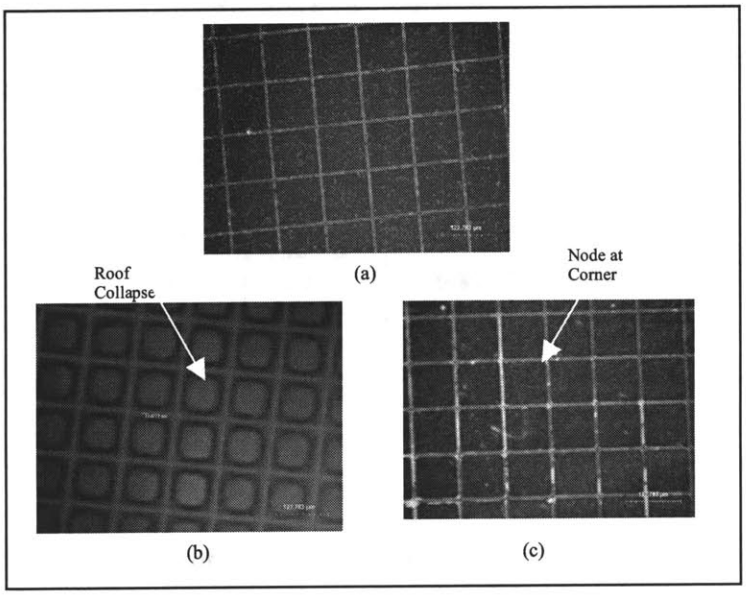

Fig 7.3.1A shows visual defects of the printed pattern in the first experimental set. (a) Sample (4rpm, 6psi) is a very faint pattern with rough edges. (b) Sample (4rpm, 15psi) with roof collapse over a large area. (c) Sample (4rpm, 15psi) having nodes at the corners of the grid.

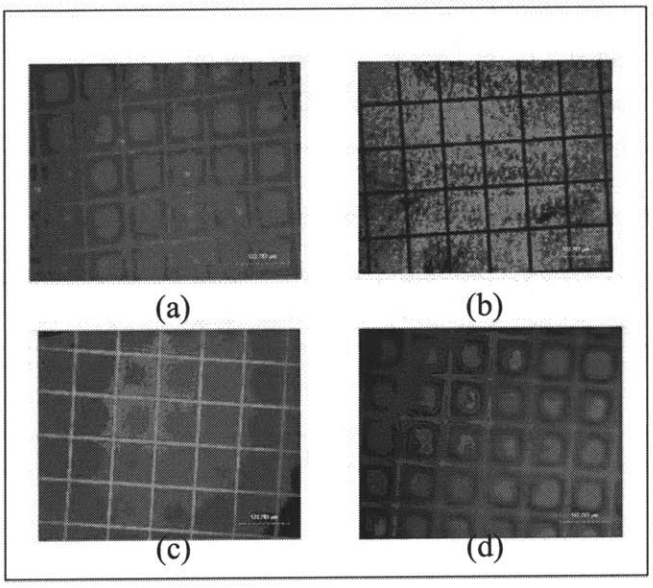

Fig 7.3.1B shows visual defects of the printed pattern in the first experimental set. (a) (25rpm, 15psi) has roof collapse over a large area. (b) (25rpm, 15psi) with complete pattern and good edges on some regions of the substrate. (c) (10rpm, 15psi) showing a pattern with well defined edges. (d) (10rpm, 15psi) showing roof collapse in some regions of the substrate.

'*Roof Collapse*' and '*incomplete printing*' were the predominant phenomena in this set of experiments. Overall the quality of the printed pattern was poor.

Stamps used for micro-contact printing have isolated high regions that transfer ink to the substrate upon physical contact. When these features are small i.e. their aspect ratio is very small, it indicates that the width of the features is large compared to the height of the features. When this is the case, the roof of the stamp is more susceptible to touching the substrate when a threshold of applied printing pressure is exceeded [33]. Consequently, all the patterns that were printed at high values of pressure (> 10 psi), exhibit roof collapse as shown in fig 7.3.1A and fig 7.3.1B.

The concentration of ink used for the experiments was 10mM. However, because of insufficient inking of the stamp, the prints obtained were very faint and not very conducive to quantitative analysis. The non-uniformity of the stamp on the stamping cylinder led to an uneven distribution of pressure over the substrate. This means that some regions of the substrate were in conformal contact with the stamp while some were not in contact with the stamp at a given instant of time during printing. This explains the incomplete printing phenomenon where only certain regions of the pattern were printed onto the substrate.

Table 7.3.1 summarizes the reasoning made above.

Defects Observed	Reason
Roof collapse	Aspect ratio 1:10
	Excessive Printing Pressure ranging from 6 to 15 psi
Incomplete Printing & Faint Pattern	Ink Concentration 10mM
	Inking time insufficient < 15 minutes
	Non uniform Inking of Stamp
	In sufficient Drying

Table 7.3.1 summarizes the reasons for the observations made in experimental set 1.

The conclusions that were drawn from experimental set 1 were:

1. Uniformity in the thickness of the stamp is extremely important for a complete printing of the pattern
2. Inking having both the inking and the stamping cylinder in mesh for a period of up to 30 minutes followed by proper drying is required for an ink concentration of 10mM.
3. Printing pressures of less than 8psi should be tried for the next set of experiments as high pressures result in roof collapse for a stamp having an aspect ratio of 1:10.

Accordingly, the next set of experiments was designed with a different range of pressure and a different method of flow of substrate (Continuous flow) by changing the wrap angle as described in chapters 3 and 4. A proper method of casting the stamps uniformly was also devised which involved the use of levelers and tilt stages to ensure flatness of the stamp as described in chapter 4.

7.3.2 Results of Experimental Set 2

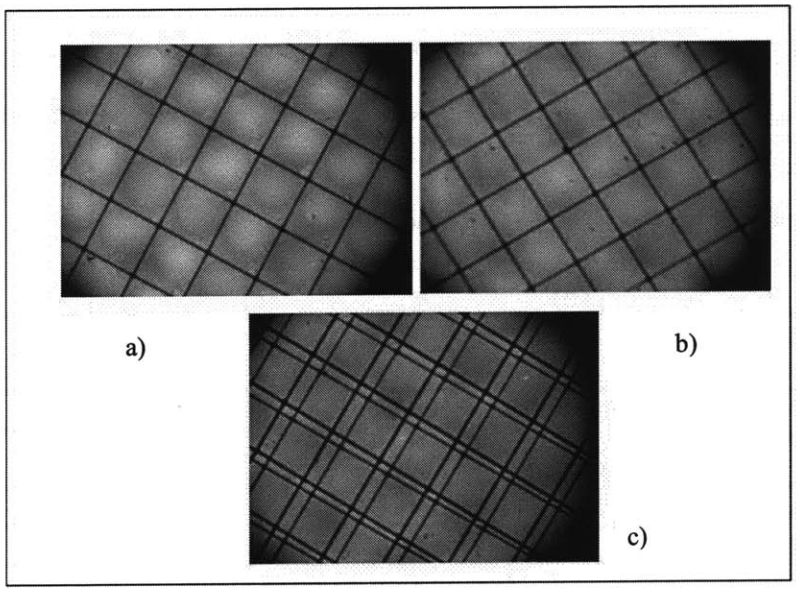

Fig 7.3.2A shows visual defects of the printed pattern in the second experimental set. (a) Sample (10rpm, 3psi) is a very visually good print with well defined edges. (b) Sample (10rpm, 3psi) shows another region of the substrate. (c) Sample (10rpm, 8psi) clearly shows 'double printing' phenomenon.

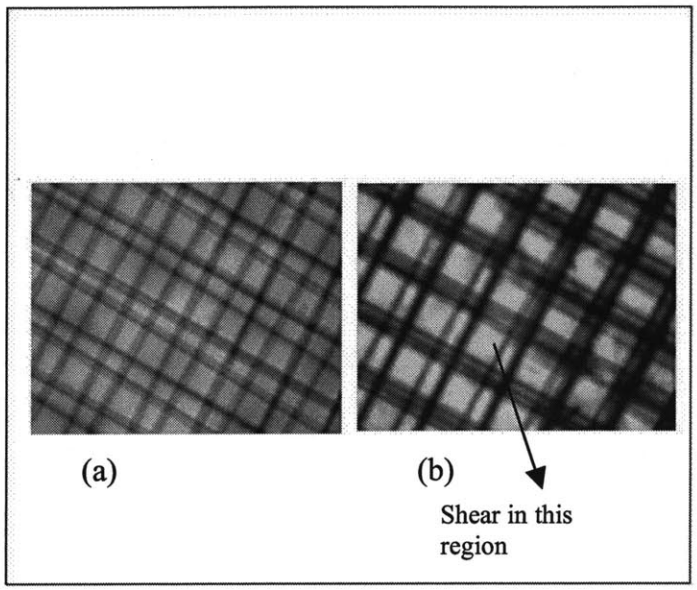

Fig 7.3.2B shows visual defects of the printed pattern in the second experimental set. (a)Sample (50rpm, 3psi) clearly shows multiple printing and distortion of the printed pattern. (b) Sample (50rpm, 8psi) shows multiple printing and there is also a sign of shear that seems to have taken place.

The predominant response in set 2 was "double" or "multiple" printing as shown in fig 7.3.2A (c) and 7.3.2B. This can be explained as follows.

When the substrate flow is continuous it is pulled over an additional rod placed between the stamping and the inking cylinders as shown in the schematic below, Fig 7.3.2C.

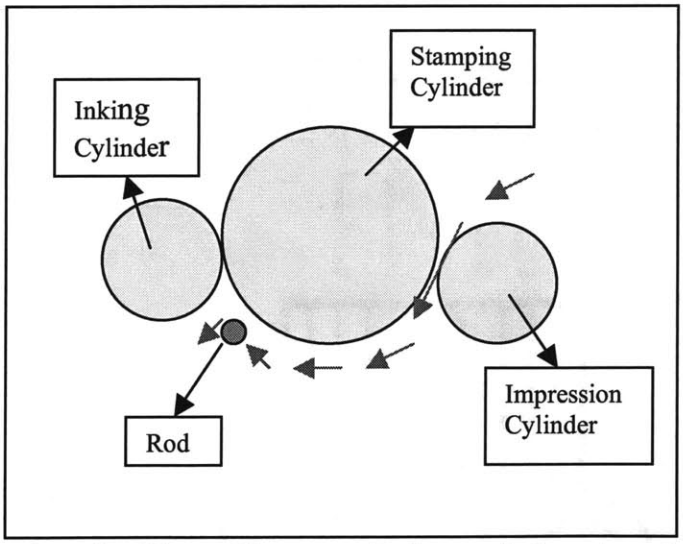

Fig 7.3.2C shows a schematic of the machine system. Red arrows indicate the path of the substrate and the grey circle is the position of the rod used to make the wrap angle large for continuous flow of substrate.

Since the feeding and removal of substrate is manual, tension control on the substrate is highly variable. As a result, there is a small amount of slack which can cause the substrate to touch the stamping cylinder multiple times causing multiple printing. Accordingly, experimental set 2 just resulted in one good print, which was obtained from the experiment conducted at a speed of 10 rpm and a pressure of 3 psi yielded a complete print without any roof collapse.

The conclusions drawn from experimental set 2 was that with a high concentration of ink (50mM) a pressure of 3 psi is sufficient for the formation of the monolayer onto the substrate with a good quality of print. However, in order to eliminate the problem of double printing, proper tension is required to be maintained at the both ends of the substrate.

7.3.3 Results of Speed Tests conducted in Experimental Set 3

The third set of qualitative experiments was conducted at a fixed pressure of 3 psi, a high ink concentration and reverse flow (small wrap angle) of substrate. With these parameters as a constant, the throughput rate of the machine was tested by varying the speed from 10 rpm to 100 rpm.

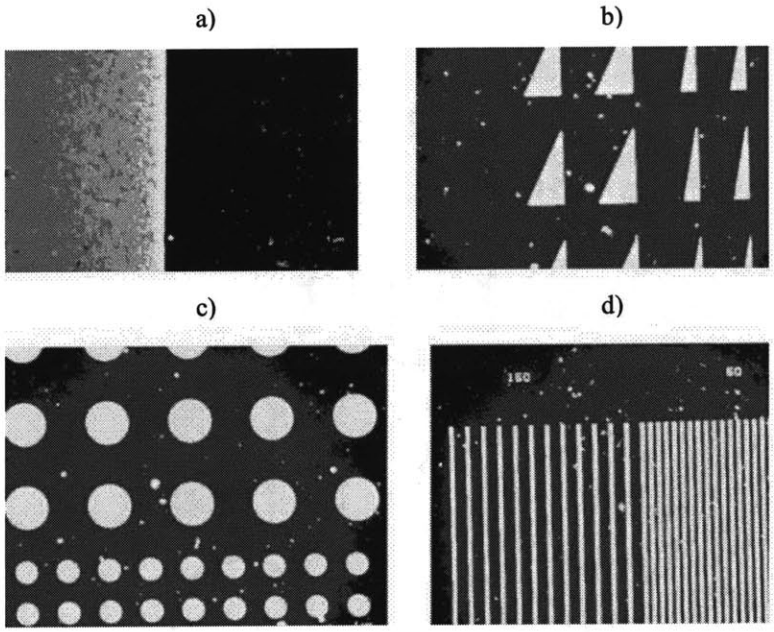

Fig 7.3.3A shows visual defects of the printed pattern in the third experimental set (10rpm, 3psi). (a) Shows a good print with a very sharp edge. (b) Shows triangles printed without any collapse. (c) Shows dots printed. (d) Shows lines printed with a spacing of 50 and 150 microns.

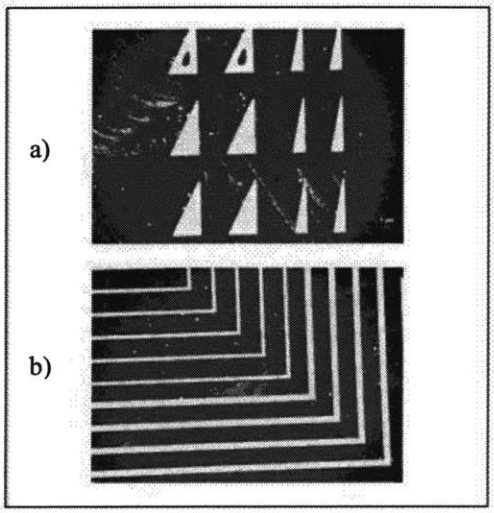

Fig 7.3.3B shows visual defects of the printed pattern in the third experimental set (25rpm, 3psi). (a) Shows a good print with a very sharp edge but some collapse in the triangles. (b) Shows perpendicular lines printed completely with well defined edges and corners.

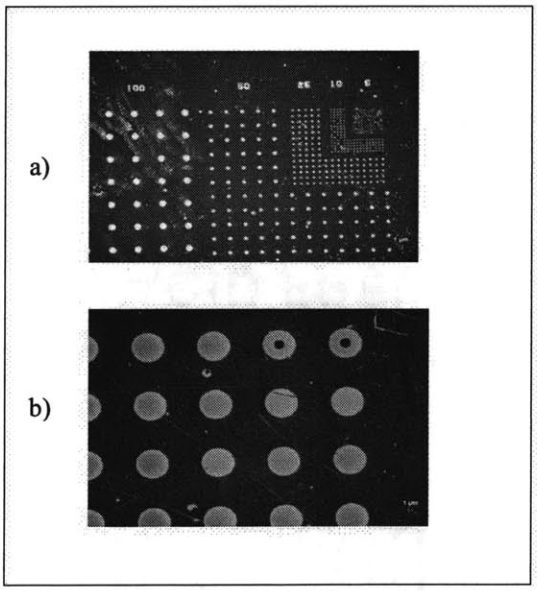

Fig 7.3.3C shows visual defects of the printed pattern in the third experimental set (50rpm, 3psi). (a) Shows a good print of dots of various sizes from 5 to 100 microns. (b) Shows some collapse observed in larger dots in a different region of the substrate.

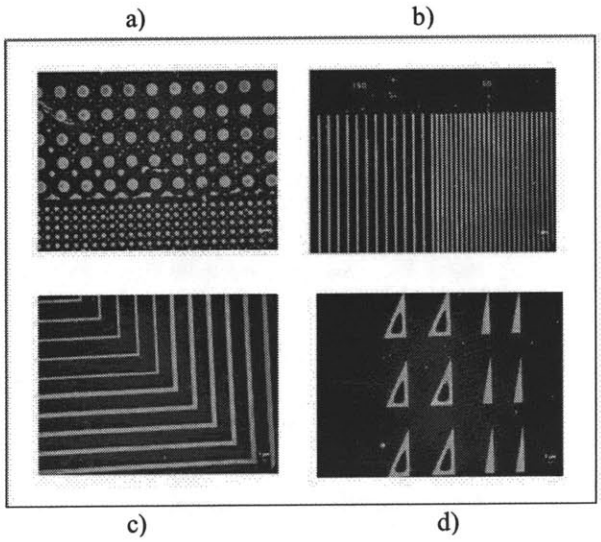

Fig 7.3.3D shows visual defects of the printed pattern in the experiment (100rpm, 3psi). (a) Shows a good print but with unusual presence of small dots uniformly spaced between the dots on the pattern. (b) Shows well defined lines. (c) Shows perpendicular lines with sharp corners. (d) Shows triangles printed with collapse of the roof.

The speed tests which were conducted successfully *transferred* the pattern from the stamp to the substrate even at speeds of 100 feet per minute as shown in the results above. Some regions of collapse are evident as the speed increases to 100 rpm. This was caused by improper adherence of PDMS sheets onto the cylinders and non uniformity of the stamp. Non uniformity in the stamp thickness makes it difficult to set a desired value of pressure between the stamp and the substrate. With non uniform PDMS sheets wrapped around the cylinders, there were regions of gap and excessive contact pressure when the stamping cylinder and the impression cylinder are brought together. This was unavoidable.

7.3.4 Conclusions to Qualitative Analysis

Over all, the qualitative experiments demonstrate that it is possible to achieve a visually good print as fast as 100 feet per minute.

It is to be kept in mind that, we were unable to conduct a proper statistical analysis to determine the capability of this machine. There are several reasons for this.

One, statistical analysis requires a large amount of data which were unable to collect. Two, since the thickness of the stamp was a random variable and its uniformity was a noise factor, every set of experiments was a random process that yielded random results. To determine the capability of the process would require the printing to be a more stable process. Hence, these experiments were simply conducted to determine whether micro-contact printing is feasible on the test hardware. This chapter now continues with some quantitative analyses that were done on visually good prints.

7.4 Quantitative Analysis: Variations in Printed Feature Line Width

In this section we quantitatively analyze the variations in the printed feature lines on substrates using the lab-scale flexographic machine. Two kinds of variations have been studied: absolute variation in the line width compared to the target value and relative variations compared to one another.

After analyzing visually, data was collected for the best prints that we got from the three sets of experiments. The first two sets were aimed at identifying the best parameters of speed and pressure at which the print quality was good while in the third one, we challenged the machine capabilities by running it at a constant pressure and very high speeds.

By 'best prints', we refer to the samples, which on visual inspection showed sharp and clear features, minimal collapse, no double printing, and had a good print registration.

The table 7.4 summarizes the kind of dimensions taken for the best prints from each set of experiments.

Experiment Number*	Experiment Goals	Print Parameters	Pattern Printed	Dimensions taken
1. Continuous Printing	Get best parameters for high throughput and good print quality	25rpm, 15psi 10rpm, 15psi	Grid with 25 microns thick lines. Each square: 250 μmX 250 μm	Width of lines in vertical and horizontal directions
2 Continuous Printing	Get best parameters for high throughput and good print quality	10rpm, 3psi 10rpm, 3psi	Grid with 15 microns thick lines. Each square: 225 μmX225 μm	Width of lines in vertical and horizontal directions
3 Reverse Printing	Challenge machine capabilities	50rpm, 3psi	Gratings with 400, 150, 50 and 10 micron spacing	Spacing between the lines

Table 7.4: Best print parameters from 3 sets of experiments. Note that each experiment number used a different stamp.

7.4.1 Data collection

The data was collected on just 4 substrates, referred to as best prints from the first two sets of experiments as shown in the table 7.4. Our capacity to analyze all samples and collect data on them was limited not only because of the bad print quality and defects (explained in section 7.2) but also the inability of the Veritas[1] microscope to take measurements in case of poor print registration. Hence, only those samples that had the best prints in each set of experiments were quantitatively studied.

For the first two sets of experiments, substrates with grids of line widths 25 μm (each square: 250 μmX 250 μm) and 15 μm (each square: 225 μmX 225 μm) respectively printed on them were analyzed. The substrate was divided into 5 sites as shown in the figure 7.4.1 to measure spatial variations and line widths were measured in vertical and horizontal directions. Forty data points from random locations in each region were

collected and then analyzed for region to region and as well as for absolute variations. The complete data for these measurements is in Appendix B.

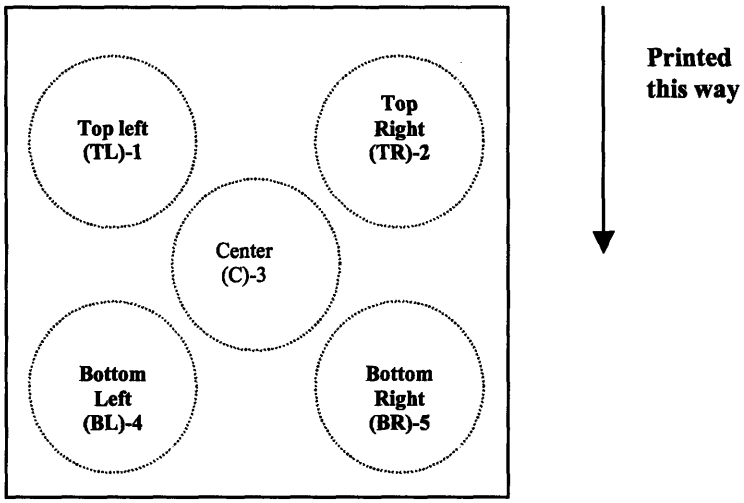

Figure 7.4.1: Square gold substrate divided into 5 sites. 40 data points in each site were collected for statistical analysis.

The third set of experiments was aimed at analyzing quality of print at very high speeds. Instead of a grid, gratings with 400, 150, 50 and 10 microns line spacing were reverse printed and then measured.

[1]Veritas: Resolution of 2 microns

7.4.2 Analysis

The quantitative analysis done in this section is an attempt to study and predict the affect of the input parameters-speed and pressure and also the effect of other variable factors on the print quality. The observations from each set of experiments have been recorded below.

Experimental Set 1: Continuous Printing

1. Data from the best print at: 25rpm, 15psi

From this set we determined that the best print quality (as seen visually) was at 25 rpm and 15 psi. A single sample from this test was measured and the mean and standard deviation of each of the 5 spatial regions was collected.

From this data, the coefficient of variation (mean / standard deviation) was calculated for vertical and horizontal dimensions in each region as shown in the table 7.4.2 A.

	Mean (microns)		Standard Deviation		Coefficient of Variation in %	
	V	H	V	H	Vertical	Horizontal
TL	0.02880	0.03356	0.00164	0.00177	5.1	5.2
TR	0.02874	0.03316	0.00033	0.00058	1.1	1.75
C	0.02946	0.03223	0.00034	0.00054	1.1	1.7
BL	0.02755	0.02867	0.00072	0.000564	2.6	1.9
BR	0.02837	0.03113	0.000446	0.001214	1.5	3.9

Table 7.4.2 A: Coefficient of Variation for vertical and horizontal dimensions in different regions.

In this print, we observed that the relative variation in dimensions was between approximately 1-5% in most of the regions. This can be attributed to non-uniform thickness of the stamp resulting into unequal pressure application, and hence high variations. Also, since the feeding and tension control is manual, there is a possibility of slippage that can result into wider features or even double printing in some regions causing variations.

In addition, we can look at the actual width error for the part. Accordingly, the deviation of average horizontal and vertical line widths from the target value was plotted for each region, as shown in Fig. 7.4.2A.

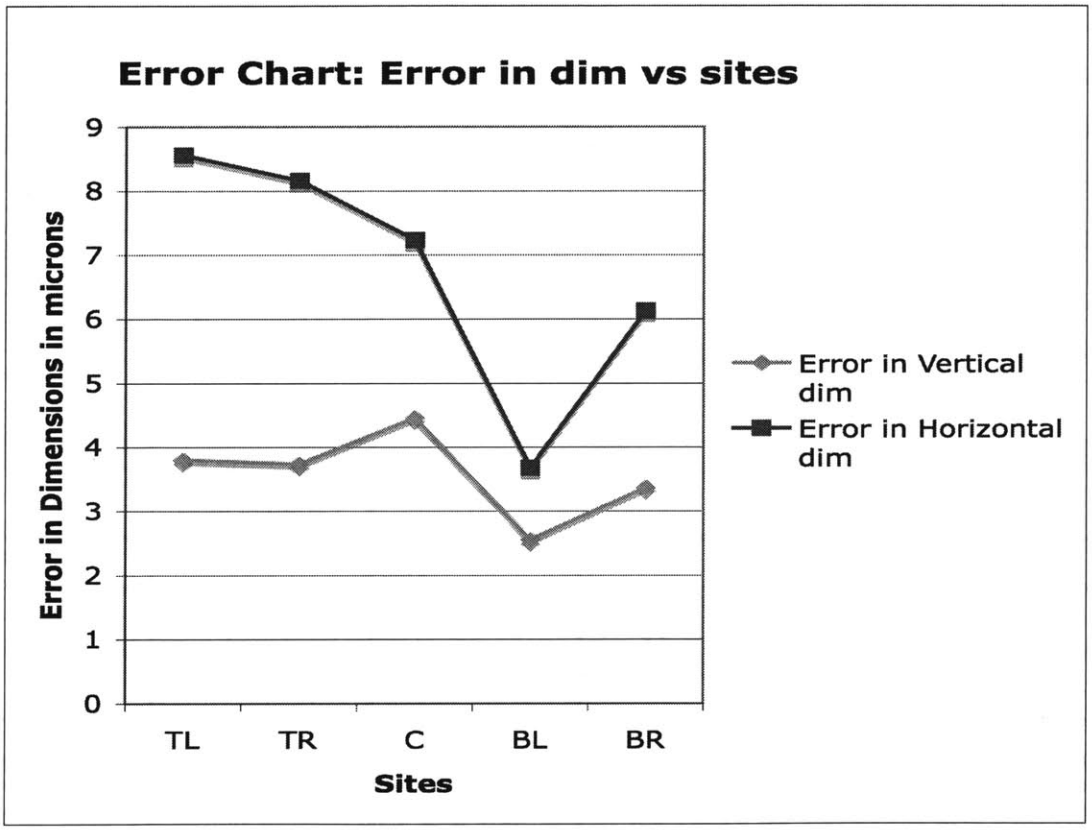

Figure 7.4.2 A: Error in dimensions of vertical and horizontal line widths as compared to the target value~25 μm

Absolute Errors: Clearly, the average printed width is greater than the actual pattern size and lies within the range of 10 microns. This sample was printed at a very high pressure of 15 psi and high speed. Such high pressures can result into greater deformation in elastomeric stamp. Also, high speeds can result into slipping which can also increase the

width of the features. Moreover, since the continuous printing method was used, the area of contact was large. If proper tension is not provided at both ends of the substrate, it can slip between the two cylinders resulting in smearing or multiple printing, thereby increasing the thickness of the features. Hence, at high speeds, reverse printing, which minimizes the area of contact, should be used to prevent slipping.

Relative Errors: The average width of printed horizontal lines is greater than that of vertical lines. This is because printing was done in the direction of vertical lines. Hence these features experience a longitudinal force while the horizontal line experience a lateral force, making the horizontal lines wider than the vertical ones.

1. Data from the best print at: 10rpm, 15psi

From experiment 1, we determined another good print quality (as seen visually), which was at 25 rpm and 15 psi. A single sample from this test was measured and the mean and standard deviation of each of the 5 spatial regions was collected.

Again the coefficient of variation was calculated for vertical and horizontal dimensions in each region as shown in the table below.

	Mean (microns)		Standard Deviation		Coefficient of Variation in %	
	V	H	V	H	Vertical	Horizontal
TL	0.02715	0.02764	0.00030	0.000395	1.1	1.4
TR	0.0259	0.02902	0.000465	0.000593	1.7	2
C	0.02697	0.02724	0.000292	0.000438	0.8	1.6
BL	0.02796	0.02834	0.000745	0.000605	2.6	2.1
BR	0.02592	0.02687	0.00025	0.000811	0.9	3

Table 7.4.2 B: Coefficient of Variation for vertical and horizontal dimensions in different regions.

As can be seen from table 7.3.2B, in some regions we have been able to achieve coefficient of variation less than 1%. Hence, if the variable factors like stamp non-uniformity, manual feed and tension control are taken care of, this machine can give a high quality print with minimal distortions.

Again, the deviation of average horizontal and vertical line widths from the target value was plotted for each in Figure 7.3.2B region.

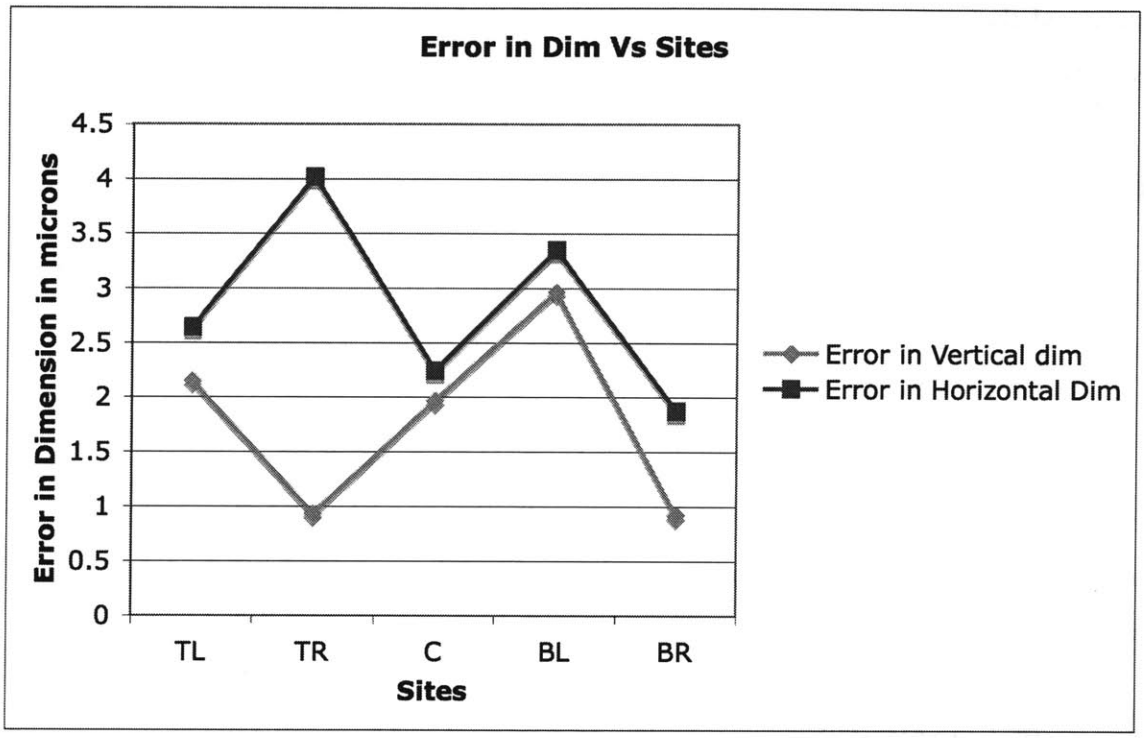

Figure 7.4.2 B: Error Chart: Error in dimensions of vertical and horizontal line widths as compared to the target value~25 μm

Absolute Errors: We again observed that the average printed width in this case was greater than the actual pattern size and was within the range of 4 microns and averaged about 2 microns. This sample was printed at same pressure~15psi as before, but at lower speed and showed a drastic reduction in line width variations. This is because, at low speeds, the manual tension control provided to the substrate was enough to prevent the slipping.

Relative Errors: The average width of printed horizontal lines is greater than that of vertical lines.

From the above analysis we can say that in case of continuous printing, low speeds should be preferred for high quality prints. To increase the production rate, reverse printing should be used. Proper tension control is important in either case to prevent slipping.

However, it is important to note that 15 psi pressure was in general too high. It not only increased the width of features as shown above, but also resulted into a lot of feature collapse.

Experimental Set 2: Continuous Printing

In this set of experiments, the best prints we got were at 10rpm, 8psi and other at 10rpm, 3psi. A grid with line width of 15 μm and spacing of 225 μm was printed.

1. Data from the best print at: 10 rpm, 8psi

From experiment 2, we determined the best quality (as seen visually) was at 10 rpm and 8 psi. A single sample from this test was measured and the mean and standard deviation of each of the 5 spatial regions was collected.

The coefficient of Variation was calculated for vertical and horizontal dimensions in each region as shown in the table 7.4.2C.

	Mean (microns)		Standard Deviation		Coefficient of Variation in %	
	V	H	V	H	Vertical	Horizontal
TL	0.02359	0.02772	0.00033	0.000695	1.4	2.4
TR	0.02416	0.02981	0.00043	0.00069	1.8	2.3
C	0.02480	0.02866	0.000304	0.001414	1.2	4.9
BL	0.02291	0.02399	0.00108	0.00086	4.7	3.6
BR	0.01877	0.02176	0.000656	0.000742	3.4	3.5

Table 7.4.2 C: Coefficient of Variation for vertical and horizontal dimensions in different regions.

For this test, the coefficient of variation was between 1.2 and 4.9%., and averaged (over the entire surface) ~ 2.8%.

The error in vertical and horizontal line width dimension is shown in Fig. 7.4.2 C.

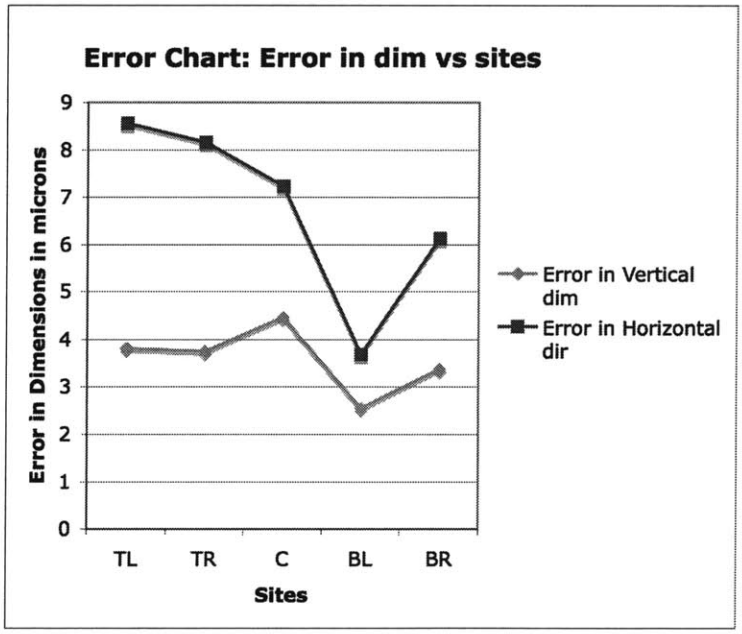

Figure 7.4.2 C: Error Chart: Error in dimensions of vertical and horizontal line widths as compared to the target value~15 μm

As can be seen form the figure 7.4.2C, the average width of the printed lines was in the range of 9 microns at these parameters. It can be attributed to the fact that printing was being done at a high pressure, which can result into significant elastomeric deformations leading to such variations.

2. Data from the best print at: 10 rpm, 3psi

From experiment 2, we determined another good print quality (as seen visually), which was at 10 rpm and 3 psi. A single sample from this test was measured and the mean and standard deviation of each of the 5 spatial regions was collected.

Again the coefficient of variation was calculated for vertical and horizontal dimensions in each region as shown in the table below.

	Mean (microns)		Standard Deviation		Coefficient of Variation in %	
	V	H	V	H	Vertical	Horizontal
TL	0.01857	0.01974	0.00067	0.00061	3.6	3.0
TR	0.01991	0.02004	0.000378	0.00030	1.8	1.5
C	0.01749	0.01817	0.000194	0.000710	1.1	3.9
BL	0.01928	0.0194	0.00046	0.000260	1.4	2.9
BR	0.01838	0.01890	0.000508	0.000439	2.0	1.2

Table 7.4.2 D: Coefficient of Variation for vertical and horizontal dimensions in different regions.

It can be seen from the table, the coefficient of variation for all regions is much less than the previous case- 10rpm, 8psi, and averages 2.2% with a range of 1.1 to 3.6%.
The deviation of average horizontal and vertical line widths from the target value are plotted in Fig. 7.4.2 D.

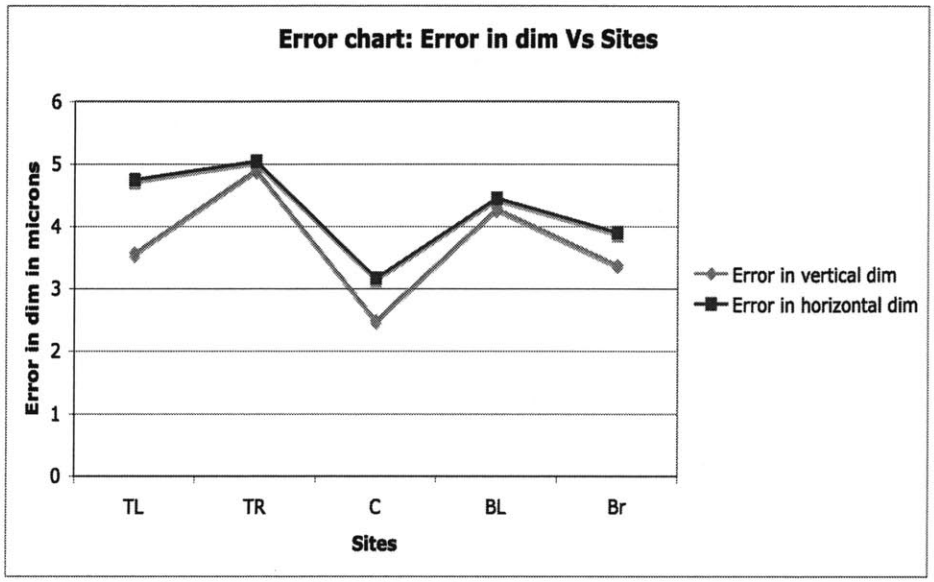

Figure 7.4.2 D: Error Chart: Error in dimensions of vertical and horizontal line widths as compared to the target value~15 μm

As expected, we again observed that the average printed width in this case was greater than the actual pattern size but was within the range of 5 microns. This sample was printed at same speed as before~10rpm, but at lower pressure, and it showed a significant reduction in line width variations. This is because, at low speeds and low pressures, the manual tension control provided to the substrate was enough to prevent the slipping and also elastomeric stamp deformation was under control.

Variations between samples printed using same stamp

We have also tried to study the variations between the samples printed using the same stamp. For this, we analyzed the line width variations in the center of the substrate as it can be assumed as the most stable printing area. Problems like non-uniformity in stamp, unequal pressure application, pattern distortions have been found more towards the edges of the stamp. The results from experiment 1 are shown in Fig. 7.4.2.E and F.

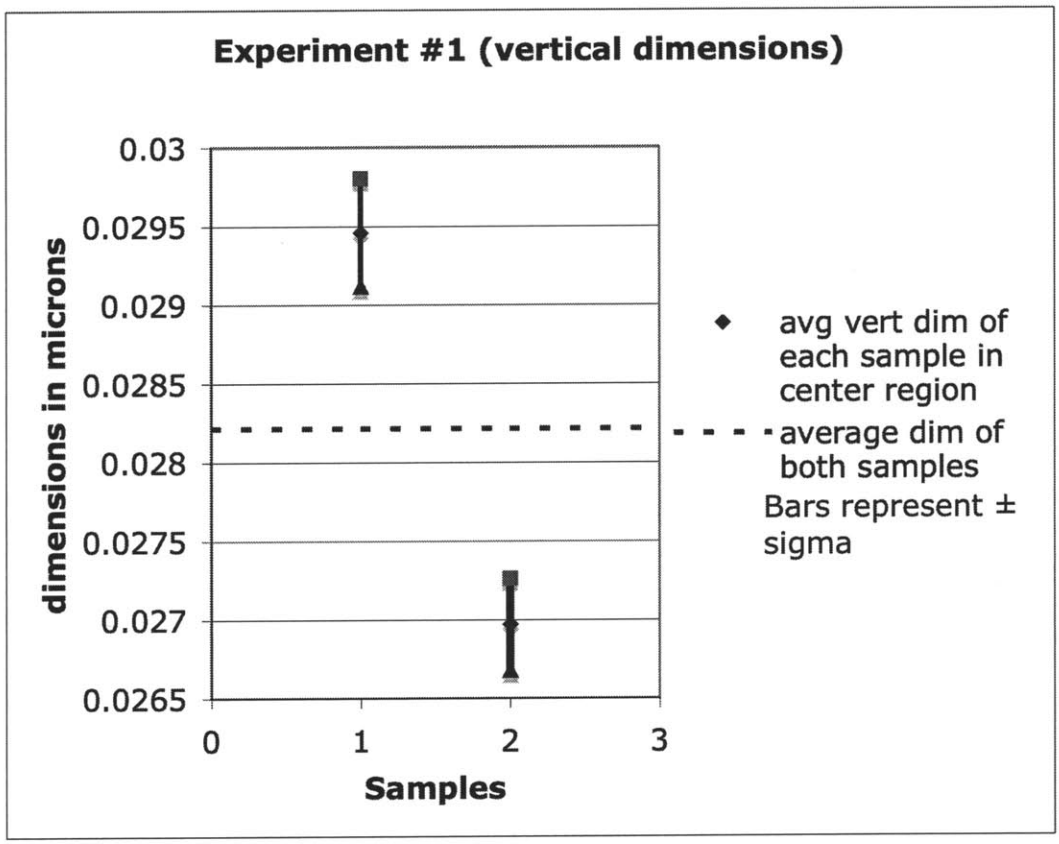

Figure 7.4.2 E: Spatial Variation Graph for vertical line width dimensions: Variations in dimensions within 1 sigma limit have been shown for both samples printed with the same stamp having 25 μm thick line widths.

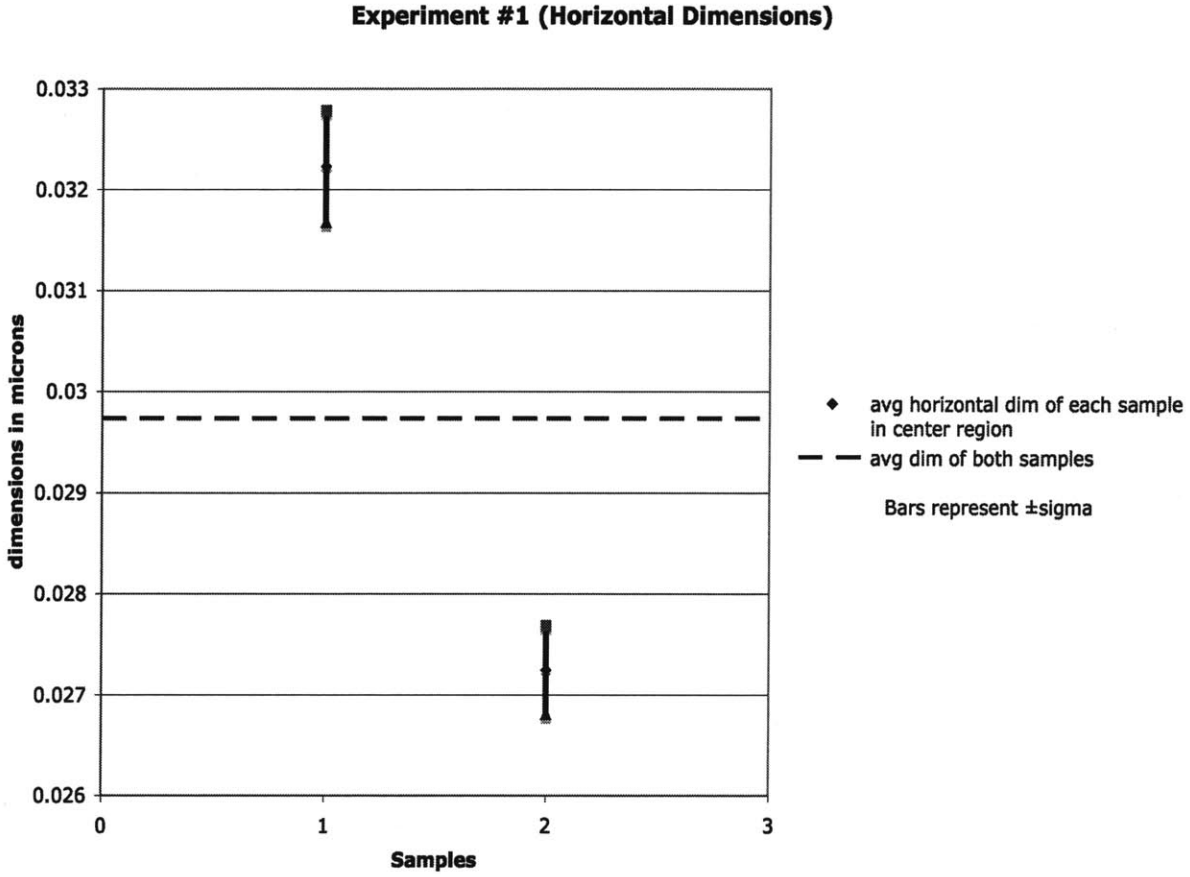

Figure 7.4.2 F: Spatial Variation Graph for horizontal line width dimensions: Variations in dimensions within 1 sigma limit have been shown for both samples printed with the same stamp having 25 μm thick line widths.

In the figures 7.4.2 E and F, the sample 1 represents the one printed at 25rpm, 15 psi and sample 2 was printed at 10rpm, 15 psi. The mean value of horizontal and vertical line widths for the second sample is much closer to the target dimension~25 μm than the first sample. Within a substrate, spatial variation seems to be same for both of them. However, there is a difference of 3-5 μm between the mean dimensional values (horizontal and vertical) of the two substrates. This likes most likely from deformation in stamps and unequal pressure application because of manual feeding and tension control.

In the figures 7.4.2 G and H, the sample 1 represents the one printed at 10rpm, 3 psi and sample 2 was printed at 10rpm, 8psi. The mean value of horizontal and vertical line widths for the first sample is much closer to the target dimension~15 μm than the second sample. Within a substrate, spatial variation seems to be little bit more for the second

sample. However, there is a difference of 5-10 μm between the mean dimensional values (horizontal and vertical) of the two substrates. This can be attributed to the variable factors like deformation in stamps and unequal pressure application because of manual feeding and tension control.

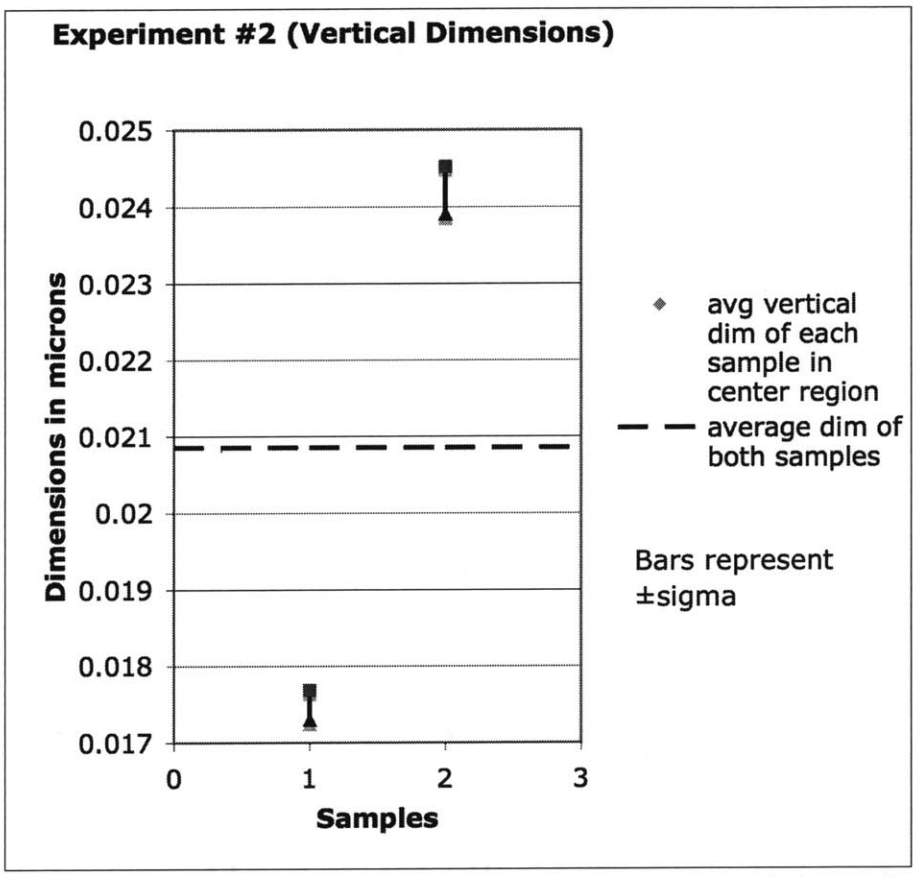

Figure 7.4.2 G: Spatial Variation Graph for vertical line width dimensions: Variations in dimensions within 1 sigma limit have been shown for both samples printed with the same stamp having 15 μm thick line widths.

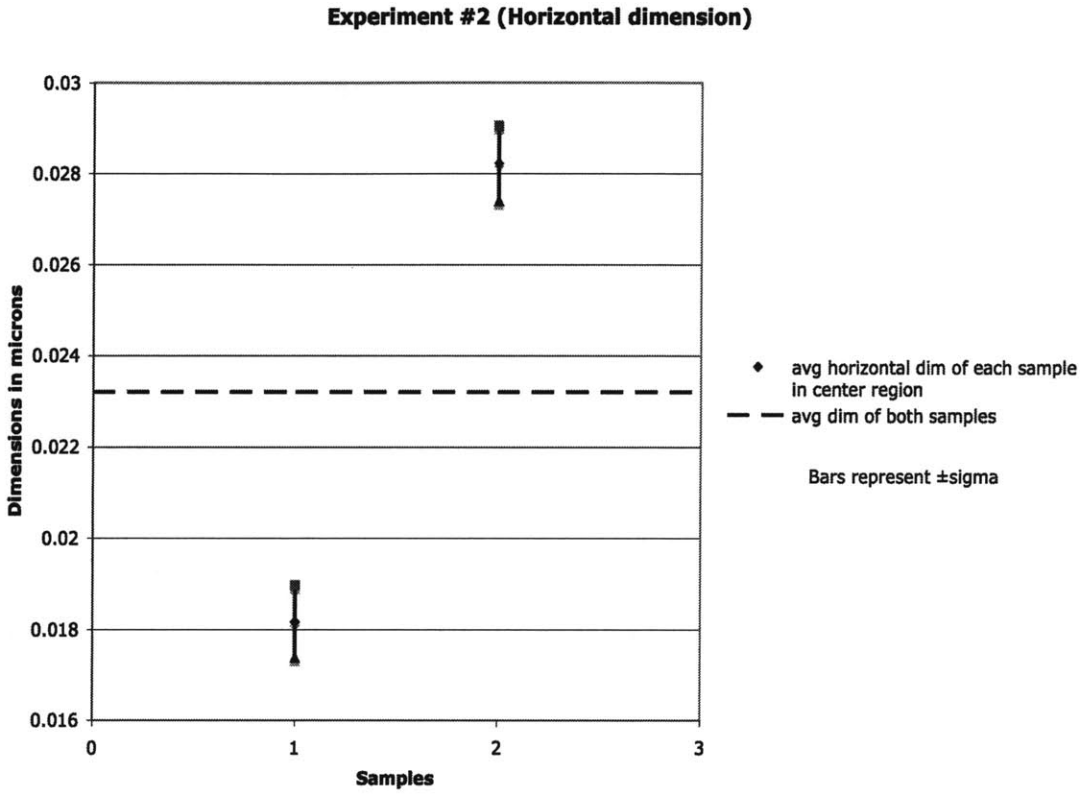

Figure 7.4.2 H: Spatial Variation Graph for horizontal line width dimensions: Variations in dimensions within 1 sigma limit have been shown for both samples printed with the same stamp having 15 μm thick line widths.

Experimental Set 3: Data from High Speed Tests

As discussed in Chapter 5, we conducted a third set of experiments to challenge the capability of the machine and were successful in printing even at 100rpm with low wrap angles.

For this analysis, the data from 50 rpm and 3 psi was used.

Since the printing was done at very high speed, reverse printing was used to keep the contact area low. Instead of a grid, we printed a grating with different line spacing ranging from 10 to 400 microns.[2] and the pitch between the lines was measured. For each set of lines, 70 measurements were taken (Appendix B) and coefficient of variation was calculated as shown in the table. As the relief size increased, the coefficient of variation decreased because larger features are more robust from a stiffness perspective.

[1]Our aim was to see how well we could print at very high speeds. Hence, we tried printing different patterns like arrays of circles, rectangles and triangles.

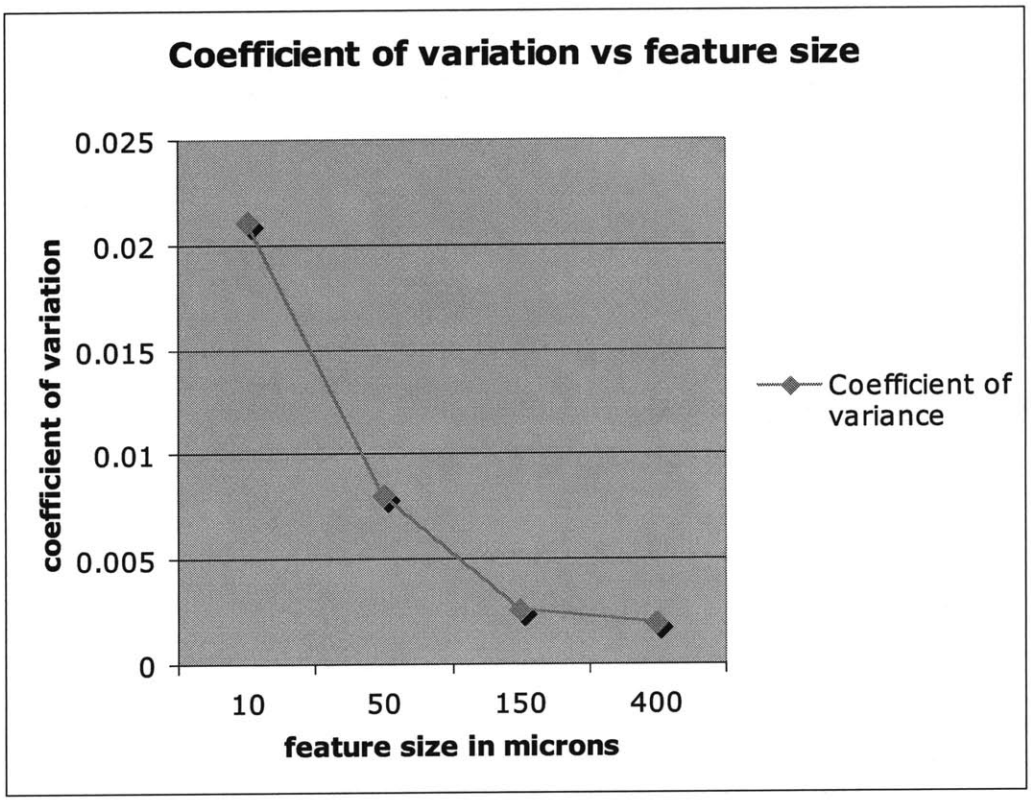

Figure 7.4.2 I: Coefficient of Variation for different line spacing.

Again, because of poor registration the number of measurements that could be taken was limited.

This kind of a quantitative analysis of the variations in printed line widths is an attempt to predict the affect of the input parameters-speed and pressure and also the affect of other variable factors on the print quality. Also, there were a few prints, which were not dark enough for the Veritas to collect data.

7.5 Analysis using Moiré Concept

In order to determine the regional distortion across a whole substrate, we employed a Moiré technique. This method allows us to compare the shape of printed pattern (grid preferred) to a reference pattern, normally the mask, to obtain a map of overall distortion.

7.5.1 Introduction to Moiré

The overlay of two periodic or quasiperiodic structures with periodicities and alignment similar to each other produces a new coarse structure, known as a moiré pattern. For many years, these patterns have been used as powerful tools in scientific and engineering metrology [1]. To evaluate distortions in our substrates, we applied moiré patterns produced by overlay of a printed substrate and the tooling mask with same grid patterns in micron feature sizes. We will begin by describing moiré patterns formed with arrays of parallel lines. Results obtained from this special case can be applied in a straightforward way to analysis of moiré patterns formed from grids with micron dimensions [32, 34].
Quantitative determination of distortions of the arrays from distortions of the moiré patterns requires a description of the patterns and their relation to the geometry of the underlying arrays. For simplicity, consider moiré patterns produced with a reference array of lines with periodicity d and a test array of lines with periodicity ad, where a is a constant. Figure 7.4.2.1 illustrates the geometry. The periodicity of the moire pattern, d_M, and its angular orientation, φ, depends on the angle, θ, between the two arrays of lines, and the values of a and d in the following fashion:

$$d_M = \frac{a}{(1+a^2-2a\cos\theta)^{1/2}}d \quad (1)$$

And

$$\sin\varphi = \frac{\sin\theta}{(1+a^2-2a\cos\theta)^{1/2}} \quad (2)$$

In our case, $a \approx 1, \theta \leq 4^\circ$, simplified forms can be used for (1) and (2)[1,2]:

$$d_M \approx \frac{d}{|\theta|} \quad (3)$$

$$\sin\varphi \approx 1 \qquad (4)$$

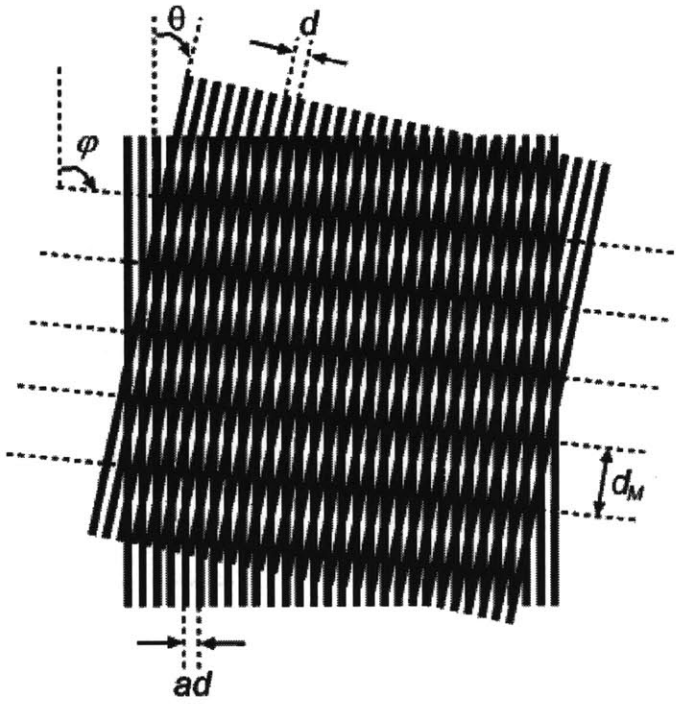

Fig 7.5.1 shows Moiré fringes formed by two linear arrays of lines and spaces [32].

Formula (3) and (4) are the mathematic foundation for the algorithm used in our software developed for distortion analysis. If the intersections of the moiré fringes formed between substrate and mask can be located, the underlying distortion of the substrate shall be calculated accordingly. The two primary advantages of applying moiré concept in distortion analysis are:

- Cost effective, no expensive microscope or other equipment is required in the analysis;
- Fast analysis, it gives the distortion distribution for the whole substrate in one test.

7.5.2 Software introduction

The Mat lab image processing tool box provides a very powerful tool to develop software specifically for imaging processing. Our program was developed in this environment.

Two approaches were considered for locating the intersections of moiré pattern in the early stage, manual pick-up and automated selection. The two methods have different strengths and weakness.

- Manual pick-up: In this method, substrate and mask are superimposed with a certain angle, θ, at which the scale of the moiré pattern is desirable. They are then placed directly on the screen of the computer. An operator should click the intersections in a predefined sequence while the software takes in all the locations. The advantage of this method is it's highly flexible and can be applied even when the distortion is significant. However, it takes a long time for an operator to select all a points on a moiré pattern.

- Automated selection: In this approach, the first step is the same as in manual pick-up method. The second step, instead of placing substrate and mask on a computer screen, is to take a picture of moiré pattern and use the software to read the image. The intersections will be selected automatically by the software. The main advantage of this method is its throughput which can be hundreds time faster than manual pick-up, however, the application of this method is limited to substrates with small distortion. When the distortion is significant, the software shall have problems selecting points in the right sequence.

Both methods were tested. In our case, substrate distortion is always significant compared to traditional micro contact printing, so the manual pick-up method was finally adopted. However, as more research is done and the process optimization moves forward, automated selection can replace this method in the near future.

After the points are selected, the software will generate a perfect reference grid and display the grid and the selected points on the screen with lines between them indicating the distortion of the moiré pattern. Then, using the algorithm introduced in the previous section, the software calculates the actual distortion of the underlying pattern and gives a diagram showing the distortion. It also provides several distortion distribution histograms. Fig 7.5.2 illustrates the whole process using manual pick-up approach.

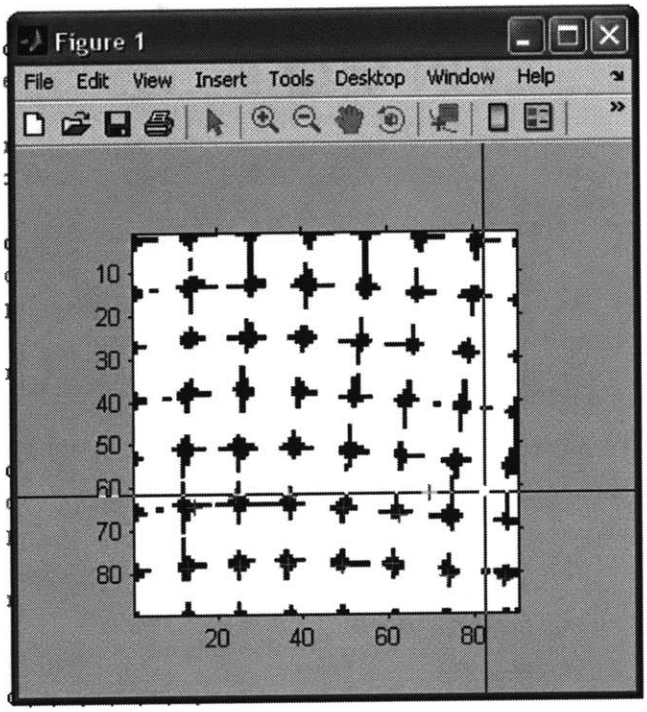

Fig 7.5.2 (a) The interface of intersection selection step, intersections are picked up from bottom to top, from left to right; red crosses mark the points selected. Please note that real interface is only a white background without black dots. Those black dots here are used to for illustration purpose, representing the intersections on the moiré pattern formed between the substrate and the mask, both of which are fixed on the screen with tap. Unit of both ax.: 1/20 inch

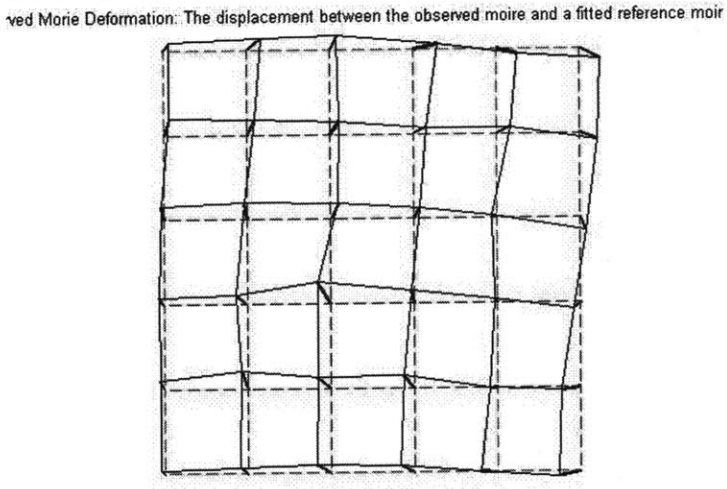

Fig 7.5.2 (b) Observed moiré deformation. Based on the selected points, a perfect grid (the red dashed grid) is generated by the software as the reference to quantify the deformation; then the selected points are compared to the perfect grid to find the deformation of the moiré pattern at each intersection (the short blue lines are the deformation vectors).

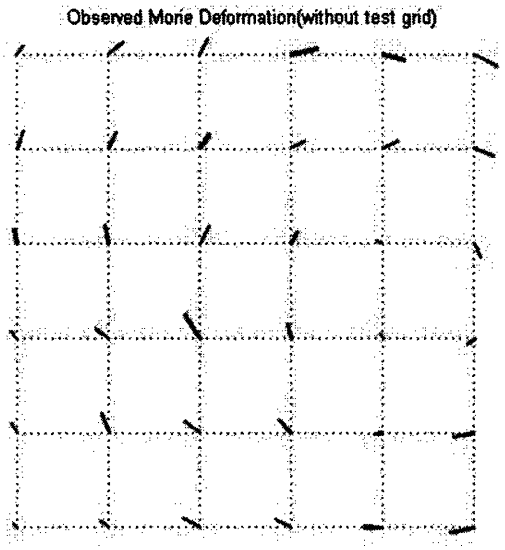

Fig 7.5.2 (c) The simplified picture of observed moiré deformation. Dotted lines form the perfect grid while short red lines are the deformation vectors.

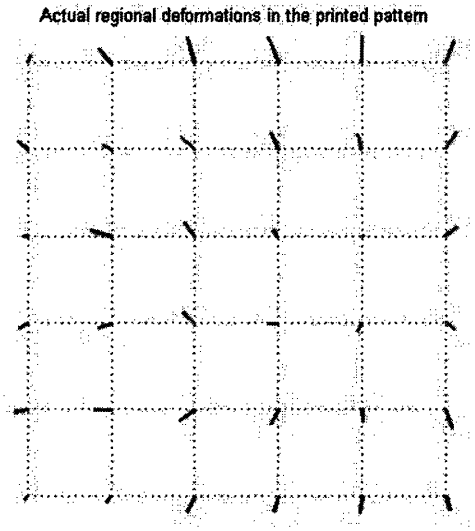

Fig 7.5.2 (d) Actual regional deformations in the printed pattern. Based on the observed moiré pattern, using the algorithm described earlier in this chapter, the actual regional deformations in the printed pattern are calculated and represented in the short red lines.

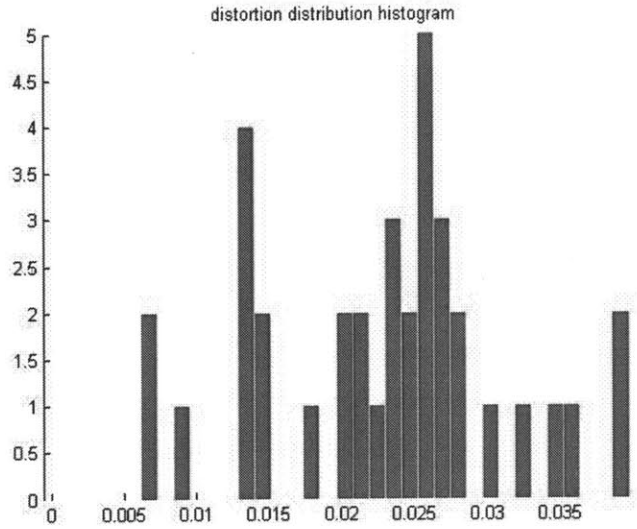

Fig 7.5.2 (e) Distortion distribution histogram. This histogram categorizes intersections based on their distortions from the perfect grid. Unit of X axis: mm, unit of Y axis: number.
Figure 7.4.2.2 Process of manual pick-up approach

7.5.3 Analysis

The quality of the patterns printed significantly affects the reliability of the moiré analysis. Four types of substrates are not suitable for this method:

A. Substrates with faint patterns: they make it very difficult for the operators to eye spot and pick up intersections because the contrast in moiré pattern will be so weak that intersections are hard to identify.
B. Substrates with double or multiple prints: double or multiple prints forms two or multiple moiré patterns interfering with each other, making it impossible to select points.
C. Substrates with many collapses: collapses covering large area actually change the pattern printed, thus change the moiré pattern.
D. Substrates with a pattern of good quality in only a small area: in a small area, the advantages of moiré analysis are greatly reduced. In addition, it is hard to collect enough points to provide reliable results.

In our groping experiments, only two substrates fall out of the four types. Moiré analysis was applied to these two. The first one is printed at 15 rpm with 10 psi

pressure. The second one is printed at 25 rpm with 10 psi pressure. Both used continuous printing method. The results are shown in Fig 7.5.3. Note that the distortions (red lines) displayed in (a) and (c) are amplified by a factor of $1/\theta$ with value equaling 57.3 and 60.2 respectively.

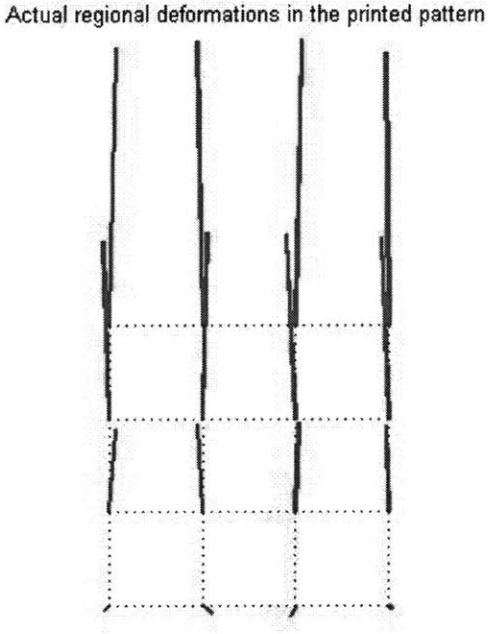

Fig 7.5.3 (a) Actual deformations calculated from 16 selected intersections. Dotted lines form the perfect grid while short red lines are the deformation vectors

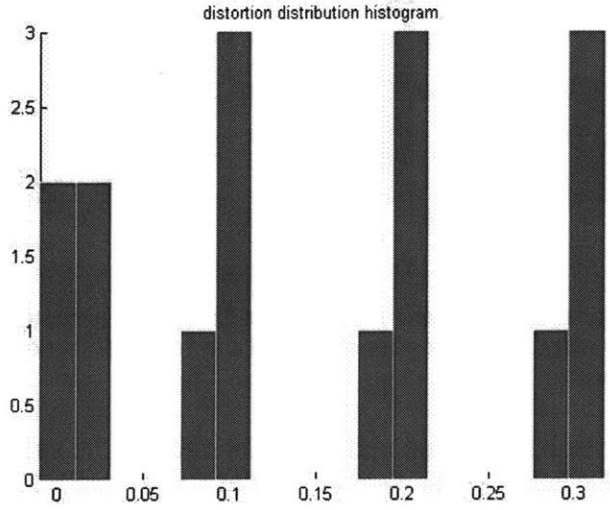

(b)

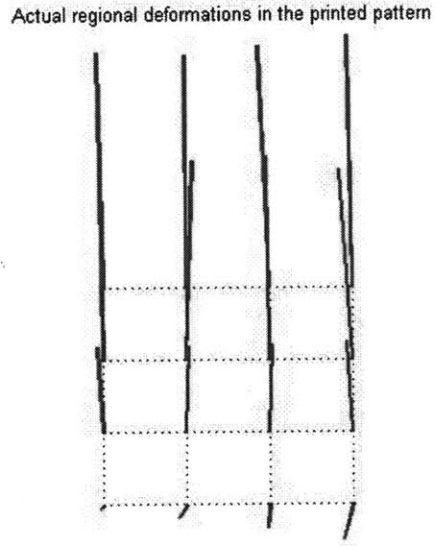

Fig 7.5.3 (c) Actual deformations calculated from 16 selected intersections. Dotted lines form the perfect grid while short red lines are the deformation vectors

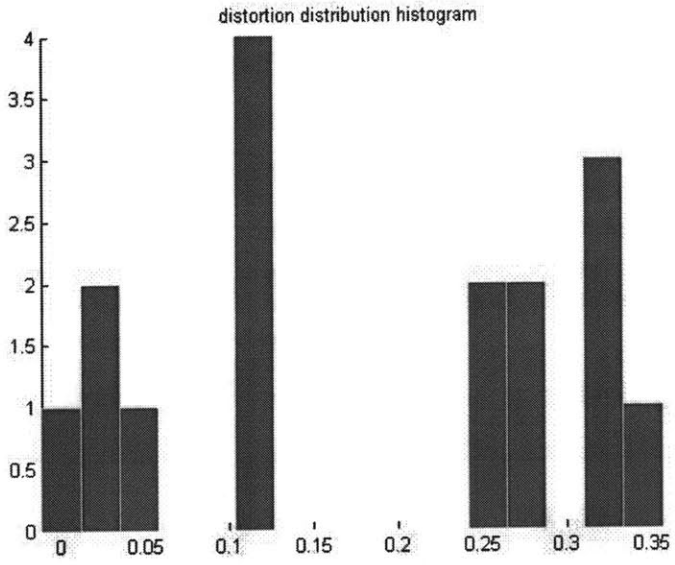

(d)

Fig 7.5.3 (a), (b) actual regional deformations and distortion distribution histogram of substrate printed at 15 rpm and 10 psi; (c), (d) actual regional deformations and distortion distribution histogram of substrate printed at 25 rpm and 10 psi.

The results show very significant regional distortions across the substrate, 300-350μms within 40mm. Another important observation is that the distortions are highly directional, indicating anisotropic underlying causes. After comparing the direction of distortion and

the direction of printing, we notice that the stretch happens along the feeding direction. Three factors can be attributed for the phenomenon:

A. While mounting, the stamp is always stretched for certain amount around the cylinder to guarantee the mounting quality in current situation.

B. Ten PSI, a high pressure value, can cause considerable deformation while printing.

C. The friction between substrate and stamp also play a role in stretching the stamp while printing takes place. This can explain the higher distortion value of substrate printed with higher speed.

Currently, we don't know exactly how distortions are divided among these factors due to limited experiment results. In the future, with cleverly designed experiments and more data, detailed conclusion can be drawn.

7.6 Conclusion

In this chapter we saw three methods of analyzing the data. Qualitative analysis simply distinguished between good and bad prints and traced back to their root causes while Quantitative analysis measured the variation in the feature size and the regional distortions in the printed pattern. Although results suggest that there is a lot of distortion, it helps us in deciding the next step in the process development phase. The next chapter discusses all the improvements in the hardware that can be made and gives a rough plan for future work on this project.

Chapter 8

Conclusions and Future Work

A working prototype was developed that was used to demonstrate the feasibility of integrating the flexography concept into micro contacting. The prototype was designed to achieve continuous high volume production with good quality. The prototype demonstrates that with the integration of flexography elements, high quality, high flexibility, high production rate and low cost manufacturing using micro contact printing is indeed possible.

A series of following experiments were conducted on the prototype to explore the capability of the machine and the effects of pressure, ink concentration and printing time on the printing quality. The printing time is again broken into two factors, printing speed and wrap angle. The results from the experiments suggest that with current machine setup, to achieve the best printing quality, the ideal combination of parameters is high ink concentration, low wrap angle, 10 feet/min printing speed with 3 psi pressure. Several other important observations are also drawn from those results:

A. The prototype is capable of printing at 100 feet/min. Although the printing quality deteriorates with increasing printing speed, but the deterioration is not significant. In addition, there is no evidence that the ink transfer process is affected by the printing time which is controlled by the printing speed or that 100 feet/min is the speed limitation. This observation suggests that the chemistry of micro contact printing will not be the bottle neck when the printing speed is within a large range for a given wrap angle, leaving more room and motivation for improvement of the system.
B. All the parameters tested, namely pressure, printing speed, wrap angle and ink concentration, and are important for the output quality. However, the primary parameter is ink concentration, which has to be kept high to achieve a good

printing quality.

C. Distortions of the printed substrates are high and always highly directional. Three factors are considered to be the main causes: (1) stretching of stamp during mounting; (2) sheer force caused by the friction between stamp and substrates while printing; (3) non-uniformity of the stamp.
D. Print with large wrap angle is susceptible to double or multiple printing. The lack of good tension control for substrate feeding is considered to be the primary cause.

Based on all the observations, in order to optimize and industrialize the prototype system, it's recommended that future work should focus on three aspects:

A. Fabrication of highly uniform PDMS stamp. Non-uniformity as small as tens of microns would cause a disaster in the printing, which means highly uniform PDMS stamp is the foundation of the printing system. Current fabrication technique is not reliable and efficient enough to meet industrial standard. Methods like using large silicon wafer mask to cast one big stamp at one time should be considered and tested.
B. Automation of the system. Currently, much of the printing process is not automated, causing a lot of problem and slowing down the whole process. Substrate feeding system with precise tension control and real-time pressure monitor and control system should be added.
C. Mounting of stamp. This is another critical step for successful printing. Current process should be modified to be more robust, otherwise different methods like using magnetic stamps or vacuum should be adopted to replace the current process.

As the last suggestion, many more designed experiments should be conducted on either this prototype or an improved device to really optimize the process parameters. It is expected that not only will this lead to better knowledge about the process but may also play an important role in creating new chemistries for better outcomes. Suggested improvements to the prototype include:

A. An absolute measure of printing pressure. This will enable a better control of pressure. Possible solution can be to instrument the machine bearing holders with load cells.

B. A tension control system for the substrate and a feeding – take-up system for handing. The system can prevent the substrates from slid and multiple print, enabling the machine to conduct high speed print experiment. The required techniques and equipment can be borrowed from flexography.

C. A one-piece tool molding method that will give more uniform tool thickness. The method shall expedite the stamp preparation process and more importantly, provides highly uniform stamps that are essential for the printing quality. One solution is to use a big silicon wafer to cast PDMS stamps with dimensions enough to wrap on the plate cylinder.

D. A synchronized driving system. The system provides better speed control of printing and reduces the chance of slid between cylinders. The required techniques and equipment can again be borrowed from flexography industry.

References

[1] Shaw,J.M.; Seidler, P.F., "Organic Electronics," *IBM Journal of Reasearch and Development*, Vol. 45, No.1, 2001

[2] Marinelli, C.; Gammel, P., "Rise of Printed Organic Electronics," *Future Fab Intl.*,Vol. 22, 2007

[3] Jaeger, R.C., "Introduction to MicroElectronic Fabrication," Vol.5, 2002

[4] Xia, Y.; Qin, D.; Whitesides, G.M., "Microcontact Printing with a Cylindrical Rolling Stamp: A Practical Step Toward Automatic Manufacturing of Patterns with Submicrometer Sized Features," *Adv. mater.*, 1996, Vol.8(12), pp.1015-1017

[5] Xia, Y.; Whitesides, G.M.,"Soft Lithography," *Annu. Rev. Mater. Sci.*1998, Vol. 28,pp.153-184

[6] Zhao, X.-M., et al.1996. Fabrication of single-mode polymeric waveguides using micromolding in capillaries. *Adv. Mater.* 8: 420-24.

[7] Kumar, A.; Whitesides, G.M.,"Features of Gold having Micrometer to Centimeter Dimensions Can Be Formed Through a Combination of Stamping with an Elastomeric Stamp and an Alkanethiol 'Ink' Followed by Chemical Etching," *App. Phys. Lett.,* 1993, Vol. 63(14), pp.2002-2004

[8] Xia, Y.; Whitesides, G.M.,"Soft Lithography," Angew. Chem. Int. Ed. 1998.37.550-575

[9] B. Michel, et al. "Understanding Microcontact Printing," IBM J. RES. & DEV. VOL. 45 NO. 5 SEPTEMBER 2001

[10] Kim, E.; Xia, Y.; Whitesides, G.M ., "Polymer microstructures formed by moulding in capillaries," *Nature *, 1995, Vol.376, pp.581-584

[11] Xia, Y.;Kim, E.; Whitesides, G.M., "Microcontact Printing of Alkanethiols on Silver and Its Application in Microfabrication," *J. Electrochem. Soc., *1996, Vol.143(3), pp.1070-1079

[12] Kim, E.; Xia, Y.; Zhao, X.-M.; Whitesides, G.M.,"Solvent-assisted microcontact molding: A convenient method for fabricating three-dimensional structures on surfaces of polymers," *Adv. Mater. *, 1997, Vol.9 (8), pp. 651-65

[13] Love, J. C.; Estroff, L. A.; Kriebel, J. K.; Nuzzo, R. G.; Whitesides, G. M.,"Self-Assembled Monolayers of Thiolates on Metals as a Form of Nanotechnology," *Chem. Rev.,2005 Vol.**105* (4),pp.1103-1170

[14] Kumar, A.; Abbott, N.L.; Kim, E.; H. Biebuyck; Whitesides G.M., "Patterned Self-Assembled Monolayers and Meso-Scale Phenomena," *Acc. Chem. Res.,*1995, Vol.28, pp.219

[15] Li, X.-M.; Huskens, J.; Reinhoudt, D.N. "Reactive self-assembled monolayers on flat and nanoparticle surfaces, and their application in soft and scanning probe lithographic nanofabrication technologies," *J. Mater. Chem*., 2004, Vol.14, pp.2954-2971

[16] James L Wilbur, Amit Kumar, Hans A Biebuyck, Enoch Kim and George M Whitesides Department of Chemistry, Harvard University, Cambridge, MA 02138, USA

[17] Hui, C. Y.; Jagota, A; Lin, Y. Y.; Kramer, E.J.,"Constraints on Microcontact Printing Imposed by Stamp Deformation *Langmuir*," 2002, Vol.18, pp.1394-1407

[18] Xia Y. Geroge M Whitesides, Soft Lithography pp155-165

[19] Masuda, T.;Isobe, E.;Higashimura, T.;Tagada., K.," Poly[1-(trimethylsilyl)-1-propyne]: a new high polymer synthesized with transition-metal catalysts and characterized by extremely high gas permeability," *J. Am. Chem. Soc.,* 1983, Vol.105, pp.7473

[20] Bain CD, Whitesides GM.1989. Angew Chem. Int. Ed. Engl. 28:506-12

[21] Gardner TJ, Frisbie CD, Whrighton MS. 1995. J. Am. Chem. Soc. 117:6927-33

[22] A.M. Kendale, Automation of soft lithographic microcontact printing. S.M. Thesis, Massachusetts Institute of Technology, 2001

[23] Xia, Y.; Qin, D.; Whitesides, G.M., "Microcontact Printing with a Cylindrical Rolling Stamp: A Practical Step Toward Automatic Manufacturing of Patterns with Submicrometer Sized Features," *Adv. mater.*, 1996, Vol.8(12), pp.1015-1017

[24] Rogers, J.A.,"Toward Paperlike Displays," ***Science,*** 2001, Vol.291, pp.1502-1503

[25] Delamarche, E.; Geissler, M.; Vichiconti, J.; Graham, W. S.; Andry, P. A.; Flake, J. C. et al., "Electroless Deposition of NiB on 15 Inch Glass Substrates for the Fabrication of Transistor Gates for Liquid Crystal Displays," ***Langmuir,2003,*** Vol.19 (14), pp.5923-5935

[26] *Odom, T. W.; Love, J. C.; Wolfe, D.B.; Paul, K.E.; Whitesides, G.M.,"Improved Pattern Transfer in Soft Lithography Using Composite Stamps," *Langmuir, *2002, Vol.18(13), pp.5314-5420

[27] Xia, Y.; Zhao, X-M.; Whitesides, G.M. *Microelectron. **Eng.,* 1996, Vol.32, pp.255.

[28] Delamarche, E.; Schmid, H.; Bietsch, A.; Larsen, N. B.; Rothuizen, H.; Michel, B.; Biebuyck, H.,"Transport Mechanisms of Alkanethiols during Microcontact Printing on Gold," *J. Phys. Chem. B.,*1998, Vol. 102(18), pp.3324-3334

[29] Libioulle L.; Bietcvh A.; Schmid H.; Michel B.; Delamarche E., "Contact Inking Stamps for Microcontact Printing of Alkanethiols on Gold".

[30] Siconolfi, F.N., et al., "Flexography: Principles and Practices," Fourth Edition, 1995

[31] Zhao, X.M.; Wilbur, J.L.; Whitesides, G.M., *Langmuir,* 1996, 12, pp. 3257-3264

[32] John A. Rogers, Kateri E. Paul, and George M. Whitesides, ''Quantifying distortions in soft lithography'', J. Vac. Sci. Technol. B 16.1., Jan/Feb 1998

[33] Blackman, S., Gregory; Jagota, A.; Sharp, K., "Mechanical Behavior of Elastomeric Stamps during Microcontact Printing Patterns: Direct Observations of Stamps and Inks," E.I Du Pont de Nemours and Co., Inc., Central Research Department, Wilmington, DE 19880-0323

[34] Yi Zhao, Xin Zhang, ''Determination of the Deformations in Polymeric Nanostructures using Geometric Moiré Techniques for Biological Applications'', 13th International Conference on Solid-State Sensors, Actuator and Microsystems (Transducer '05), Seoul, Korea, June 5–9, 2005

[35] www.wikipedia.com ."Quality," Site accessed on 08/21/2007.

[36] Decré, M.M.J et al., "Wave Printing (I): Towards Large-Area, Multilayer Microcontact Printing". Philips Research Laboratories Eindhoven,
Mass Products and Technologies Department, Philips Center for Industrial Technology, Prof. Holstlaan 4, 5656AA Eindhoven, The Netherlands.

[37] Parallax Inc, Flexiforce Demo Kit (#28017), 03/2003

[38] www.usdigital.com, Technical Data sheet-MS23C, USDigitals. Accessed on 08/2007

[39] www.tekscan.com, Technical Datasheet (Model#A101), Tekscan incl, Accessed on 08/2007

Appendix A

MS23C

Size 23 Stepper Motor

Description:

The MS23C is an industry standard NEMA size 23 stepper motor featuring high torque and all metal construction. The MS23C is optimized for microstepping and offers 1.8° per full step with 200 full steps per revolution. The stepper motor is manufactured especially for US Digital by NMB Technologies, a well-established industry leader in the designing and manufacturing of precision stepper motors and ball bearings.

The standard MS23C is a 4-wire connector interface that has already been configured for Bipolar Parallel operation. The MS23C comes with a 12" long cable / connector assembly (custom cable lengths are available). The MS23C configuration is ideal for use with our MD2S microstepping motor driver and is highly recommended. When driving in Bipolar Series, Bipolar Half Coil or Unipolar modes the MS23C is available with 8-wire leads.

The MS23C stepper motor may be ordered from stock with or without a pre-attached US Digital kit encoder. Compatible kit encoders include the E5D, E5S, E6D and E6S. US Digital will mount these encoders at no extra cost. Combined pricing is available on the fifth page of this data sheet.

This product is part of US Digital's Motion Control Building Block. To learn more, please see the corresponding section on the fifth page of this data sheet.

The stepper motor has a 0.250" diameter shaft on the front and rear. The shaft endplay has been limited to 0.010" for excellent encoder performance and minimum vibration.

Features:

- Industry standard size 23 stepping motor
- Two phase, 1.8° step angle, 200 full steps per rev.
- High angle accuracy
- Optimized for microstepping applications
- 8-wire motor lead or 4-pin connector for maximum versatility
- 110 oz-in running torque
- High quality NMB ball bearings
- Minimal endplay
- All metal construction
- Double-ended shaft construction
- Encoder ready, available with or without US Digital encoder attached
- US Digital warrants its products against defects and workmanship for two years. See complete warranty for details.

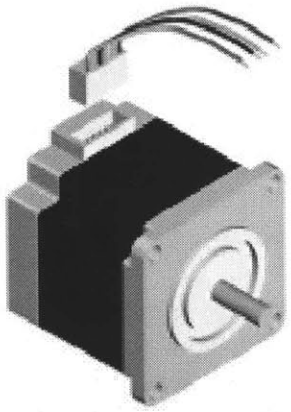

MS23C (standard)
4-wire connector

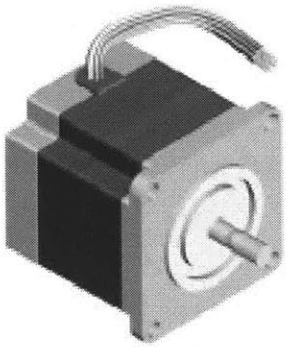

MS23
8-wire leads

Mechanical Drawing (Shown with MS23C):

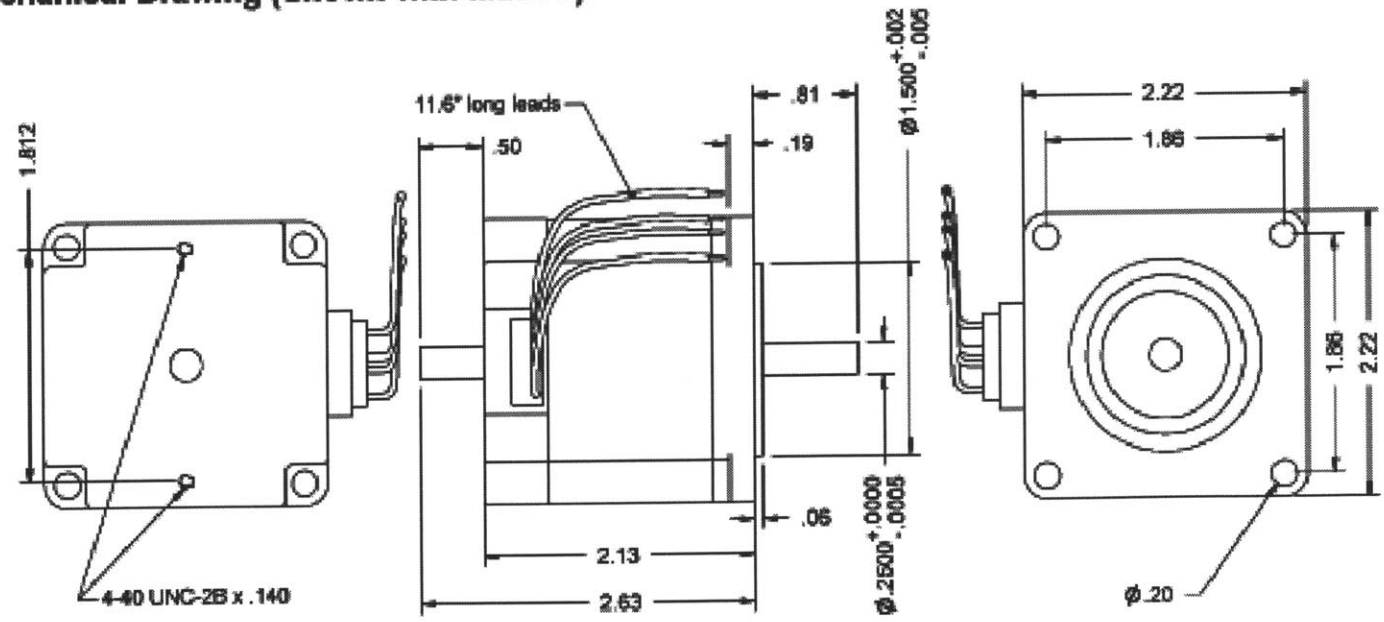

US DIGITAL
info@usdigital.com ▪ www.usdigital.com
Local: 360.260.2468 ▪ Sales: 800.736.0194
Support: 360.397.9999 ▪ Fax: 360.260.2469
1400 NE 136th Ave. ▪ Vancouver, Washington ▪ 98684 ▪ USA

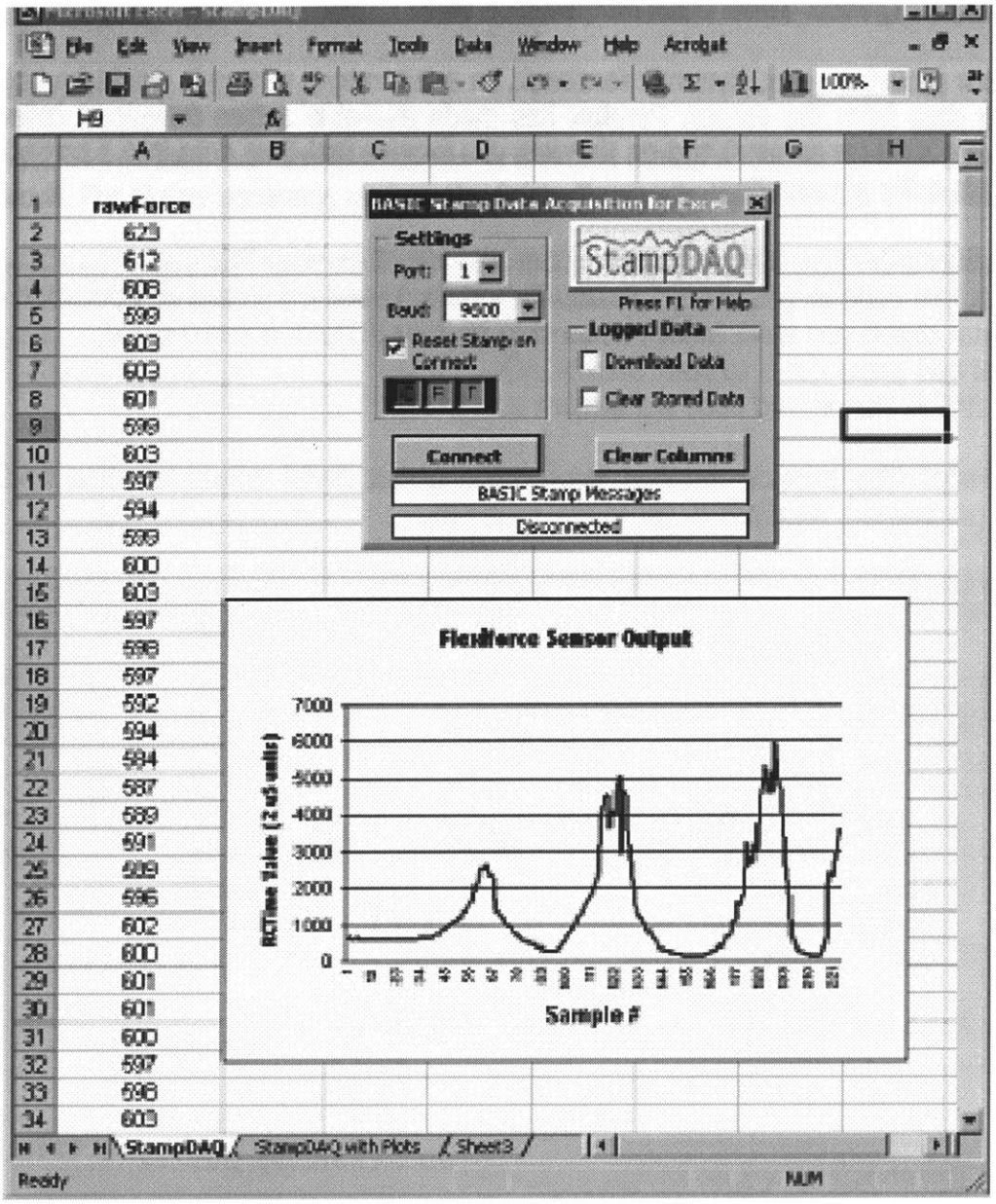

Figure 3: Example StampDAQ Output

The Flexiforce sensor provides quick, dynamic feedback. In a laboratory setting it would be helpful to obtain real-time streaming data from the sensor. Parallax has made available a free download called StampDAQ. StampDAQ is an Excel 2000 (or greater) add-on that lets you receive real-time data into a spreadsheet. To use StampDAQ follow this order of operation:

1. Download StampDAQ from www.parallax.com and install on your PC.
2. Run the sample code in your BASIC Stamp 2 module. Leave the Board of Education (or whatever experimental circuit you have made) connected to your PC with a serial cable.
3. Open Excel and press ctrl-S to start StampDAQ.
4. Reset the BASIC Stamp and data will stream into Excel.

The StampDAQ "Help" files provide detailed information about serial communication and baud rates, configuration and parameters required to setup the program.

```
' Flexiforce StampDAQ.bs2

' Example with the Flexiforce sensor and StampDAQ
' ($STAMP BS2)
' ($PBASIC 2.5)

' -----[ Declarations ]----------------------------------------------------

rawForce        VAR     word            ' Stores raw output
sensorPin       CON     15              ' Flexiforce sensor circuit
sPin            CON     16              ' Serial transmit pin
Baud            CON     84              ' 9600, 8-bit, no polarity, true

' -----[ Main Routine ]----------------------------------------------------

Initialize:
  PAUSE 1000
  SEROUT sPin,Baud,[CR]                 'prep StampDAQ buffer
  SEROUT sPin,Baud,[CR,"LABEL,rawForce",CR]
                                        'Label column with rawForce
  SEROUT sPin,Baud,["CLEARDATA",CR]     'Clear all data

Display:
  HIGH 15                               'Discharge capacitor
  PAUSE 2
  RCTIME sensorPin,1,rawForce           'Measure R/C charge time
  SEROUT sPin,Baud,["DATA,rawForce,", DEC rawForce,CR]
                                        'Send data to StampDAQ

GOTO Display
```

Example #1: Simple Output Example

The first example demonstrates the Flexiforce sensor in a BASIC Stamp resistor/capacitor time-discharge measurement circuit. For higher accuracy, replace the 0.01 uF capacitor with the 0.1 uF capacitor.

```
' Flexiforce Simple.bs2
' Displays R/C Discharge Time in BASIC Stamp DEBUG Window
' {$STAMP BS2}
' {$PBASIC 2.5}

' -----[ Declarations ]----------------------------------------------------

rawForce        VAR     word            ' Stores raw output
sensorPin       CON     15              ' Flexiforce sensor circuit

' -----[ Main Routine ]----------------------------------------------------

Measure:
  HIGH sensorPin                        ' Discharge the capacitor
  PAUSE 2
  RCTIME sensorPin,1,rawForce           ' Measure RC charge time
  DEBUG Home, "Flexiforce raw output = ", dec rawForce,CR
GOTO Measure
```

Flexiforce Specifications

Physical Properties	
Thickness	0.005" (0.127 mm)
Length	8.000" (203 mm)
Width	0.55" (14 mm)
Active Sensing Area	0.375" (9.53 mm) diameter
Connector	3 pin post connector

Typical Performance	
Linearity (error)	< ±5% (Line drawn from 0 to 50% load)
Repeatability	< ±2.5% of Full Scale (Conditioned Sensor, 80% of Full Force Applied)
Hysteresis	< 4.5 % of Full Scale (Conditioned Sensor, 80% of Full Force Applied)
Drift	< 3% / logarithmic time (Constant Load - 25 lb.)
Rise Time	< 20 µsec (Impact load - recorded on Oscilloscope)
Operating Temperature	15°F - 140°F (-9°C - 60°C)*

Figure 1: Flexiforce Specifications

The force response of this sensor is approximately 1.6 lbs. using the Flexiforce Sample Drive Circuit on www.tekscan.com. However, the best way to determine the correlation is by placing known weights on the end of the sensor and recording your RCTime values from the sample BASIC Stamp programs.

Example Circuit

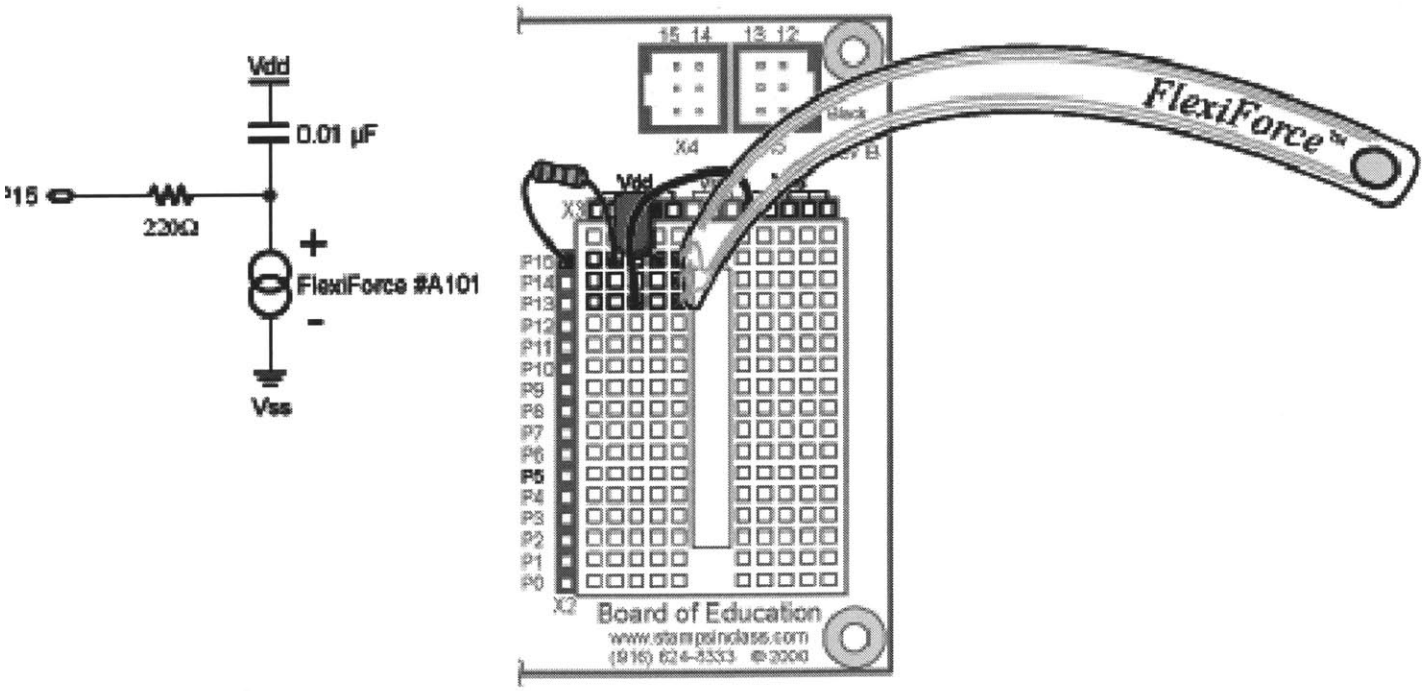

Figure 2: Example Schematic and Pictorial

PARALLAX
599 Menlo Drive, Suite 100
Rocklin, California 95765, USA
Office: (916) 624-8333
Fax: (916) 624-8003

General: info@parallaxinc.com
Technical: support@parallaxinc.com
Web Site: www.parallaxinc.com
Educational: www.stampsinclass.com

Flexiforce Demo Kit (#28017)

Single Element Pressure Sensor

Tekscan's FlexiForce® sensor measures force between two surfaces. The sensor output exhibits a high degree of linearity, low hysteresis and minimal drift compared to other thin-film force sensors. The Flexiforce single element sensor acts as a resistor in an electrical circuit. When the sensor is unloaded, its resistance is very high. Resistance decreases when force is applied to the sensor. The resistance can be read by connecting an ohmmeter to the outer two pins of the sensor and applying a force to the round tab sensing area at the end of the film.

The resistance of the Flexiforce sensor is proportional to weight. The sensor included in your kit is rated at 1.6 lbs.[1] The purpose of the Parallax example circuit is only to demonstrate the resistive nature of the sensor with a resistor/capacitor discharge time measurement circuit; no correlations to weight are made in these examples.

Packing List

Verify that your Flexiforce Demo Kit has the following components:

- (1) Flexiforce thin-film sensor
- (1) 220 ohm resistor
- (1) 0.1 uF capacitor
- (1) 0.01 uF capacitor

The sample code and circuit uses the Parallax BASIC Stamp 2 module. With a change of directive at the top of each PBASIC program the code may also be used in BASIC Stamp 2SX, 2e, 2p, and 2pe modules. The second sample program uses StampDAQ, an Excel add-on which receives real-time data into an Excel spreadsheet. StampDAQ works with Excel 2000 or higher and can be downloaded for free from www.parallax.com.

[1] Based on resistor values in the Tekscan "Flexiforce Sample Drive Circuit" drawing on the manufacturer's web site http://www.tekscan.com. Standard force range of this sensor can be changed to have a full-scale 1 lb – 1,000 lb response by changing driving voltage and feedback resistors and driving voltage in their sample circuit.

MS23C

Size 23 Stepper Motor

Motion Control Building Block:

The MS23C may be combined with US Digital's MD2S microstepping motor driver and one of our switching power supplies to provide a motion control building block that simply requires step and direction input signals to set the MS23C stepper motor in motion. Alternatively, the quadrature outputs from an optical encoder may be connected to the step and direction inputs to control the motor position.

Switching Power Supplies:
For more detailed information on the power supplies, see either the PS-24, PS-48, PS-150 and PS-320 data sheets.

Part Number: PS-24 (24V, 2.5A)	$25.20 / 1 • $19.64 / 100
Part Number: PS-48 (48V, 2.5A)	$50.40 / 1 • $39.27 / 100
Part Number: PS-320-24 (24V, 12.5A)	$177.45 / 1 • $145.95 / 100
Part Number: PS-320-48 (48V, 6.5A)	$177.45 / 1 • $145.95 / 100


PS-24


PS-48

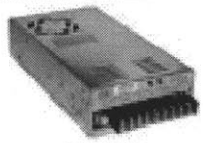
PS-320

Microstepping Motor Driver:
US Digital offers a programmable microstepping motor driver that interfaces with size 17 through size 42 stepper motors. The MD2S is specially tuned to match US Digital's size 23 stepper motor and provide excellent Speed-Torque characteristics.

For more detailed information on the microstep drive, see the MD2S data sheet.

Part Number: MD2S	$136.00 / 1 • $104.00 / 100

Ordering Information:

Motor Only :
$62.00 / 1
$55.65 / 10
$50.40 / 50
$45.00 / 100

Part #:

Motor only — Optical Encoder Version (optional)

MS23C — ☐ — ☐ — ☐ — ☐

Interface:
C = 12" 4-wire connector assembly.*
(blank) = 8-wire leads.

Optical Encoder:
E5D = Differential 1" encoder.
E5S = Single-ended 1" encoder.
E6D = Differential 2" encoder.
E6S = Single-ended 2" encoder.

CPR:

E5S / E5D		E6S / E6D
32***	500	64***
50	512	100
96	540**	200
100	720***	400
110**	900***	500
120**	1000	512**
192	1016**	1000
200	1024	1024
250	1250***	1800***
256		2000
360		2048
400		2500

Options:
I = Index (3rd channel).
L = Avago compatible pin-out.****

Notes:
* Recommended for use with the Motion Control Building Block.
** Index option not available.
*** 32, 64, 720, 900, 1250 and 1800 only available with index.
**** Only available with differential versions (E6D and E6D).

Motor with Optical Encoder:

E5D Standard:	E5D Index/HiRes: (Hi Res >=1000 CPR)	E5S Standard:	E5S Index/HiRes: (Hi Res >=1000 CPR)	E6D Standard:	E6D Index/HiRes: (Hi Res >=2000 CPR)	E6S Standard:	E6S Index/HiRes: (Hi Res >=2000 CPR)
$116.60 / 1	$125.88 / 1	$102.95 / 1	$112.37 / 1	$127.20 / 1	$136.87 / 1	$113.45 / 1	$122.71 / 1
$104.22 / 10	$112.48 / 10	$92.09 / 10	$100.47 / 10	$116.55 / 10	$125.69 / 10	$102.90 / 10	$111.41 / 10
$91.82 / 50	$98.86 / 50	$81.47 / 50	$88.62 / 50	$107.10 / 50	$115.61 / 50	$93.45 / 50	$101.20 / 50
$81.72 / 100	$87.96 / 100	$72.53 / 100	$78.86 / 100	$98.55 / 100	$106.58 / 100	$85.95 / 100	$93.32 / 100

Technical Data, Rev. 06.22.07, June 2007
All information subject to change without notice.

US DIGITAL
info@usdigital.com • www.usdigital.com
Local: 360.260.2468 • Sales: 800.736.0194
Support: 360.397.9999 • Fax: 360.260.2469
1400 NE 136th Ave. • Vancouver, Washington • 98684 • USA

MS23C

Size 23 Stepper Motor

Motor Winding Diagrams:

MS23C (4-wire connector):

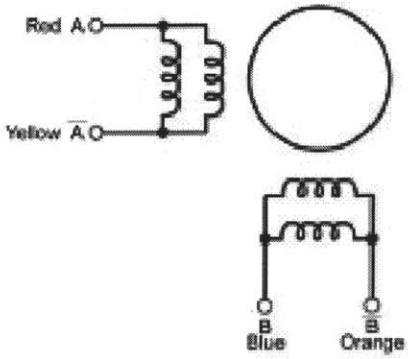

MS23 (8-wire leads):

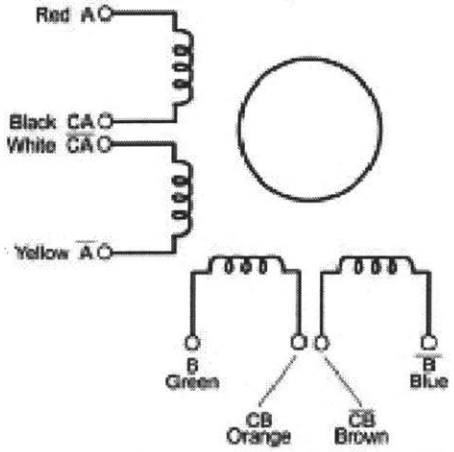

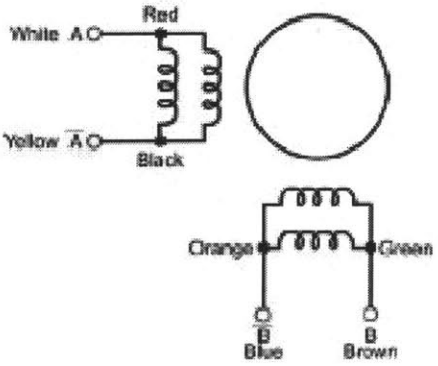

MS23C Pin-out:

Pin	Description	Color
1	A channel	Red
2	NC	-
3	A- channel	Yellow
4	B channel	Blue
5	NC	-
6	B- channel	Orange

Switching Sequence:

Step	A	B	$\overline{A}$	$\overline{B}$
1	+	+	-	-
2	-	+	+	-
3	-	-	+	+
4	+	-	-	+

> For clockwise rotation facing motor output shaft.

Absolute Maximum Ratings:

Parameter	Max.	Units
Case Temperature	100	°C
Winding Temperature	130	°C
Ambient Temperature	50	°C
Motor Power Dissipation	7.65	Watts
Maximum Phase Current*	-	-

* See bipolar parallel specifications below.

Mechanical Specifications:

Parameter	Dimension	Units	Notes
Weight	23.94	oz.	
Full Step Angle	1.8	degrees	
Step Angle Accuracy	±5	%	
Insulation Resistance	100 500	MOhm VDC	Min.
Dielectric Strength	500	VAC	for 1 minute
Radial Play	0.0008	in.	Max. (1 lbs load)
End Play	0.010	in.	Max.
Detent Torque	4.9	oz-in	
Rotor Inertia	3.96×10^{-3}	oz-in-s^2	

Bipolar Parallel Specifications:

Parameter	Value	Units
Full Step Current	4.20	Amps
Micro Step Current	5.90	Amps
DC Resistance	0.43	Ohms
Inductance	1.73	mH
Power Per Phase	7.65	Watts
Power Total	15.3	Watts
Holding Torque (static torque)	140	oz-in
Running Torque	110	oz-in

Compatible Cables / Connectors:

Encoder Version:

Finger-latching:		
5-pin	10-pin	Description
CON-FC5-22*	CON-FC10	Connector
CA-3133-1FT**		Connector on one end with 4 12" wires
CA-3132-1FT**		Connector on one end with 5 12" wires
CA-3131-6FT**	CA-4217-6FT	Connector on one end of a 6' shielded round cable
	CA-4174-6FT***	Same as CA-4217, but for L-option only
CA-3620-6FT**	CA-3619-6FT	Connectors on both ends of a 6' shielded round cable
	CA-3807-FT***	Same as CA-3807, but for L-option only

* 22 AWG is standard. 24, 26 and 28 AWG are also available.
** Single-ended output and accompanying cables are typically designed for cable lengths of 6 feet or less; for longer cable lengths, differential output and accompanying cables are recommended.
*** Avago / Agilent / HP compatible cable assembly.

Attention:
> Specify cable length when ordering.
> Custom cable lengths are available. See the Cables / Connectors data sheet for more information.

MS23C:

Stepper Motor Connector:	
6-pin	Description
CA-6352-1FT	Connector on one end with 4 12" wires (two pins are left open)

> The above cable is included with the MS23C and does not need to be ordered separately.

Encoder Version Pin-outs:

Pin	5-pin Single-ended	10-pin Differential Standard	10-pin Differential Avago (L-option)
1	Ground	Ground	No connection
2	Index	Ground	+5VDC power
3	A channel	Index-	Ground
4	+5VDC power	Index+	NC
5	B channel	A- channel	A- channel
6		A+ channel	A+ channel
7		+5VDC power	B- channel
8		+5VDC power	B+ channel
9		B- channel	Index-
10		B+ channel	Index+

US DIGITAL
info@usdigital.com ▪ www.usdigital.com
Local: 360.260.2468 ▪ Sales: 800.736.0194
Support: 360.397.9999 ▪ Fax: 360.260.2469
1400 NE 136th Ave. ▪ Vancouver, Washington ▪ 98684 ▪ USA

MS23C

Size 23 Stepper Motor

Mechanical Drawings (Encoder Version):

- The drawings below only show the MS23C (4-wire connector); the MS23 (8-wire leads) *IS ALSO* available with an encoder attached.
- For encoder information see each encoder's data sheet.

E5D:

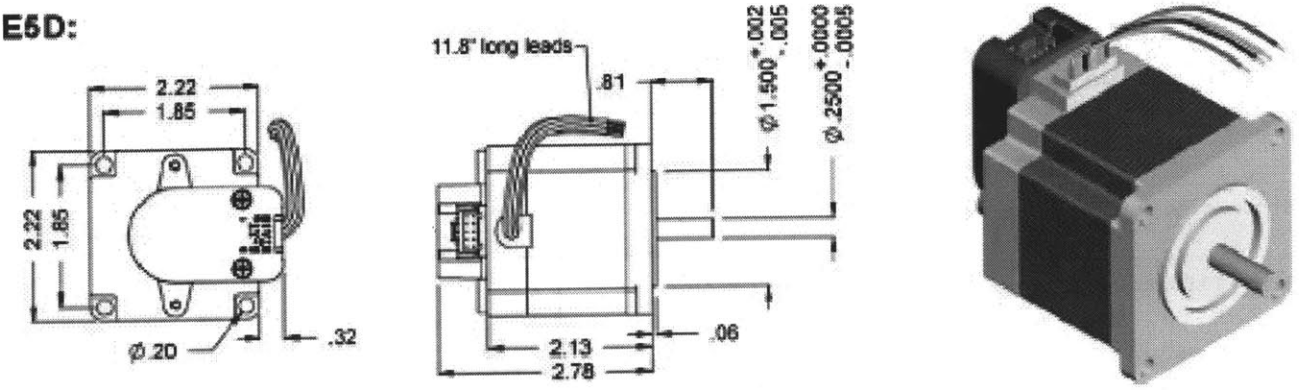

E5S:

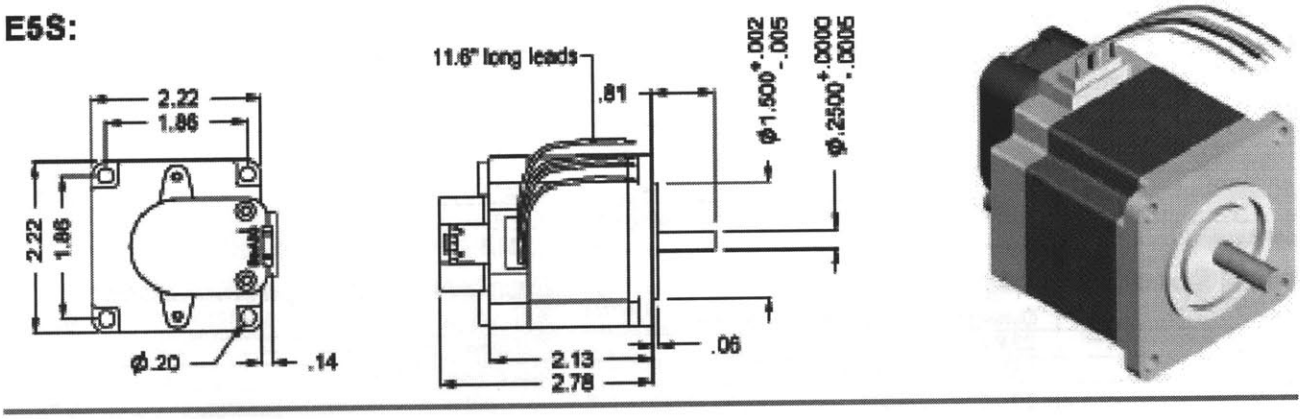

E6D:

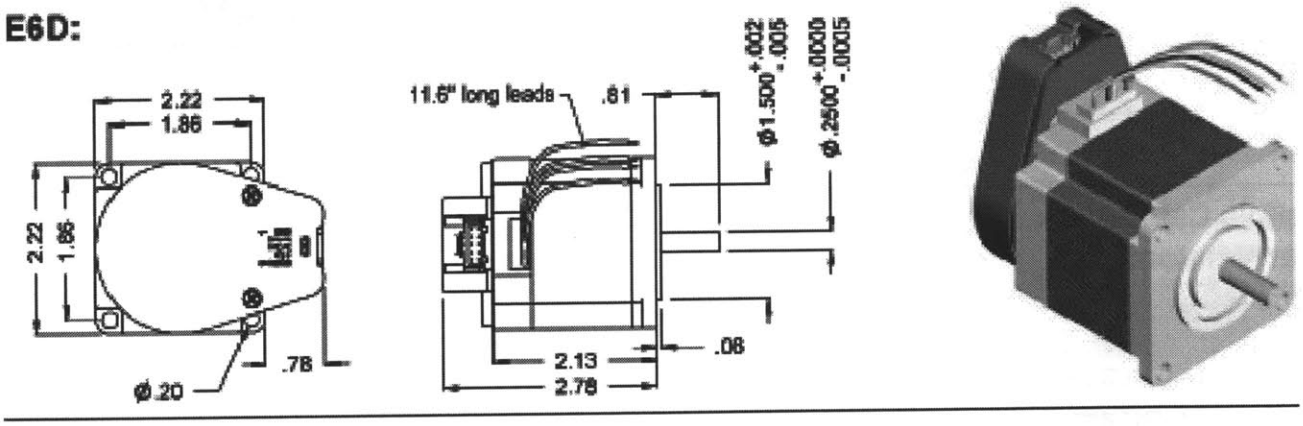

E6S:

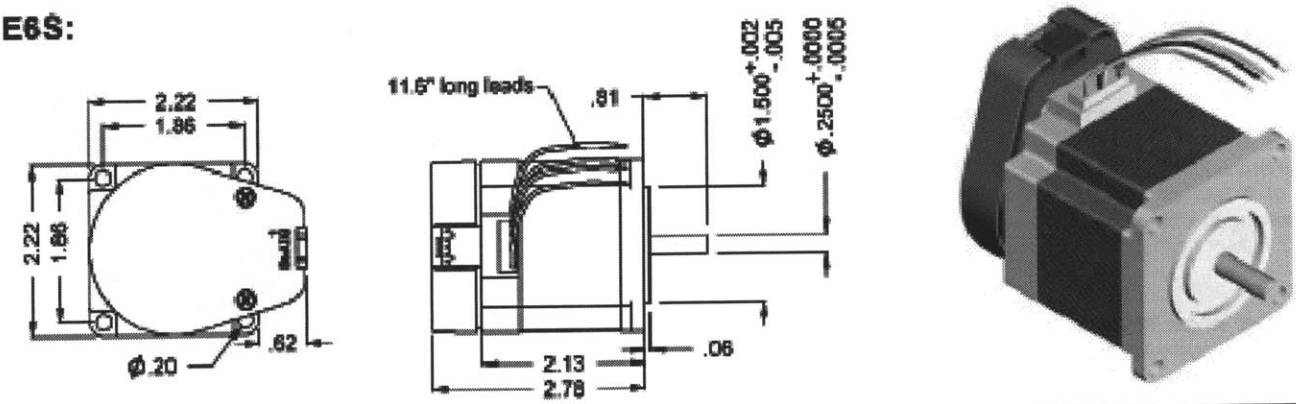

US DIGITAL

info@usdigital.com ▪ www.usdigital.com
Local: 360.260.2468 ▪ Sales: 800.736.0194
Support: 360.397.9999 ▪ Fax: 360.260.2469
1400 NE 136th Ave. ▪ Vancouver, Washington ▪ 98684 ▪ USA

MS23C

Size 23 Stepper Motor

Speed-Torque Curves:

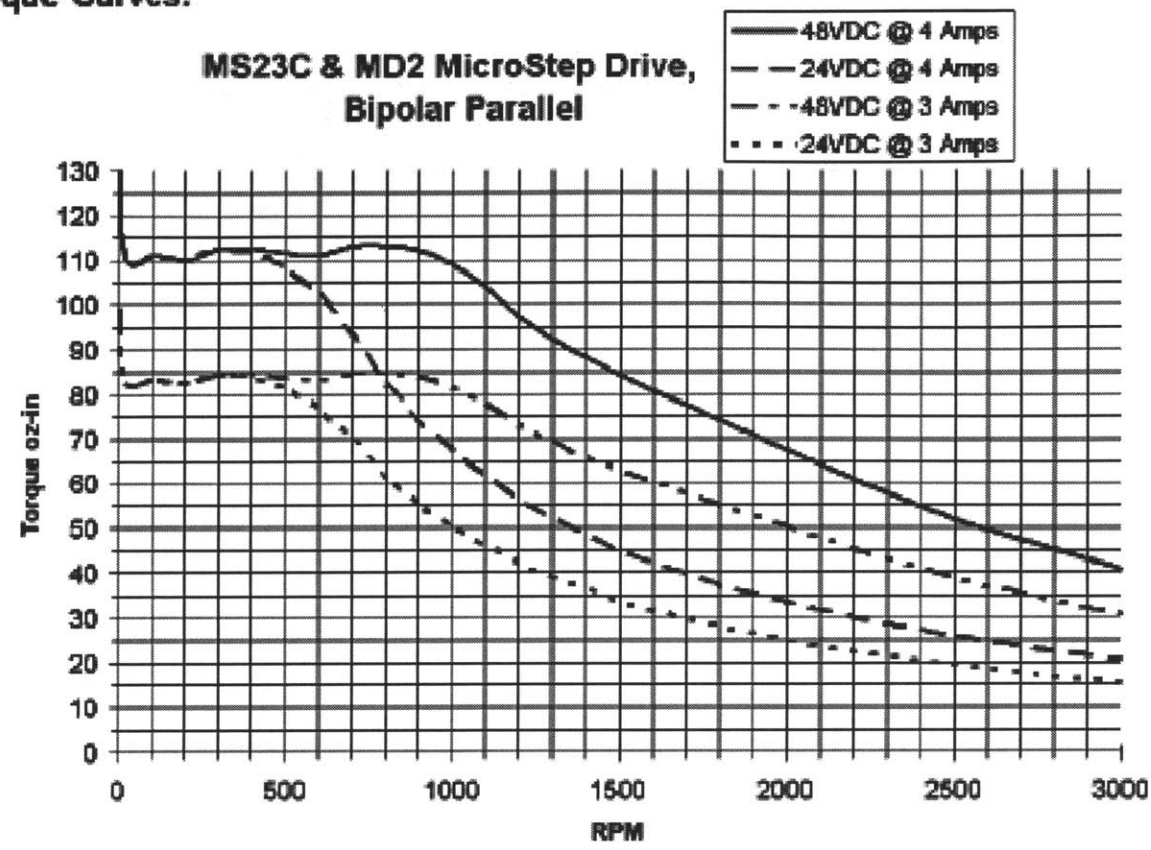

Terms & Definitions:

Wiring Configuration:

Bipolar Parallel Mode: Both coils of phase A are connected in parallel, likewise for phase-B. The inductance seen by the external motor driver is one fourth that of Bipolar Series Mode. This mode provides the highest speed performance for the lowest power supply voltage.

Bipolar Series Mode: Both coils of phase A are connected in series, likewise for phase-B. The inductance seen by the external motor driver is four times greater than that of Bipolar Parallel Mode. This mode allows the motor to be driven with a lower current for lower speed applications.

Stepping:

Full Stepping: The process of switching the motor current from -100% to +100% (two increments) in a four step quadrature sequence. Each step (quadrature state) moves the rotor 1.8 degrees (one full step). This type of driver is simple and low cost, and produces maximum vibration and noise.

Half Stepping: The process of switching the motor current in three levels from -100% to 0 to +100% (three increments) in an eight step sequence. Each step moves the rotor 0.9 degrees (one half step). This type of driver is also relatively simple and produces medium vibration and noise.

Microstepping: The process of progressively metering the motor current from -100% to +100% in many small increments, moving the rotor from one pole position to the next in tiny steps (microsteps). The current waveform is similar to a sine wave. One full sine wave will move the rotor 1.8 degrees (one full step). This driver is currently the most popular and provides smooth, quiet movement with very fine control of rotor position. Typical microstepping drivers provide selectable resolutions from 1 to 256 microsteps per full step (200 to 51,200 microsteps per motor revolution). For best microstepping performance, the shape of the internal motor poles are modified for smooth pole-to-pole transitions. This minimizes the natural detent force, linearizing the movement, and minimizing vibration. The MS23C has been optimized for microstepping.

Torque:

Detent Torque: The amount of torque required to rotate a stepper motor shaft without power applied to the windings.

Holding Torque: The amount of torque required to rotate the stepper motor shaft while the windings are energized with maximum DC current at zero speed.

Pull In Torque: The amount of torque a stepper motor can produce without losing synchronism starting from a zero speed state, then given a fixed frequency step sequence.

Pull Out Torque: The amount of torque a stepper motor can produce at a particular operating speed without losing synchronism.

Speed / Torque Limits:

Why does the torque decline as the speed increases, and what sets the maximum speed? Torque is directly proportional to the current flowing in the motor coils. The current must ramp up to +100%, then -100% 50 times per revolution (200 quadrature states). The coil inductance opposes changes in current. The current does not have enough time to ramp up to maximum at higher speeds. Before it reaches maximum, it must reverse and ramp the other direction. The maximum rate of current change is inversely proportional to the square of the inductance and directly proportional to the power supply voltage. Maximum speed with minimum torque loss is obtained by minimizing the coil inductance and maximizing the power supply voltage. Since bipolar parallel mode has one fourth the inductance, of bipolar series mode, the torque is much greater at higher speeds. The MS23C motors have been designed for minimum inductance.

US DIGITAL

info@usdigital.com ▪ www.usdigital.com
Local: 360.260.2468 ▪ Sales: 800.736.0194
Support: 360.397.9999 ▪ Fax: 360.260.2469
1400 NE 136th Ave. ▪ Vancouver, Washington ▪ 98684 ▪ USA

Technical Data Sheet (Model #A101)

This data sheet provides technical performance characteristics for *FlexiForce*® Sensors.

Physical Properties

Thickness	.005" (0.127 mm)
Length	8.00" (203 mm), 6.00", 4.00", or 2.00"
Width	0.55" (14 mm)
Sensing Area	.375" diameter (9.53 mm)
Connector	3-pin Male Square Pin

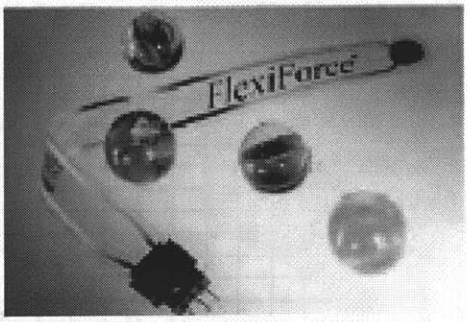

Recommended Excitation Circuit

$V_o = -V_T * (R_F/R_S)$; where $R_F = 20$ kΩ

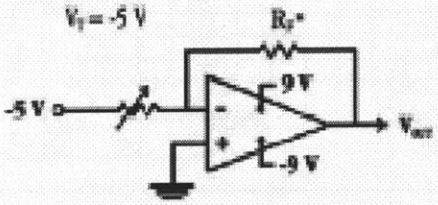

*The range for R_F is 1 kΩ to 100 kΩ
**Resistance at no load is 20 MΩ

Typical Performance / Evaluation Conditions

Linearity (Error)	< ±5%	Line drawn from 0 to 50% load
Repeatability	< ±2.5% of Full Scale	Conditioned Sensor, 80% of Full Force Applied
Hysteresis	< 4.5 % of Full Scale	Conditioned Sensor, 80% of Full Force Applied
Drift	< 3% per Logarithmic Time	Constant Load of 25 lbs. (111 N)
Rise Time	< 20 µsec	Impact Load, Output recorded on Oscilloscope
Operating Temperature	15°F - 140°F (-9°C - 60°C)*	

*Force reading change per degree of temperature change: ±0.2%/°F (0.36%/°C)
*For loads less than 10 lbs., the operating temperature can be increased to 165°F (74°C)

Tekscan, Inc. - 307 W. First Street - S. Boston, MA 02127 - USA - www.tekscan.com
T(800)248-3669(617)464-4500x223 - F(617)464-4266\269-8389 - flexiforce@tekscan.com

Appendix B

Data Used for Quantitative Analysis

25 rpm, 15 psi: Exp #1

Top Left Corner Vertical		0.0299
		0.0294
		0.03
		0.0293
		0.0297
		0.0292
		0.0292
		0.0289
		0.029
		0.0275
		0.0292
		0.0293
		0.0296
		0.0222
		0.0283
		0.0291
		0.0291
		0.0293
		0.0289
SD	0.00164588	0.029
Mean		**0.028805**

Top Right Corner Vertical		0.0288
		0.0289
		0.0285
		0.0288
		0.0284
		0.0285
		0.0288
		0.0289
		0.0292
		0.0286
		0.0287
		0.0283
		0.028
		0.0285
		0.0286
		0.0295
		0.0288
		0.0288
		0.0291
SD	0.000339349	0.0291
Mean		**0.02874**

Top Left Corner horizontal		0.0329
		0.0342
		0.0331
		0.0322
		0.0342
		0.0341
		0.0336
		0.0333
		0.0356
		0.0296
		0.0343
		0.0298
		0.0356
		0.0307
		0.0339
		0.0351
		0.0354
		0.035
		0.0346
SD	0.001773608	0.034
Mean		**0.03356**

Top Right Corner Horizontal		0.0313
		0.0326
		0.0328
		0.0327
		0.0327
		0.0333
		0.0331
		0.0331
		0.0335
		0.0328
		0.0334
		0.0334
		0.0332
		0.0336
		0.0337
		0.0338
		0.0333
		0.0333
		0.0338
SD	0.000583456	0.0338
Mean		**0.03316**

Bottom Left Corner Vertical		0.0275
		0.0272
		0.0271
		0.0273
		0.0271
		0.0267
		0.0272
		0.03
		0.0276
		0.0275
		0.0265
		0.0272
		0.0274
		0.0282
		0.0275
		0.028
		0.0279
		0.0282
		0.0272
SD	0.000725839	0.0277
Mean		**0.02755**

Bottom Left Corner Horizontal		0.0285
		0.0286
		0.0283
		0.0277
		0.0283
		0.0282
		0.029
		0.0293
		0.0286
		0.0287
		0.0283
		0.0285
		0.0276
		0.0291
		0.0291
		0.0292
		0.0289
		0.0297
		0.0296
SD	0.000564638	0.0283
Mean		**0.028675**

Bottom Right Corner Vertical		0.0284
		0.0283
		0.0283
		0.0287
		0.0286
		0.0286
		0.0286
		0.0287
		0.0287
		0.0279
		0.0272
		0.0285
		0.0289
		0.028
		0.0281
		0.0283
		0.0286
		0.0291
		0.0283
SD	0.000446153	0.0276
Mean		**0.02837**

Bottom Right Corner Horizontal		0.0304
		0.0296
		0.0311
		0.0316
		0.0307
		0.031
		0.0305
		0.0296
		0.0316
		0.0328
		0.0328
		0.0311
		0.029
		0.0303
		0.0329
		0.0332
		0.0326
		0.031
		0.0308
SD	0.001214864	0.03
Mean		**0.03113**

	Center Vertical	0.0299
		0.0298
		0.0292
		0.0296
		0.0298
		0.0294
		0.0295
		0.0291
		0.0295
		0.0292
		0.0293
		0.0287
		0.0291
		0.0294
		0.0299
		0.0302
		0.0294
		0.0293
		0.0295
SD	0.000342437	0.0294
	Mean	**0.02946**
	Center Horizontal	0.0325
		0.0326
		0.0329
		0.0325
		0.0316
		0.0314
		0.0325
		0.0325
		0.0327
		0.0325
		0.0319
		0.032
		0.0328
		0.0327
		0.0323
		0.0307
		0.0322
		0.0318
		0.0319
SD	0.000549737	0.0326
	Mean	**0.03223**

10 rpm, 15 psi: Exp#1

Top Left Corner				**Top Right Corner**	
Horizontal		0.0279		**Horizontal**	0.0287
		0.0278			0.0288
		0.0276			0.0279
		0.0286			0.0284
		0.028			0.029
		0.0275			0.0293
		0.0277			0.0288
		0.0275			0.0288
		0.0268			0.0295
		0.0277			0.0296
		0.0274			0.0293
		0.0274			0.0285
		0.0278			0.0287
		0.0275			0.0284
		0.0279			0.0297
		0.0282			0.0292
		0.0278			0.0294
		0.0273			0.0302
		0.0272			0.0299
SD	0.000395235	0.0272	**SD**	0.000593473	0.0283
Mean		**0.02764**	**Mean**		**0.02902**
Top Left Corner vertical		0.0271	**Top Right Corner Vertical**		0.0257
		0.0269			0.0267
		0.0272			0.0255
		0.0267			0.0253
		0.0269			0.0259
		0.0271			0.0264
		0.0275			0.0262
		0.027			0.0265
		0.0267			0.0258
		0.027			0.0251
		0.0269			0.0255
		0.027			0.026
		0.0275			0.026
		0.027			0.0258
		0.0275			0.0253
		0.0274			0.0263
		0.0271			0.0265
		0.0272			0.0266
		0.0279			0.0259
SD	0.000303488	0.0274	**SD**	0.000465974	0.0257
Mean		**0.02715**	**Mean**		**0.025935**

Bottom Left Corner horizontal			Bottom Right Corner horizontall		
		0.0277			0.0262
		0.0282			0.0256
		0.0289			0.0262
		0.0289			0.0263
		0.0283			0.0269
		0.0279			0.0261
		0.0292			0.0264
		0.0283			0.0265
		0.028			0.0265
		0.0291			0.0266
		0.0297			0.027
		0.0291			0.028
		0.0279			0.0272
		0.0273			0.0272
		0.0282			0.0269
		0.0282			0.027
		0.0282			0.0276
		0.028			0.0271
		0.028			0.0294
SD	0.000605653	0.0278	**SD**	0.000811675	0.0268
Mean		**0.028345**	**Mean**		**0.026875**
Bottom Left Corner Vertical			**Bottom Right Corner Vertical**		
		0.0279			0.0258
		0.0273			0.026
		0.028			0.0258
		0.0268			0.0261
		0.0278			0.0263
		0.0281			0.0261
		0.0275			0.0261
		0.029			0.0258
		0.0275			0.0258
		0.0265			0.0263
		0.0274			0.0265
		0.0281			0.0259
		0.0278			0.0258
		0.0275			0.0257
		0.0278			0.0258
		0.0287			0.0259
		0.0291			0.0258
		0.0293			0.0257
		0.0285			0.0254
SD	0.000745001	0.0287	**SD**	0.00025105	0.0259
Mean		**0.027965**	**Mean**		**0.025925**

	Center Horizontal	0.0274
		0.0266
		0.0268
		0.027
		0.0278
		0.0272
		0.0276
		0.0284
		0.0278
		0.0269
		0.0272
		0.0276
		0.0276
		0.027
		0.0271
		0.027
		0.0271
		0.0271
		0.0268
SD	0.000438268	0.0269
	Mean	**0.027245**
	Center Vertical	0.0267
		0.0269
		0.027
		0.0269
		0.0271
		0.0262
		0.0269
		0.0272
		0.027
		0.0269
		0.0265
		0.0271
		0.0273
		0.0268
		0.027
		0.0271
		0.0271
		0.0276
		0.0269
SD	0.000292179	0.0272
	Mean	**0.02697**

10 rpm, 8 psi: Exp#2

Top Left Corner Horizontal		
		0.0281
		0.0279
		0.0285
		0.0289
		0.029
		0.0287
		0.0277
		0.0276
		0.0274
		0.0273
		0.0273
		0.0274
		0.0272
		0.0269
		0.0267
		0.0278
		0.0279
		0.0279
		0.0264
SD	0.000695	0.0279
Mean		**0.027725**
Top Left Corner vertical		0.0238
		0.0237
		0.0235
		0.0239
		0.0236
		0.0236
		0.0236
		0.0235
		0.024
		0.0241
		0.0241
		0.0238
		0.0239
		0.0229
		0.023
		0.0234
		0.0235
		0.0233
		0.0233
SD	0.00033003	0.0234
Mean		**0.023595**

Top Right Corner Horizontal		
		0.031
		0.0315
		0.0314
		0.029
		0.0296
		0.0297
		0.0298
		0.03
		0.0299
		0.0298
		0.0295
		0.0294
		0.0293
		0.0292
		0.0291
		0.0294
		0.0295
		0.0297
		0.0298
SD	0.000697571	0.0297
Mean		**0.029815**
Top Right Corner vertical		0.023
		0.0232
		0.0239
		0.0241
		0.0243
		0.0244
		0.0244
		0.0245
		0.0246
		0.0245
		0.0245
		0.0238
		0.0239
		0.024
		0.0241
		0.0242
		0.0244
		0.0245
		0.0245
SD	0.000438028	0.0245
Mean		**0.024165**

Bottom Left Corner Horizontal		0.025
		0.0258
		0.0248
		0.0242
		0.0245
		0.0239
		0.0233
		0.024
		0.0235
		0.0237
		0.0236
		0.0229
		0.0227
		0.0225
		0.023
		0.0241
		0.0242
		0.0248
		0.025
SD	0.00086139	0.0243
Mean		**0.02399**

Bottom Left Corner vertical		0.0239
		0.0238
		0.0239
		0.0242
		0.0239
		0.0243
		0.0235
		0.0229
		0.021
		0.021
		0.0215
		0.0218
		0.0219
		0.023
		0.0239
		0.0235
		0.0233
		0.0229
		0.0221
SD	0.00108792	0.022
Mean		**0.022915**

Bottom Right Corner Horizontal		0.025
		0.0248
		0.0243
		0.0239
		0.0236
		0.0238
		0.0239
		0.0229
		0.0225
		0.0224
		0.0229
		0.0234
		0.0233
		0.0231
		0.0239
		0.024
		0.0242
		0.0243
		0.0245
SD	0.000742878	0.0246
Mean		**0.023765**

Bottom Right Corner vertical		0.018
		0.0185
		0.02
		0.0178
		0.0189
		0.0195
		0.02
		0.0187
		0.0189
		0.019
		0.0193
		0.0195
		0.019
		0.0185
		0.0189
		0.0185
		0.018
	3.6	0.0183
	0.04747627	0.0182
SD	0.000656225	0.0179
Mean		**0.01877**

	Center Horizontal	0.029
		0.0298
		0.03
		0.0303
		0.0305
		0.031
		0.0298
		0.0288
		0.0279
		0.0277
		0.0278
		0.0269
		0.0268
		0.0265
		0.0264
		0.0278
		0.028
		0.029
		0.03
SD	0.001414734	0.0292
	Mean	**0.02866**
	Center Vertical	0.0242
		0.0245
		0.02457
		0.0247
		0.0246
		0.0249
		0.025
		0.0251
		0.0248
		0.0249
		0.025
		0.0247
		0.0246
		0.0245
		0.0245
		0.0248
		0.0249
		0.025
		0.0253
SD	0.000304584	0.0255
	Mean	**0.0248035**

10 rpm, 3 psi: Exp#2

Top Left Corner				**Top Right Corner**		
Horizontal		0.0202		**Horizontal**		0.0203
		0.0202				0.02
		0.0203				0.0201
		0.0199				0.0199
		0.0191				0.0201
		0.0203				0.0189
		0.0197				0.0202
		0.019				0.0201
		0.0215				0.0198
		0.0195				0.0199
		0.02				0.0199
		0.0189				0.02
		0.0194				0.0201
		0.0191				0.0202
		0.0201				0.0203
		0.0192				0.0201
		0.0195				0.0202
		0.0198				0.0202
		0.0194				0.0202
SD	0.00061084	0.0198	**SD**		0.000305045	0.0203
Mean		**0.019745**		**Mean**		**0.02004**
Top Left Corner vertical		0.0173		**Top Right Corner vertical**		0.0198
		0.0184				0.0196
		0.0181				0.0194
		0.0185				0.0196
		0.0183				0.0194
		0.0177				0.0198
		0.0181				0.0203
		0.0185				0.0198
		0.0185				0.0199
		0.0189				0.0195
		0.0186				0.0199
		0.0182				0.0201
		0.0182				0.0201
		0.0181				0.0196
		0.0195				0.0208
		0.0192				0.02
		0.0183				0.0198
		0.0194				0.0207
		0.0198				0.0201
SD	0.00067207	0.0198	**SD**		0.000378223	0.02
Mean		**0.01857**		**Mean**		**0.01991**

Bottom Left Corner Horizontal		0.0196		**Bottom Right Corner Horizontal**	0.0187
		0.0192			0.01912
		0.0192			0.01912
		0.0199			0.0189
		0.0191			0.0186
		0.0195			0.0192
		0.0199			0.0186
		0.0194			0.0197
		0.0195			0.0193
		0.0193			0.0193
		0.0194			0.0191
		0.0195			0.0188
		0.0194			0.0199
		0.0191			0.0181
		0.0199			0.0187
		0.0196			0.0185
		0.0191			0.0184
		0.0193			0.0187
		0.0193			0.0186
SD	0.00026052	0.0197	**SD**	0.0004399	0.0187
Mean		**0.019445**	**Mean**		**0.018902**
Bottom Left Corner vertical		0.0189		**Bottom Right Corner vertical**	0.0175
		0.0193			0.0179
		0.0194			0.018
		0.0197			0.0183
		0.0196			0.0188
		0.0195			0.0187
		0.0195			0.0189
		0.0197			0.0186
		0.0201			0.0184
		0.0195			0.0185
		0.0194			0.019
		0.0195			0.01902
		0.0196			0.019
		0.0196			0.0184
		0.0197			0.0185
		0.0189			0.0187
		0.0189			0.0189
		0.0187			0.0179
		0.0186			0.0179
		0.0185			0.0176
SD	0.00046614	0.0184	**SD**	0.000508799	0.0175
Mean		**0.0192857**	**Mean**		**0.0183819**

	Center Horizontal	0.0189
		0.0197
		0.0193
		0.0178
		0.018
		0.0189
		0.0178
		0.0179
		0.0174
		0.0174
		0.0174
		0.0173
		0.0173
		0.0179
		0.0178
		0.018
		0.0189
		0.0186
		0.0186
SD	0.000710893	0.0185
	Mean	**0.01817**
	Center Vertical	0.0177
		0.0177
		0.0176
		0.0173
		0.0179
		0.0173
		0.0173
		0.0176
		0.0178
		0.0174
		0.0174
		0.0175
		0.0175
		0.0173
		0.0173
		0.0175
		0.0172
		0.0173
		0.0176
SD	0.000194395	0.0176
	Mean	**0.01749**

Experiment #3 Grating (left to right) 400 microns spacing:	top to bottom	Spacing 1	spacing 2	spacing 3	spacing 4	spacing 5
		0.4443	0.4442	0.4427	0.4429	0.4427
		0.4439	0.4442	0.443	0.4431	0.4427
50 rpm, 3 psi reverse		0.4452	0.4451	0.4426	0.4426	0.4425
		0.4455	0.4452	0.4425	0.4426	0.4429
		0.4445	0.4439	0.4431	0.443	0.4426
		0.4444	0.4437	0.4432	0.4431	0.4428
		0.4439	0.4436	0.4396	0.4432	0.4428
		0.4438	0.4433	0.4436	0.4436	0.4431
		0.4441	0.4432	0.4437	0.4435	0.4435
		0.4438	0.4431	0.4445	0.4441	0.4434
		0.4442	0.4431	0.4445	0.4441	0.4432
		0.4438	0.4435	0.4448	0.4442	0.4437
		0.4438	0.4434	0.4445	0.4442	0.4435
		0.4438	0.4432	0.4446	0.4442	0.4438
		0.4438	0.4437	0.4444	0.4448	0.261
		0.4438	0.4435	0.4447	0.4445	0.4442
		0.4438	0.4438	0.4444	0.4441	0.4438
		0.4439	0.4438	0.4442	0.4443	0.4438
150 microns		0.1459	0.1458	0.1459	0.1456	0.1452
		0.1464	0.1459	0.1464	0.146	0.1453
		0.146	0.146	0.146	0.1466	0.1458
		0.1464	0.1463	0.1464	0.1463	0.1464
		0.1461	0.1458	0.1461	0.1462	0.1454
		0.1462	0.1464	0.1462	0.1461	0.1463
		0.146	0.1461	0.146	0.1459	0.1458
		0.1458	0.1461	0.1458	0.1459	0.1459
		0.1456	0.1461	0.1456	0.146	0.1455
		0.1463	0.1463	0.1463	0.1462	0.1456
		0.1446	0.146	0.1446	0.1461	0.146
		0.1458	0.1464	0.1458	0.1455	0.1454
		0.1459	0.146	0.1459	0.1455	0.1453
		0.1453	0.146	0.1453	0.1455	0.1453
		0.1458	0.146	0.1458	0.1455	0.1453

50 microns

0.0499	0.05	0.0498	0.0501
0.05	0.0501	0.0502	0.0503
0.0499	0.05	0.0502	0.0501
0.0501	0.0478	0.05	0.0502
0.0501	0.0501	0.0503	0.0501
0.0501	0.0502	0.05	0.0501
0.0499	0.0501	0.0501	0.0501
0.0502	0.0501	0.0501	0.0501
0.0499	0.0501	0.0501	0.0503
0.0501	0.0501	0.0503	0.0504
0.05	0.0504	0.0504	0.0504
0.0497	0.0504	0.0504	0.0504

10 microns

0.0122	0.0123	0.0122	0.0121
0.0126	0.0122	0.0122	0.0123
0.0123	0.0122	0.012	0.012
0.0122	0.0121	0.012	0.012
0.0122	0.012	0.012	0.012
0.0121	0.0119	0.0121	0.0118
0.0121	0.0118	0.0119	0.0112
0.012	0.017	0.0119	0.0115
0.012	0.0116	0.0118	0.0118
0.0118	0.0116	0.0117	0.0119
0.0116	0.0116	0.0118	0.0119
0.016	0.0115	0.0118	0.0116
0.016	0.0117	0.0118	0.0116
0.015	0.0117	0.0117	0.0118
0.015	0.0115	0.0117	0.0118

Matlab Code for Moiré Analysis

```
function answer=c(m,n,xstep,xlength,ystep,ylength)
% m:The row number for points taken from moire pattern
% n:The column number for points taken from moire pattern
% xstep:For the search grid(used to find the least mean position),steps to
% be taken in x direction.
% xlength:The length to be covered by xstep
% ystep:For the search grid(used to find the least mean position),steps to
% be taken in y direction.
% ylength:The length to be covered by ystep


%input background, pick points
image=imread('1.bmp');
image=rgb2gray(image);
i2=im2bw(image,0.01);
i2=medfilt2(i2,[2, 2]);
figure;title('thresholded and smoothed image');
imshow(i2);
axis on;
hold on
testMoireCoordinates=cell(m,n);
for i=1:m
for j=1:n
[x_test,y_test]=ginput(1);
plot(x_test,y_test,'r+');
d=[x_test,y_test];
testMoireCoordinates(i,j)={d};
end
end
hold off;

%find the average length in x direction
x_unit=0;
for i=1:m
testC=cell2mat(testMoireCoordinates(i,1));
x_Ctest1=testC(1,1);
testC=cell2mat(testMoireCoordinates(i,n));
x_Ctest3=testC(1,1);
xdif=x_Ctest3-x_Ctest1;
x_unit=x_unit+xdif/m;
end

%find the average length in y direction
y_unit=0;
for j=1:n
testC=cell2mat(testMoireCoordinates(1,j));
y_Ctest1=testC(1,2);
testC=cell2mat(testMoireCoordinates(m,j));
y_Ctest3=testC(1,2);
ydif=y_Ctest3-y_Ctest1;
y_unit=y_unit+ydif/n;
end
```

```
%Make the reference grid with the left bottom corner perfectly match the
%one in the test grid
testfOrigin=cell2mat(testMoireCoordinates(1,1));
xOrigin=testfOrigin(1,1);
yOrigin=testfOrigin(1,2);
xdest=xOrigin+x_unit;
ydest=yOrigin+y_unit;

x=linspace(xOrigin,xdest,n)
y=linspace(yOrigin,ydest,m)
set(gca,'YDir','reverse');%reverse the y axis direction
[x,y]=meshgrid(x,y);

referenceMoireCoordinates=cell(m,n);
for i=1:m
for j=1:n
d=[x(i,j),y(i,j)];
referenceMoireCoordinates(i,j)={d};
end
end


distMat=zeros(m,n); % will store the dm value
angleMat=zeros(m,n);

for i=1:m
for j=1:n
testC=cell2mat(testMoireCoordinates(i,j));
x_Ctest=testC(1,1);
y_Ctest=testC(1,2);
refC=cell2mat(referenceMoireCoordinates(i,j));
x_Cref=refC(1,1);
y_Cref=refC(1,2);
set(gca,'YDir','reverse');
X=[x_Cref,x_Ctest]; Y=[y_Cref,y_Ctest];
%line(X,Y,'color','r');
%hold on;
distMat(i,j)=sqrt((x_Ctest-x_Cref)^2+(y_Ctest-y_Cref)^2 );
angleMat(i,j)=atan((y_Ctest-y_Cref)/(x_Ctest-x_Cref));
end
end

%determine the position of reference grid with least mean
x_testMoireCoordinates=zeros(m,n);
y_testMoireCoordinates=zeros(m,n);

for i=1:m
for j=1:n
testC=cell2mat(testMoireCoordinates(i,j));
x_testMoireCoordinates(i,j)=testC(1,1);
y_testMoireCoordinates(i,j)=testC(1,2);
end
end

least=1000;
xmove=0;
```

```
ymove=0;
for c=1:xstep  %% MAKE IT MORE GENERAL SO THAT INSTEAD OF 9, WE CAN USE ANY
NUMBER...EG. GXH
for d=1:ystep
sum=0;
for i=1:m
for j=1:n
testC=cell2mat(testMoireCoordinates(i,j));
x_Ctest=testC(1,1);
y_Ctest=testC(1,2);
refC=cell2mat(referenceMoireCoordinates(i,j));
x_Cref=refC(1,1);
y_Cref=refC(1,2);

distMat(i,j)=sqrt((x_Ctest-xlength*0.5/xstep+xlength/xstep-x_Cref)^2+(y_Ctest-
ylength*0.5/ystep+ylength/ystep-y_Cref)^2);
sum=sum+distMat(i,j);
end
end

if sum<least
least=sum;
xmove=0.625-c/8;
ymove=0.625-d/8;
else
least=least;
xmove=xmove;
ymove=ymove;
end
end
end

%put the reference grid on the right position
finalreferenceMoireCoordinates=cell(m,n);
for i=1:m
for j=1:n
testC=cell2mat(referenceMoireCoordinates(i,j));
x_Ctest=testC(1,1)+xmove;
y_Ctest=testC(1,2)+ymove;
k=[x_Ctest, y_Ctest];
finalreferenceMoireCoordinates(i,j)={k};
end
end

distMat=zeros(m,n); % will store the dm value
angleMat=zeros(m,n);


%Determine and illustrate the observed moire deformation
figure;
title('Observed Morie Deformation: The displacement between the observed moire and a fitted reference
moire pattern');
set(gca,'YDir','reverse');
x=linspace(xOrigin,xdest,n);
y=linspace(yOrigin,ydest,m);
[x,y]=meshgrid(x,y);
```

```
%line(x,y,'color','k');
%line(y,x,'color','k');
axis equal;
for i=1:m
for j=1:n
testC=cell2mat(testMoireCoordinates(i,j));
x_Ctest=testC(1,1);
y_Ctest=testC(1,2);
refC=cell2mat(finalreferenceMoireCoordinates(i,j));
x_Cref=refC(1,1);
y_Cref=refC(1,2);
X=[x_Cref,x_Ctest]; Y=[y_Cref,y_Ctest];
line(X,Y,'color','b','LineWidth',2);
hold on;
distMat(i,j)=sqrt((x_Ctest-x_Cref)^2+(y_Ctest-y_Cref)^2 );
angleMat(i,j)=atan((y_Ctest-y_Cref)/(x_Ctest-x_Cref));
end
end

x_finalreferenceMoireCoordinates=zeros(m,n); % Storing the x and y coordinates of hte final reference
moire in 2 matrices
y_finalreferenceMoireCoordinates=zeros(m,n);

for i=1:m
for j=1:n
refC=cell2mat(finalreferenceMoireCoordinates(i,j));
x_finalreferenceMoireCoordinates(i,j)=refC(1,1);
y_finalreferenceMoireCoordinates(i,j)=refC(1,2);
end
end
hold on;
h=drawGrid(x_finalreferenceMoireCoordinates,y_finalreferenceMoireCoordinates,'r',1,'--');
h=drawGrid(x_testMoireCoordinates,y_testMoireCoordinates,'k',1,'-');
axis off;
hold off;
set(gcf, 'color', 'white');


figure;
title('Observed Morie Deformation(without test grid)')
axis equal;
set(gca,'YDir','reverse');
hold on;
for i=1:m
for j=1:n
testC=cell2mat(testMoireCoordinates(i,j));
x_Ctest=testC(1,1);
y_Ctest=testC(1,2);
refC=cell2mat(finalreferenceMoireCoordinates(i,j));
x_Cref=refC(1,1);
y_Cref=refC(1,2);
X=[x_Cref,x_Ctest]; Y=[y_Cref,y_Ctest];
line(X,Y,'color','r','LineWidth',2);
hold on;
distMat(i,j)=sqrt((x_Ctest-x_Cref)^2+(y_Ctest-y_Cref)^2 );
angleMat(i,j)=atan((y_Ctest-y_Cref)/(x_Ctest-x_Cref));
```

```
end
end
h=drawGrid(x_finalreferenceMoireCoordinates,y_finalreferenceMoireCoordinates,'k',1,':');
hold off;
axis off;
set(gcf, 'color', 'white');



%Calculating the real pattern deformations using the moire deformations.

figure;
title('Actual regional deformations in the printed pattern');
actualdistMat=zeros(m,n); % will store the dm value
actualangleMat=zeros(m,n);
defdis=zeros(1,m*n);%use to save the distortion for each point
def_x=zeros(1,m*n);
def_y=zeros(1,m*n);
axis equal;
maxmx=0;%use to find the maximum distortions
maxmy=0;
maxmdis=0;
for i=1:m
for j=1:n
testC=cell2mat(testMoireCoordinates(i,j));
x_Ctest=testC(1,1);
y_Ctest=testC(1,2);
refC=cell2mat(finalreferenceMoireCoordinates(i,j));
x_Cref=refC(1,1);
y_Cref=refC(1,2);
set(gca,'YDir','reverse');
X=[x_Cref,x_Cref-y_Cref+y_Ctest]; Y=[y_Cref,y_Cref+x_Cref-x_Ctest];
line(X,Y,'color','r','LineWidth',2); hold on;axis equal;
actualdistMat(i,j)=sqrt((x_Cref+y_Cref-y_Ctest-x_Cref)^2+(y_Cref-x_Cref+x_Ctest-
y_Cref)^2)*0.01;%assume theta=0.01
def_x(1,(i-1)*n+j)=sqrt((y_Cref-y_Ctest)^2)*0.01;
def_y(1,(i-1)*n+j)=sqrt((-x_Cref+x_Ctest)^2)*0.01;
defdis(1,(i-1)*n+j)=sqrt((x_Cref+y_Cref-y_Ctest-x_Cref)^2+(y_Cref-x_Cref+x_Ctest-y_Cref)^2)*0.01;
actualangleMat(i,j)=atan((y_Cref-x_Cref+x_Ctest-y_Cref)/(x_Cref+y_Cref-y_Ctest-x_Cref));
if def_x(1,(i-1)*n+j)>maxmx
maxmx=def_x(1,(i-1)*n+j);
else
maxmx=maxmx;
end
if def_y(1,(i-1)*n+j)>maxmy
maxmy=def_y(1,(i-1)*n+j);
else
maxmy=maxmy;
end
if defdis(1,(i-1)*n+j)>maxmdis
maxmdis=defdis(1,(i-1)*n+j);
else
maxmdis=maxmdis;
end
end
```

```
end
h=drawGrid(x_finalreferenceMoireCoordinates,y_finalreferenceMoireCoordinates,'k',0.5,':')
axis off;
set(gcf, 'color', 'white');
xline=linspace(0,maxmx,m*n);
yline=linspace(0,maxmy,m*n);
disline=linspace(0,maxmdis,m*n);

defdis=defdis';
def_x=def_x';
def_y=def_y';
figure;
title('distortion distribution histogram');
hold on
hist(defdis,disline);
tt= findobj(gca,'Type','patch');
set(tt,'FaceColor','r','EdgeColor','w')
hold off
axis tight;
meandefdis=mean2(defdis)

figure;
title('x direction distortion distribution histogram');
hold on
hist(def_x,xline);
tt= findobj(gca,'Type','patch');
set(tt,'FaceColor','r','EdgeColor','w')
hold off
axis tight;
meandef_x=mean2(def_x)

figure;
title('y direction distortion distribution histogram');
hold on
hist(def_y,yline);
tt= findobj(gca,'Type','patch');
set(tt,'FaceColor','r','EdgeColor','w')
hold off
axis tight;
meandey_x=mean2(def_y)
```